

Modeling and LQR Control of a Two-Dimensional Airfoil

Shana D. Olds

Thesis submitted to the Faculty of the Virginia Polytechnic Institute and State University in partial fulfillment of the requirements for the degree of

MASTERS OF SCIENCE IN MATHEMATICS

APPROVED:

Dr. John Burns, Chairman

Dr. Terry Herdman

Dr. Robert Rogers

April 21, 1997

Blacksburg, VA

Copyright 1997, Shana D. Olds

Keywords: LQR, stability, pitch, plunge, flap angle

MODELING AND LQR CONTROL OF A TWO-DIMENSIONAL AIRFOIL

Shana D. Olds

(ABSTRACT)

In this paper we develop a mathematical model of a two-dimensional aeroelastic airfoil. This model is used to design a flutter suppression controller. Flutter is a vibration in a wing caused by airstream energy being absorbed by the lifting surface. Flutter increases with increasing speed. For simplicity, we consider a flat plate in a two-dimensional flow. The model is developed in the frequency domain and then transformed into the time domain.

The uncontrolled model is numerically simulated using MATLAB. Linear Quadratic Regulator (LQR) theory is used to design a state feedback controller. The LQR control scheme consists of using a full state feedback controller of the form $u = -K_c x$, where K_c is a control gain matrix. The goal is to use LQR theory to suppress flutter and to maintain stability of the closed loop system.

ACKNOWLEDGMENTS

I would like to thank the chairman of my committee, Dr. John Burns, for directing me into a field study that I thoroughly enjoy. His insight and motivation has shown me that mathematics is not just something school teachers study. I would like to thank Dr. Rogers for being on my committee and giving good, sound advice and guidance through the undergraduate years. I would also like to thank Dr. Herdman for serving on my committee.

I would like to thank God, for there were times when I thought I would not make it, but He saw me through.

I thank you to my parents for their undying love, encouragement, and motivation. You have always supported me and I love you very much. To all of my family and friends: thank you so much for being there for me and taking an interest in control theory even though most of you do not like mathematics.

A special thanks to all of my friends in the mathematics department, especially Tom Bail. We persevered and made it!! I would not have made it without you.

May God bless all of you!

Contents

1	Introduction	1
2	The Two-Dimensional Aeroelastic Airfoil	2
2.1	The Positions and Motions of the Airfoil Model	2
2.2	The Aerodynamic Loads	2
2.3	The Aeroelastic Model	5
3	The First Order System	13
4	Numerical Simulations	17
4.1	Open Loop Simulations	19
5	The LQR Problem	33
5.1	LQR Control	33
5.2	Closed Loop Simulations: Control Initiated at $t=0$	36
5.3	Closed Loop Simulations: Control Initiated at $t>0$	50
6	Conclusions	63
A	Nomenclature	65
B	MATLAB Codes	67

List of Figures

2.1	The 2-D cross-section of a typical airfoil.	11
2.2	Free body diagram of the main body and trailing edge control surface. . . .	12
4.1	The plunge, pitch, and flap angle for the open loop system: Stable, $V=950$.	20
4.2	The velocities of the plunge, pitch, and flap angle for the open loop system: Stable, $V=950$	21
4.3	The aerodynamic lag states B_1 and B_2 for the open loop system: Stable, $V=950$	22
4.4	The aerodynamic lag states A_1 and A_2 for the open loop system: Stable, $V=950$	23
4.5	The plunge, pitch, and flap angle for the open loop system: Marginally stable, $V=V_f$	24
4.6	The velocities of the plunge, pitch, and flap angle for the open loop system: Marginally Stable, $V=V_f$	25
4.7	The aerodynamic lag states B_1 and B_2 for the open loop system: Marginally Stable, $V=V_f$	26
4.8	The aerodynamic lag states A_1 and A_2 for the open loop system: Marginally Stable, $V=V_f$	27
4.9	The plunge, pitch, and flap angle for the open loop system: Unstable, $V=1000$.	29
4.10	The velocities of the plunge, pitch, and flap angle for the open loop system: Unstable, $V=1000$	30
4.11	The aerodynamic lag states B_1 and B_2 for the open loop system: Unstable, $V=1000$	31
4.12	The aerodynamic lag states A_1 and A_2 for the open loop system: Unstable, $V=1000$	32
5.1	The plunge, pitch, and flap angle for the closed loop system: Stable, $V=950$.	37
5.2	The velocities of the plunge, pitch, and flap angle for the closed loop system: Stable, $V=950$	38

5.3	The aerodynamic lag states B_1 and B_2 for the closed loop system: Stable, $V=950$	39
5.4	The aerodynamic lag states A_1 and A_2 for the closed loop system: Stable, $V=950$	40
5.5	The plunge, pitch, and flap angle for the closed loop system: Stable, $V=V_f$	41
5.6	The velocities of the plunge, pitch, and flap angle for the closed loop system: Stable, $V=V_f$	42
5.7	The aerodynamic lag states B_1 and B_2 for the closed loop system: Stable, $V=V_f$	43
5.8	The aerodynamic lag states A_1 and A_2 for the closed loop system: Stable, $V=V_f$	44
5.9	The plunge, pitch, and flap angle for the closed loop system: Stable, $V=1000$	45
5.10	The velocities of the plunge, pitch, and flap angle for the closed loop system: Stable, $V=1000$	46
5.11	The aerodynamic lag states B_1 and B_2 for the closed loop system: Stable, $V=1000$	47
5.12	The aerodynamic lag states A_1 and A_2 for the closed loop system: Stable, $V=1000$	48
5.13	The plunge, pitch, and flap angle for the closed loop system with the control initiated at $t=.5$ seconds: $V=1000$	51
5.14	The velocities of the plunge, pitch, and flap angle for the closed loop system with the control initiated at $t=.5$ seconds: $V=1000$	52
5.15	The aerodynamic lag states B_1 and B_2 for the closed loop system with the control initiated at $t=.5$ seconds: $V=1000$	53
5.16	The aerodynamic lag states A_1 and A_2 for the closed loop system with the control initiated at $t=.5$ seconds: $V=1000$	54
5.17	The plunge, pitch, and flap angle for the closed loop system with the control initiated at $t=1$ second: $V=1000$	55
5.18	The velocities of the plunge, pitch, and flap angle for the closed loop system with the control initiated at $t=1$ second: $V=1000$	56
5.19	The aerodynamic lag states B_1 and B_2 for the closed loop system with the control initiated at $t=1$ second: $V=1000$	57
5.20	The aerodynamic lag states A_1 and A_2 for the closed loop system with the control initiated at $t=1$ second: $V=1000$	58
5.21	The plunge, pitch, and flap angle for the closed loop system with the control initiated at $t=2$ seconds: $V=1000$	59
5.22	The velocities of the plunge, pitch, and flap angle for the closed loop system with the control initiated at $t=2$ seconds: $V=1000$	60

5.23	The aerodynamic lag states B_1 and B_2 for the closed loop system with the control initiated at $t=2$ seconds: $V=1000$	61
5.24	The aerodynamic lag states A_1 and A_2 for the closed loop system with the control initiated at $t=2$ seconds: $V=1000$	62

List of Tables

2.1	List of Φ_i 's	10
3.1	List of R_i 's	15
4.1	List of Constants	18
4.2	Eigenvalues of open loop system for $V = 950$	20
4.3	Eigenvalues of open loop system for $V=Vf=975.6$	28
4.4	Eigenvalues of open loop system for $V=1000$	29
5.1	Eigenvalues of $(A - BK_V)$: $V=1000$	35
5.2	Eigenvalues of $(A - BK_V)$: $V=Vf=975.6$	35
5.3	Eigenvalues of closed loop system for $V=950$	41
5.4	Eigenvalues of closed loop system for $V=Vf=975.6$	45
5.5	Eigenvalues of closed loop system for $V=1000$	49

Chapter 1

Introduction

The goal of this thesis is to develop a state space model for the so-called typical aeroelastic airfoil and then apply LQR control to this system to dampen flutter. As stated by York in [10], flutter is an aeroelastic self-excited unstable vibration in which the airstream energy is absorbed by the lifting surface. The motion involves both bending and torsional components which are basically simple harmonic oscillations with a unique flutter frequency. The basic model may be found in York's thesis [10]. However, we repeat the derivation here in order to correctly identify all of the system's parameters in the model. We begin with the fundamental force and inertia equations. A second order dynamical system is constructed and used to develop a first order state space system of the form,

$$\dot{x}(t) = Ax(t) + Bu(t), \tag{1.1}$$

where each parameter is explicitly defined. The system is tested with $u = 0$ to analyze its behavior and to test the model for accuracy.

The control objective is to use state feedback to stabilize the system and prevent flutter. We focus on the infinite time Linear-Quadratic Regulator problem. This approach leads to a full state-feedback controller of the form $u = -K_c x$ to maintain stability. We show that a stable solution exists and use the algebraic Riccati equation to solve for an optimal control u^* . MATLAB is used in all numerical simulations. In particular, we use the Control System Toolbox to compute the gain matrix K_c and the ordinary differential equation solver ODE45 to run time simulations.

Chapter 2

The Two-Dimensional Aeroelastic Airfoil

In this chapter we derive a state space model for a two-dimensional airfoil in an unsteady flow. We start by describing the positions and motions of the airfoil and then discuss the aerodynamic loads. We make heavy use of York's work [10].

2.1 The Positions and Motions of the Airfoil Model

Consider the typical airfoil as described in Figure 2.1. We develop the basic dynamic equations for the airfoil in terms of the airfoil's position, velocity, and so-called aerodynamic lag states. For this paper, the airfoil is viewed as a flat plate suspended from a fixed object by a spring. The motion of the airfoil is described by three positions: the plunge h , the pitch α , and the flap angle β . The plunge h is the position along the y-axis measured positive down. The pitch α is the angle measured from the x-axis. The flap angle β is the angle of the flap with respect to the airfoil. To provide the correct forces so that this cross-section behaves like part of the attached wing, we will use linear and torsional springs. The linear spring that provides a restoring force for the plunge of the airfoil is assumed to have stiffness constant K_h . Likewise the torsional spring has stiffness constant K_α and the flap spring has stiffness constant K_β .

2.2 The Aerodynamic Loads

The airfoil is subjected to three aerodynamic loads. The lift L is measured positive in the upward direction. The pitching moment M is assumed to be centered about the one-quarter chord of the airfoil. The flap torque T is applied to the flap hinge. The goal is to

develop a state space model that can be used for control design.

We first derive the equations of motion. Newton's second law of motion and the moment equation for a rigid body in planar motion are given by

$$\sum \vec{F}_y = m_i \vec{a}_{c.m.} \quad (2.1)$$

and

$$\sum \vec{M}_{c.m.} = I_{c.m.} \dot{\omega}, \quad (2.2)$$

respectively. Here F is force, m is mass, \vec{a} is acceleration, $M_{c.m.}$ is momentum, $I_{c.m.}$ is inertia, and $\dot{\omega}$ is the angular acceleration. The free body diagram is shown in Figure 2.2. Equations (2.1) and (2.2) are applied to the main body and to the trailing edge control surface. We assume angles α and β are small so that we can linearize about the zero equilibrium point. In particular, we assume that

$$\alpha = \beta = \dot{\alpha} = \dot{\beta} = \ddot{\alpha} = \ddot{\beta} = 0 \quad (2.3)$$

is an equilibrium for the system.

Assuming the angles are small and linearizing yields the system (see [10])

$$K_h h - q_y + L_1 + m_1 [\ddot{h} + b x_1 \ddot{\alpha}] = 0, \quad (2.4)$$

$$I_Q \ddot{\alpha} + M_1 + K_\alpha \alpha - K_\beta \beta - K_h h b x_1 - L_1 \left[d b - \frac{b}{2} + b x_1 \right] - q_y [c b - b x_1] = 0, \quad (2.5)$$

$$q_y + L_2 + m_2 [\ddot{h} + b c \ddot{\alpha} + l(\ddot{\beta} + \ddot{\alpha})] = 0, \quad (2.6)$$

and

$$-(q_y + L_2)l + K_\beta + M_2 + I_G(\ddot{\alpha} + \ddot{\beta}) = 0. \quad (2.7)$$

The subscript 1 denotes equations for the main body (body 1) of the airfoil. The subscript 2 denotes equations for the trailing edge flap (body 2). Therefore, equations (2.4) and (2.5) apply to body 1 of the airfoil and equations (2.6) and (2.7) apply to body 2. Here q_y is the vertical flap hinge force, l is the distance to the trailing edge flap center of gravity from c , m_1 is the mass of body 1, m_2 is the mass of body 2, x_1 is the nondimensionalized distance of the main section center of gravity, I_Q is the inertia per unit length of the total section, I_G is the moment of inertia per unit span of trailing edge flap about point G, b is a normalizing constant, and c is the nondimensionalized distance to the flap hinge line. Adding equations (2.4) and (2.6) yields the plunge equation

$$(mb) \frac{\ddot{h}}{b} + [m_1 b x_1 + m_2 (bc + l)] \ddot{\alpha} + m_2 l \ddot{\beta} + (b K_h) \frac{h}{b} = -L. \quad (2.8)$$

Equations (2.4) through (2.7) are combined so that the pitching moment about the one-quarter chord point has the form

$$M = M_1 + M_2 + L_2 \left[c + d - \frac{1}{2} \right] b. \quad (2.9)$$

Equations (2.4) through (2.7) are combined as

$$\left(d - \frac{1}{2} + x_1 \right) b [\text{eq.}(2.4)] + 1 [\text{eq.}(2.5)] + \left[b \left(c + d - \frac{1}{2} \right) + l \right] [\text{eq.}(2.6)] + 1 [\text{eq.}(2.7)], \quad (2.10)$$

so that the pitch equation becomes

$$\begin{aligned} & \left[m_1 b^2 \left(d - \frac{1}{2} + x_1 \right) + m_2 b^2 \left(c + d - \frac{1}{2} + \frac{l}{b} \right) \right] \frac{\ddot{h}}{b} \\ & + \left[m_1 b^2 x_1 \left(d - \frac{1}{2} + x_1 \right) + I_Q + m_2 b \left(c + d - \frac{1}{2} + \frac{l}{b} \right) (bc + l) + I_G \right] \ddot{\alpha} \\ & + \left[m_2 b l \left(c + d - \frac{1}{2} + \frac{l}{b} \right) + I_G \right] \ddot{\beta} \\ & + \left[K_h b^2 \left(d - \frac{1}{2} \right) \right] \frac{h}{b} + K_\alpha \alpha = -M. \end{aligned} \quad (2.11)$$

Solving equation (2.6) for q_y and substituting this into (2.7) produces the equation

$$(bm_2 l) \frac{\ddot{h}}{b} + [m_2 l (bc + l) + I_G] \ddot{\alpha} + (m_2 l^2 + I_G) \ddot{\beta} + K_\beta \beta = -(T + T_S). \quad (2.12)$$

The torque T_S is an additional flap hinge torque used to control the flap. The open loop (or uncontrolled) system is defined by $T_S = 0$. Finally, equation (2.8) is multiplied by $-b \left[d + a - \frac{1}{2} \right]$ and added to equation (2.11). Combining (2.11), (2.8), and (2.12) produces the second order system

$$\begin{bmatrix} bm & S_\alpha & S_\beta \\ bS_\alpha & I_\alpha & I_\beta + S_\beta bc \\ bS_\beta & I_\beta + S_\beta bc & I_\beta \end{bmatrix} \begin{bmatrix} \frac{\ddot{h}}{b} \\ \ddot{\alpha} \\ \ddot{\beta} \end{bmatrix} + \begin{bmatrix} K_h & 0 & 0 \\ 0 & K_\alpha & 0 \\ 0 & 0 & K_\beta \end{bmatrix} \begin{bmatrix} \frac{h}{b} \\ \alpha \\ \beta \end{bmatrix} = \begin{bmatrix} -L \\ -M_{e.a.} \\ -(T + T_S) \end{bmatrix}. \quad (2.13)$$

We write this system in the form

$$M' \ddot{Y}(t) + KY(t) = \begin{bmatrix} -L \\ -M \\ -(T + T_S) \end{bmatrix}, \quad (2.14)$$

where

$$M' = \begin{bmatrix} bm & S_\alpha & S_\beta \\ bS_\alpha & I_\alpha & I_\beta + S_\beta bc \\ bS_\beta & I_\beta + S_\beta bc & I_\beta \end{bmatrix} \quad (2.15)$$

and

$$K = \begin{bmatrix} K_h & 0 & 0 \\ 0 & K_\alpha & 0 \\ 0 & 0 & K_\beta \end{bmatrix}. \quad (2.16)$$

This is the matrix form of the equations of motion where M' is the mass matrix and K is the stiffness matrix. In the above equations, S_α is the static moment of the airfoil per unit length about x_α measured in terms of mass and nondimensionalized distances, $S_\beta = m_2 l$ is the static moment of the trailing edge flap per unit length about c , b is a normalizing factor for h , and c is the distance between the flap hinge and the spring K_h .

2.3 The Aeroelastic Model

Following York [10], we apply the Laplace transform to equation (2.14). This converts the system to the frequency domain and the motion of the airfoil is defined as simple harmonic oscillations. We use linearized, unsteady aerodynamic theory from [5] and apply it to derive the formulas which give the pressure distribution over the wing and the aerodynamic responses of the oscillating hinges for any position of the hinge with respect to the leading edge. The linearization allows the total aerodynamic loads to be found by superposition of the forces and moments associated with each degree of freedom. Once the basic system has been derived, the inverse Fourier transform is used to construct a state space model. From [10], the three degrees of freedom are:

1. The plunging or bending oscillation of the airfoil,

$$z_1(x) = h e^{i\omega t},$$

2. The pitching oscillation of the airfoil about the one-quarter chord point,

$$z_2(x) = \alpha b \left[x + \frac{1}{2} \right] e^{i\omega t},$$

and

3. The oscillation about the leading edge or hinge line,

$$z_3(x) = \begin{cases} 0 & \text{for } 0 \leq \Theta \leq \phi \\ \beta e^{i\omega t} (\cos \phi - \cos \Theta) & \text{for } \phi \leq \Theta \leq \pi \end{cases}.$$

Here, x represents the position along the airfoil so that z_1 and z_3 are independent of x . From [5] the aerodynamic loads are defined as follows:

$$L \equiv \frac{\text{total wing lift}}{\text{unit depth}} = \pi\rho V^2 b e^{i\omega t} \sum_{g=1}^3 G k_g, \quad (2.17)$$

$$M \equiv \frac{\text{total wing moment about the 1/4 chord}}{\text{unit depth}} = \pi\rho V^2 b^2 e^{i\omega t} \sum_{g=1}^3 G m_g, \quad (2.18)$$

and

$$T \equiv \frac{\text{total flap hinge about its leading edge}}{\text{unit depth}} = \pi\rho V^2 b^2 e^{i\omega t} \sum_{g=1}^3 G n_g. \quad (2.19)$$

Here ρ is the air density, V is the velocity, t is the time, and G is the amplitude of degree of freedom g .

Since the pitching, plunging, and control surface oscillations are have small amplitudes, we omit $e^{i\omega t}$ for convenience. Finally, we substitute the expressions for k_g , m_g , and n_g from [9] into equations (2.17), (2.18), and (2.19). Hence, in the frequency domain L , M , T are given by

$$\begin{aligned} L(\omega) &= \pi\rho V^2 b \left[\left\{ i \left(\frac{\omega b}{V} \right) [2C(k)] - \frac{\omega^2 b^2}{V^2} \right\} \frac{h}{b} + \left\{ 2C(k) \left(1 + \frac{i\omega b}{V} \right) + \frac{i\omega b}{V} - \frac{\omega^2 b^2}{2V^2} \right\} \alpha \right] \\ &+ \pi\rho V^2 b \left[\left\{ \frac{1}{\pi} \left[2C(k) \left(\Phi_1 + \frac{i\omega b}{2V} \Phi_2 \right) + \frac{i\omega b}{V} \Phi_3 - \frac{\omega^2 b^2}{2V^2} \Phi_4 \right] \right\} \beta \right], \end{aligned} \quad (2.20)$$

$$M(\omega) = \pi\rho V^2 b^2 \left\{ - \left(\frac{\omega^2 b^2}{2V^2} \right) \frac{h}{b} + \left(\frac{i\omega b}{V} - \frac{3\omega^2 b^2}{8V^2} \right) \alpha + \frac{1}{\pi} \left[\Phi_5 + \frac{i\omega b}{2V} \Phi_6 - \frac{\omega^2 b^2}{4V^2} \Phi_7 \right] \beta \right\}, \quad (2.21)$$

and

$$\begin{aligned} T(\omega) &= \pi\rho V^2 b^2 \left[\left\{ \frac{1}{\pi} \left[C(k) \frac{i\omega b}{V} \Phi_8 - \frac{\omega^2 b^2}{2V^2} \Phi_4 \right] \right\} \frac{h}{b} \right] \\ &+ \pi\rho V^2 b^2 \left[\left\{ \frac{1}{\pi} \left[C(k) \left(1 + \frac{i\omega b}{V} \right) \Phi_8 + \frac{i\omega b}{2V} \Phi_9 - \frac{\omega^2 b^2}{4V^2} \Phi_7 \right] \right\} \alpha \right] \\ &+ \pi\rho V^2 b^2 \left[\left\{ \frac{1}{\pi^2} \left[C(k) \left(\Phi_1 + \frac{i\omega b}{2V} \Phi_2 \right) \Phi_8 + \Phi_{10} \right. \right. \right. \\ &\left. \left. \left. + \frac{i\omega b}{2V} \Phi_{11} - \frac{\omega^2 b^2}{4V^2} \Phi_{12} \right] \right\} \beta \right], \end{aligned} \quad (2.22)$$

respectively. Equations (2.20), (2.21), and (2.22) are written in terms of the transformed plunge, pitch, flap angle, and frequency ω . The constants Φ_i can be found in [5] and are listed in Table 2.1. The Theodorsen function $C(k)$ is a function that, in the frequency domain, determines the aerodynamic loads for a given airfoil motion. From [8] equations (2.20), (2.21), and (2.22) can be rewritten as

$$L(\omega) = -\pi\rho b^2 \left[\omega^2 h + \left(\frac{\omega^2 b}{2} - i\omega V \right) \alpha - \frac{1}{\pi} \left(i\omega V \Phi_3 - \frac{\omega^2 b}{2} \Phi_4 \right) \beta \right] \\ - 2\pi\rho V b \left[\frac{C(k)}{i\omega} \right] \left\{ \omega^2 h + (\omega^2 b - i\omega V) \alpha + \frac{V}{\pi} \left(\frac{\omega^2 b}{2V} \Phi_2 - i\omega \Phi_1 \right) \beta \right\}, \quad (2.23)$$

$$M(\omega) = \pi\rho b^3 \left[-\frac{1}{2}\omega^2 h + \left(i\omega V - \frac{3b\omega^2}{8} \right) \alpha + \left(\frac{V^2}{\pi b} \Phi_5 + \frac{i\omega V}{2\pi} \Phi_6 - \frac{\omega^2 b}{4\pi} \Phi_7 \right) \beta \right], \quad (2.24)$$

and

$$T(\omega) = \pi\rho b^2 \left\{ -\omega^2 h \left(\frac{b}{2\pi} \right) \Phi_4 + \left(\frac{i\omega b V}{2\pi} \Phi_9 - \frac{\omega^2 b^2}{4\pi} \Phi_7 \right) \alpha \right\} \\ + \pi\rho b^2 \left\{ \left(\frac{V^2}{\pi^2} \Phi_{10} + \frac{i\omega V b}{2\pi^2} \Phi_{11} - \frac{\omega^2 b^2}{4\pi^2} \Phi_{12} \right) \beta \right\} \\ + \pi\rho V b \left[\frac{C(k)}{i\omega} \right] \left\{ \left(-\frac{\omega^2 b}{\pi} \Phi_8 \right) h + \left[\frac{V b}{\pi} \left(i\omega - \frac{\omega^2 b}{V} \right) \Phi_8 \right] \alpha \right\} \\ + \pi\rho V b \left[\frac{C(k)}{i\omega} \right] \left[\frac{V b}{\pi^2} \left(i\omega \Phi_1 - \frac{\omega^2 b}{2V} \Phi_2 \right) \Phi_8 \right] \beta, \quad (2.25)$$

respectively.

These oscillatory loads are the Fourier transforms of the transient loads. Therefore, the inverse Fourier transforms of the oscillatory loads are the transient loads. The inverse Fourier transform of the terms containing the Theodorsen Function, $C(k)$, are found using the Convolution Theorem (Theorem 12.4.4 in [6]). The Fourier transform of the Wagner Function, $\Phi\left(\frac{Vt}{b}\right)$, is

$$\mathcal{F} \left\{ \Phi \left(\frac{Vt}{b} \right) \right\} = \frac{C(k)}{i\omega},$$

where $C(k)$ is the Theodorsen Function.

Applying inverse Fourier transforms to the oscillatory loads yields the transient loads. Thus, in the time domain the aerodynamic loads have the form (see [10])

$$L(t) = \pi\rho b^2 \left[\ddot{h} + \frac{b}{2}\ddot{\alpha} + \frac{b}{2\pi}\Phi_4\ddot{\beta} + V\dot{\alpha} + \frac{V}{\pi}\Phi_3\dot{\beta} \right] + 2\pi\rho V b D(t), \quad (2.26)$$

$$M(t) = \pi\rho b^3 \left[\frac{1}{2}\ddot{h}(t) + \frac{3b}{8}\ddot{\alpha}(t) + \frac{b}{4\pi}\Phi_7\ddot{\beta}(t) + V\dot{\alpha}(t) + \frac{V}{2\pi}\Phi_6\dot{\beta}(t) + \frac{V^2}{\pi b}\Phi_5\beta(t) \right], \quad (2.27)$$

and

$$\begin{aligned} T(t) &= \pi\rho b^2 \left[\left(\frac{b}{2\pi}\Phi_4 \right) \ddot{h}(t) + \left(\frac{b^2}{4\pi}\Phi_7 \right) \ddot{\alpha}(t) + \left(\frac{b^2}{4\pi^2}\Phi_{12} \right) \ddot{\beta}(t) + \left(\frac{bV}{2\pi}\Phi_9 \right) \dot{\alpha}(t) \right] \\ &+ \pi\rho b^2 \left[\left(\frac{Vb}{2\pi^2}\Phi_{11} \right) \dot{\beta}(t) + \left(\frac{V^2}{\pi^2}\Phi_{10} \right) \beta(t) \right] + \pi\rho VbG(t), \end{aligned} \quad (2.28)$$

respectively. The functions $D(t)$ and $G(t)$ are Duhamel integrals given by

$$D(t) = \int_0^t \Phi \left[\frac{V(t-\tau)}{b} \right] Q'_1(\tau) d\tau, \quad (2.29)$$

and

$$G(t) = \int_0^t \Phi \left[\frac{V(t-\tau)}{b} \right] Q'_2(\tau) d\tau, \quad (2.30)$$

where

$$Q'_1(\tau) = \frac{dQ_1(\tau)}{d\tau} = h''(\tau) + \alpha''(\tau)b + \frac{b}{2\pi}\Phi_2\beta''(\tau) + V\alpha'(\tau) + \frac{V}{\pi}\Phi_1\beta'(\tau), \quad (2.31)$$

$$Q'_2(\tau) = \frac{dQ_2(\tau)}{d\tau} = \frac{b}{\pi}\Phi_8h''(\tau) + \frac{b^2}{\pi}\Phi_8\alpha''(\tau) + \frac{b^2}{2\pi^2}\Phi_2\Phi_8\beta''(\tau) + \frac{Vb}{\pi}\Phi_8\alpha'(\tau) + \frac{Vb}{\pi^2}\Phi_1\Phi_8\beta'(\tau), \quad (2.32)$$

and $\tau = \frac{Vt}{b}$. The moment equation (2.27) does not require a Duhamel integral because the moment is assumed to be centered at the one-quarter chord of the airfoil.

In order to evaluate the Duhamel integrals, one needs the Wagner Function or a numerical approximation. We use the standard two-term Jones exponential approximation of Φ given by

$$\Phi \left(\frac{Vt}{b} \right) = 1 - \alpha_1 e^{-\frac{\beta_1 Vt}{b}} - \alpha_2 e^{-\frac{\beta_2 Vt}{b}}, \quad (2.33)$$

where, $\alpha_1 = .165$, $\beta_1 = .041$, $\alpha_2 = .335$, and $\beta_2 = .32$. Substituting this approximation into equations (2.26) and (2.28) yields the expressions

$$D(t) = Q_1(t) - \alpha_1 B_1(t) - \alpha_2 B_2(t) \quad (2.34)$$

and

$$G(t) = Q_2(t) - \alpha_1 A_1(t) - \alpha_2 A_2(t), \quad (2.35)$$

where the functions $A_1(t)$, $A_2(t)$, $B_1(t)$, and $B_2(t)$ are called aerodynamic lag states. The aerodynamic lag states are used to describe the "states" of the fluid and satisfy the first-order differential equations given by

$$\begin{aligned}
\dot{B}_1(t) + \left(\frac{\beta_1 V}{b}\right) B_1(t) &= \dot{Q}_1(t), \\
\dot{B}_2(t) + \left(\frac{\beta_2 V}{b}\right) B_2(t) &= \dot{Q}_1(t), \\
\dot{A}_1(t) + \left(\frac{\beta_1 V}{b}\right) A_1(t) &= \dot{Q}_2(t), \\
\dot{A}_2(t) + \left(\frac{\beta_2 V}{b}\right) A_2(t) &= \dot{Q}_2(t).
\end{aligned} \tag{2.36}$$

In the equations (2.31) and (2.32), we substitute t for τ and integrate with respect to t to obtain

$$Q_1(t) = \dot{h}(t) + \dot{\alpha}(t)b + \frac{b}{2\pi}\Phi_2\dot{\beta}(t) + V\alpha(t) + \frac{V}{\pi}\Phi_1\beta(t) \tag{2.37}$$

and

$$Q_2(t) = \frac{b}{\pi}\Phi_8\dot{h}(t) + \frac{b^2}{\pi}\Phi_8\dot{\alpha}(t) + \frac{b^2}{2\pi^2}\Phi_2\Phi_8\dot{\beta}(t) + \frac{Vb}{\pi}\Phi_8\alpha(t) + \frac{Vb}{\pi^2}\Phi_1\Phi_8\beta(t). \tag{2.38}$$

Therefore, the aerodynamic loads are given by

$$\begin{aligned}
L(t) &= \pi\rho b^2(b)\frac{\ddot{h}(t)}{b} + \pi\rho b^2\left(\frac{b}{2}\right)\ddot{\alpha}(t) + \pi\rho b^2\left(\frac{b}{2\pi}\Phi_4\right)\ddot{\beta}(t) + \pi\rho b^2(2V)\frac{\dot{h}(t)}{b} + \pi\rho b^2(3V)\dot{\alpha}(t) \\
&+ \pi\rho b^2\frac{V}{\pi}(\Phi_3 + \Phi_2)\dot{\beta}(t) + \pi\rho b^2\left(\frac{2V^2}{b}\right)\alpha(t) + \pi\rho b^2\left(\frac{2V^2}{\pi b}\Phi_1\right)\beta(t) \\
&- \pi\rho b^2\left(\frac{2V\alpha_1}{b}\right)B_1(t) - \pi\rho b^2\left(\frac{2V\alpha_2}{b}\right)B_2(t),
\end{aligned} \tag{2.39}$$

$$\begin{aligned}
M(t) &= \pi\rho b^2\left[\left(\frac{b^2}{2}\right)\frac{\ddot{h}(t)}{b} + \left(\frac{3b^2}{8}\right)\ddot{\alpha}(t) + \left(\frac{b^2}{4\pi}\Phi_7\right)\ddot{\beta}(t) + (Vb)\dot{\alpha}(t)\right] \\
&+ \pi\rho b^2\left[\left(\frac{Vb}{2\pi}\Phi_6\right)\dot{\beta}(t) + \left(\frac{V^2}{\pi}\right)\beta(t)\right],
\end{aligned} \tag{2.40}$$

and

$$T(t) = \pi\rho b^2\left[\left(\frac{b^2}{2\pi}\Phi_4\right)\frac{\dot{h}(t)}{b} + \left(\frac{b^2}{4\pi}\Phi_7\right)\dot{\alpha}(t) + \left(\frac{b^2}{4\pi^2}\Phi_{12}\right)\dot{\beta}(t) + \left(\frac{Vb}{\pi}\Phi_8\right)\frac{\dot{h}(t)}{b}\right]$$

$$\begin{aligned}
& + \pi \rho b^2 \left[\left[\frac{Vb}{\pi} \left(\frac{\Phi_9}{2} + \Phi_8 \right) \right] \dot{\alpha}(t) + \left[\frac{Vb}{2\pi^2} (\Phi_{11} + \Phi_2 \Phi_8) \right] \dot{\beta}(t) + \left(\frac{V^2}{\pi} \Phi_8 \right) \alpha(t) \right] \\
& + \pi \rho b^2 \left[\left[\frac{V^2}{\pi} (\Phi_{10} + \Phi_1 \Phi_8) \right] \beta(t) - \left(\frac{V\alpha_1}{b} \right) A_1(t) - \left(\frac{V\alpha_2}{b} \right) A_2(t) \right], \quad (2.41)
\end{aligned}$$

respectively.

$\Phi_1(\phi)$	$= \pi - \phi + \sin \phi$
$\Phi_2(\phi)$	$= (\pi - \phi)(1 + 2 \cos \phi) + \sin \phi(2 + \cos \phi)$
$\Phi_3(\phi)$	$= \pi - \phi + \sin \phi \cos \phi$
$\Phi_4(\phi)$	$= (\pi - \phi)2 \cos \phi + \sin \phi \frac{2}{3}(2 + \cos^2 \phi)$
$\Phi_5(\phi)$	$= \sin \phi(1 - \cos \phi)$
$\Phi_6(\phi)$	$= 2(\pi - \phi) + \sin \phi \frac{2}{3}(2 - \cos \phi)(1 + 2 \cos \phi)$
$\Phi_7(\phi)$	$= (\pi - \phi)\left(\frac{1}{2} + 2 \cos \phi\right) + \sin \phi \frac{1}{6}(8 + 5 \cos \phi + 4 \cos^2 \phi - 2 \cos^3 \phi)$
$\Phi_8(\phi)$	$= (\pi - \phi)(-1 + 2 \cos \phi) + \sin \phi(2 - \cos \phi)$
$\Phi_9(\phi)$	$= (\pi - \phi)(1 + 2 \cos \phi) + \sin \phi \frac{1}{3}(2 + 3 \cos \phi + 4 \cos^2 \phi)$
$\Phi_{10}(\phi)$	$= \Phi_{31}(\phi) \cdot \Phi_5(\phi)$
$\Phi_{11}(\phi)$	$= \Phi_2(\phi) \cdot \Phi_3(\phi)$
$\Phi_{12}(\phi)$	$= (\pi - \phi)^2\left(\frac{1}{2} + 4 \cos^2 \phi\right) + (\pi - \phi) \sin \phi \cos \phi(7 + 2 \cos^2 \phi)$ $+ \sin^2 \phi\left(2 + \frac{5}{2} \cos^2 \phi\right)$
$\Phi_{31}(\phi)$	$= \pi - \phi - \sin \phi$

Table 2.1: List of Φ_i 's

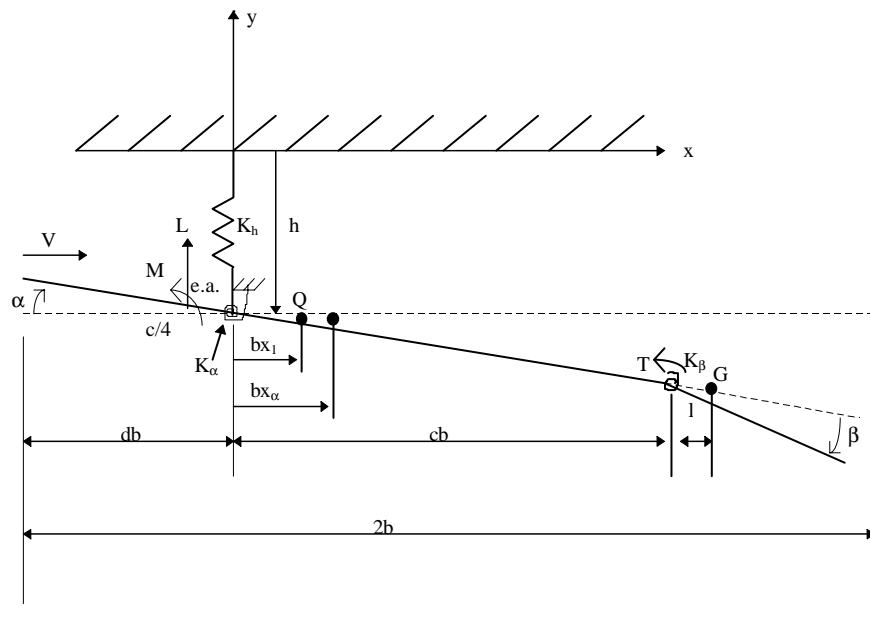


Figure 2.1: The 2-D cross-section of a typical airfoil.

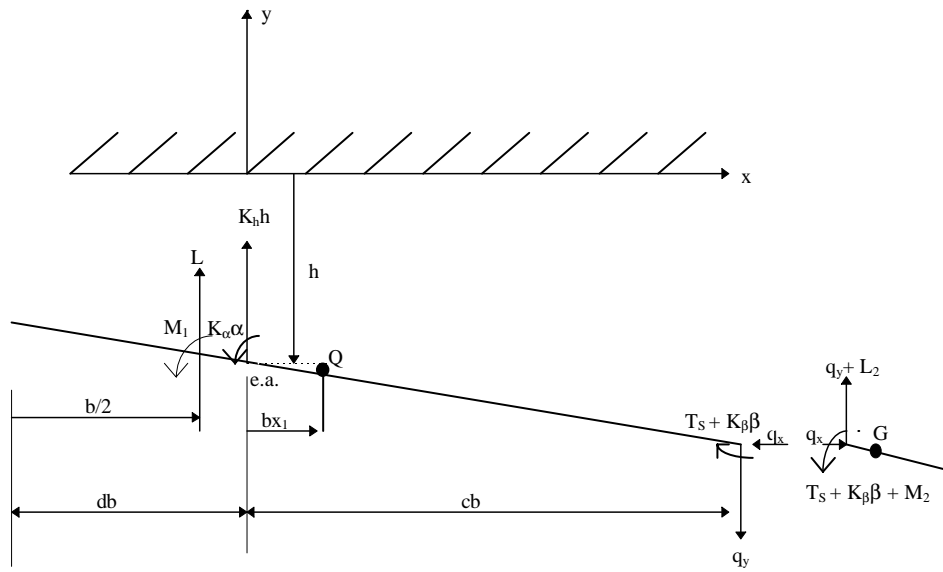


Figure 2.2: Free body diagram of the main body and trailing edge control surface.

Chapter 3

The First Order System

The goal of this chapter is to reduce our second order system to a first order system of the form

$$\dot{x}(t) = \begin{bmatrix} \ddot{Y}(t) \\ \dot{Y}(t) \\ \dot{x}_A(t) \end{bmatrix} = \begin{bmatrix} A_{11} & A_{12} & A_{13} \\ A_{21} & A_{22} & A_{23} \\ A_{31} & A_{32} & A_{33} \end{bmatrix} \begin{bmatrix} \dot{Y}(t) \\ Y(t) \\ x_A(t) \end{bmatrix} + B[u(t)] \quad (3.1)$$

where

$$Y(t) = \left[\frac{h(t)}{b} \quad \alpha(t) \quad \beta(t) \right]^T \quad (3.2)$$

and

$$x_A(t) = \left[B_1(t) \quad B_2(t) \quad A_1(t) \quad A_2(t) \right]^T. \quad (3.3)$$

To complete the model we start with the equation

$$M'\ddot{Y}(t) + KY(t) = \begin{bmatrix} -L(t) \\ -M(t) \\ -[T(t) + T_S(t)] \end{bmatrix}, \quad (3.4)$$

and use the representations for $L(t)$, $M(t)$, and $T(t)$ given by equations (2.39), (2.40), and (2.41) to rewrite equation (3.4) in the form

$$M'\ddot{Y} + KY = -\pi\rho b^2 \left[Z_1\ddot{Y} + Z_2\dot{Y} + Z_3Y + Z_4x_A \right]. \quad (3.5)$$

Here,

$$Z_1 = \begin{bmatrix} b & \frac{b}{2} & \frac{b}{2\sqrt{2}}\Phi_4 \\ \frac{b^2}{2} & \frac{3b^2}{8} & \frac{b^2}{4\pi}\Phi_7 \\ \frac{b^2}{2\pi}\Phi_4 & \frac{b^2}{4\pi^2}\Phi_7 & \frac{b^2}{4\pi}\Phi_{12} \end{bmatrix}, \quad (3.6)$$

$$Z_2 = \begin{bmatrix} 2V & 3V & \frac{V}{\pi}(\Phi_3 + \Phi_2) \\ 0 & Vb & \frac{Vb}{2\pi}\Phi_6 \\ \frac{Vb}{\pi}\Phi_8 & \frac{Vb}{\pi}\left(\frac{\Phi_9}{2} + \Phi_8\right) & \frac{Vb}{2\pi^2}(\Phi_{11} + \Phi_2\Phi_8) \end{bmatrix}, \quad (3.7)$$

$$Z_3 = \begin{bmatrix} 0 & \frac{2V^2}{b} & \frac{2V^2}{\pi b} \Phi_1 \\ 0 & 0 & \frac{V^2}{\pi} \Phi_5 \\ 0 & \frac{V^2}{\pi} \Phi_8 & \frac{V^2}{\pi^2} (\Phi_{10} + \Phi_1 \Phi_8) \end{bmatrix}, \quad (3.8)$$

and

$$Z_4 = \begin{bmatrix} \frac{-2V\alpha_1}{b} & \frac{-2V\alpha_2}{b} & 0 & 0 \\ 0 & 0 & 0 & 0 \\ 0 & 0 & \frac{-V\alpha_1}{b} & \frac{-V\alpha_2}{b} \end{bmatrix}. \quad (3.9)$$

The matrices Z_i , $i=1, 2, 3, 4$ are found by using the equation

$$\begin{bmatrix} -L(t) \\ -M(t) \\ -(T(t) + T_S(t)) \end{bmatrix} = -\pi\rho b^2 [Z_1\ddot{Y} + Z_2\dot{Y} + Z_3Y + Z_4x_A] \quad (3.10)$$

and moving all of the coefficients of \ddot{Y} into Z_1 , all of the coefficients of the \dot{Y} into Z_2 , all of the coefficients of Y into Z_3 , and all of the coefficients of x_A into Z_4 . Solving equation (3.5) for \ddot{Y} yields the second order system

$$\ddot{Y} = -[M' + \pi\rho b^2 Z_1]^{-1}[\pi\rho b^2 Z_2\dot{Y} + (K + \pi\rho b^2 Z_3)Y + \pi\rho b^2 Z_4x_A]. \quad (3.11)$$

This system yields the first six submatrices of the A matrix.

To find the elements of the last row of the A matrix, we augment the system by adding the equations in (2.36) to (3.11). From [8], the first order differential equation for the aerodynamic lag states are written as

$$\dot{x}_A = \begin{bmatrix} \dot{B}_1 \\ \dot{B}_2 \\ \dot{A}_1 \\ \dot{A}_2 \end{bmatrix} = \begin{bmatrix} \frac{-\beta_1 V}{b} & 0 & 0 & 0 \\ 0 & \frac{-\beta_2 V}{b} & 0 & 0 \\ 0 & 0 & \frac{-\beta_1 V}{b} & 0 \\ 0 & 0 & 0 & \frac{-\beta_2 V}{b} \end{bmatrix} \begin{bmatrix} B_1 \\ B_2 \\ A_1 \\ A_2 \end{bmatrix} + \begin{bmatrix} \dot{Q}_1 \\ \dot{Q}_1 \\ \dot{Q}_2 \\ \dot{Q}_2 \end{bmatrix}. \quad (3.12)$$

Equations (2.31) and (2.32) provide representations of $\dot{Q}_1(t)$ and $\dot{Q}_2(t)$ in terms of \ddot{Y} and \dot{Y} . In particular,

$$\dot{Q}_1 = [R_1 \ R_2 \ R_3] \begin{bmatrix} \frac{\ddot{h}}{b} \\ \ddot{\alpha} \\ \ddot{\beta} \end{bmatrix} + [0 \ R_4 \ R_5] \begin{bmatrix} \frac{\dot{h}}{b} \\ \dot{\alpha} \\ \dot{\beta} \end{bmatrix} \quad (3.13)$$

and

$$\dot{Q}_2 = [R_6 \ R_7 \ R_8] \begin{bmatrix} \frac{\ddot{h}}{b} \\ \ddot{\alpha} \\ \ddot{\beta} \end{bmatrix} + [0 \ R_9 \ R_{10}] \begin{bmatrix} \frac{\dot{h}}{b} \\ \dot{\alpha} \\ \dot{\beta} \end{bmatrix}, \quad (3.14)$$

respectively. We want to reduce \dot{Q}_1 and \dot{Q}_2 to first order equations. Use the representation of \ddot{Y} from equation (3.1) and substitute for \ddot{Y} in terms of \dot{Y} , Y , and x_A into equations (3.13) and (3.14) to obtain

$$\dot{Q}_1 = \begin{bmatrix} R_1 & R_2 & R_3 \end{bmatrix} \left\{ A_{11} \begin{bmatrix} \frac{\dot{h}}{b} \\ \dot{\alpha} \\ \dot{\beta} \end{bmatrix} + A_{12} \begin{bmatrix} \frac{h}{b} \\ \alpha \\ \beta \end{bmatrix} + A_{13} \begin{bmatrix} B_1 \\ B_2 \\ A_1 \\ A_2 \end{bmatrix} \right\} + \begin{bmatrix} 0 & R_4 & R_5 \end{bmatrix} \begin{bmatrix} \frac{\dot{h}}{b} \\ \dot{\alpha} \\ \dot{\beta} \end{bmatrix} \quad (3.15)$$

and

$$\dot{Q}_2 = \begin{bmatrix} R_6 & R_7 & R_8 \end{bmatrix} \left\{ A_{11} \begin{bmatrix} \frac{\dot{h}}{b} \\ \dot{\alpha} \\ \dot{\beta} \end{bmatrix} + A_{12} \begin{bmatrix} \frac{h}{b} \\ \alpha \\ \beta \end{bmatrix} + A_{13} \begin{bmatrix} B_1 \\ B_2 \\ A_1 \\ A_2 \end{bmatrix} \right\} + \begin{bmatrix} 0 & R_9 & R_{10} \end{bmatrix} \begin{bmatrix} \frac{\dot{h}}{b} \\ \dot{\alpha} \\ \dot{\beta} \end{bmatrix}. \quad (3.16)$$

$R_1 = \frac{b^2}{V}$	$R_6 = \frac{b^2}{\pi V} \Phi_8$
$R_2 = \frac{b^2}{V}$	$R_7 = \frac{b^3}{\pi V} \Phi_8$
$R_3 = \frac{b^2}{2\pi V}$	$R_8 = \frac{b^3}{2\pi^2 V} \Phi_2 \Phi_8$
$R_4 = V$	$R_9 = \frac{Vb}{\pi} \Phi_8$
$R_5 = \frac{V}{\pi} \Phi_1$	$R_{10} = \frac{Vb}{\pi^2} \Phi_1 \Phi_8$

Table 3.1: List of R_i 's

The R_i 's are listed in Table 3.1 and are found by comparing the \dot{Q}_i 's with the Q_i 's. Now, using equations (3.12), (3.15), and (3.16) collecting all of the \dot{Y} coefficients, Y coefficients, and x_A coefficients, we obtain the submatrices A_{31} , A_{32} , and A_{33} , respectively. Hence, the 10×10 A matrix in equation (3.1) is be constructed using the following submatrices:

$$A_{11} = -[M' + \pi \rho b^2 Z_1]^{-1} \pi \rho b^2 Z_2, \quad (3.17)$$

$$A_{12} = -[M' + \pi \rho b^2 Z_1]^{-1} (K + \pi \rho b^2 Z_3), \quad (3.18)$$

$$A_{13} = -[M' + \pi \rho b^2 Z_1]^{-1} \pi \rho b^2 Z_4, \quad (3.19)$$

$$A_{21} = [I_{3 \times 3}], \quad A_{22} = [0_{3 \times 3}], \quad A_{23} = [0_{3 \times 4}], \quad (3.20)$$

$$A_{31} = \begin{bmatrix} \begin{bmatrix} R_1 & R_2 & R_3 \end{bmatrix} A_{11} + \begin{bmatrix} 0 & R_4 & R_5 \end{bmatrix} \\ \begin{bmatrix} R_1 & R_2 & R_3 \end{bmatrix} A_{11} + \begin{bmatrix} 0 & R_4 & R_5 \end{bmatrix} \\ \begin{bmatrix} R_6 & R_7 & R_8 \end{bmatrix} A_{11} + \begin{bmatrix} 0 & R_9 & R_{10} \end{bmatrix} \\ \begin{bmatrix} R_6 & R_7 & R_8 \end{bmatrix} A_{11} + \begin{bmatrix} 0 & R_9 & R_{10} \end{bmatrix} \end{bmatrix}, \quad (3.21)$$

$$A_{32} = \begin{bmatrix} \begin{bmatrix} R_1 & R_2 & R_3 \\ R_1 & R_2 & R_3 \\ R_6 & R_7 & R_8 \\ R_6 & R_7 & R_8 \end{bmatrix} A_{12} \end{bmatrix}, \quad (3.22)$$

and

$$A_{33} = \begin{bmatrix} \begin{bmatrix} \frac{-\beta_1 V}{b} & 0 & 0 & 0 \\ 0 & \frac{-\beta_2 V}{b} & 0 & 0 \\ 0 & 0 & \frac{-\beta_1 V}{b} & 0 \\ 0 & 0 & 0 & \frac{-\beta_2 V}{b} \end{bmatrix} + \begin{bmatrix} \begin{bmatrix} R_1 & R_2 & R_3 \\ R_1 & R_2 & R_3 \\ R_6 & R_7 & R_8 \\ R_6 & R_7 & R_8 \end{bmatrix} A_{13} \end{bmatrix} \end{bmatrix} \quad (3.23)$$

where A_{11} is 3×3 , A_{12} is 3×3 , A_{13} is 3×4 , A_{31} is 4×3 , A_{32} is 4×3 , and A_{33} is 4×4 . The 10×1 input matrix B is given by

$$B = \frac{1}{I_\beta} \begin{bmatrix} (M')^{-1} \begin{bmatrix} 0 \\ 0 \\ 1 \end{bmatrix} \\ 0 \\ 0 \\ 0 \\ 0 \\ 0 \\ 0 \\ 0 \end{bmatrix}. \quad (3.24)$$

Chapter 4

Numerical Simulations

We now test the model to see if it behaves as a reasonable model of flutter. The constants used are listed in Table 4.1. The open loop system in equation (3.1) will be simulated using velocities of 950 feet/sec, 975.6 feet/sec, and 1000 feet/sec. The velocity $V_f = 975.6$ feet/sec is the flutter speed. The flutter speed is the speed at which the open loop system becomes marginally stable. In other words, the system is neither asymptotically stable nor unstable. We solved the systems on 5 second time intervals. The plunge, pitch, and flap angle will be graphed for all simulations. Also, we plot graphs of the plunge rate, pitch rate, flap rate, and aerodynamic lag states. However, we shall concentrate on the three degrees of freedom. The units of the plunge are feet and the units for the pitch and flap angle are radians (1 radian ≈ 57.3 degrees). The units of the plunge rate are feet/sec and the units of pitch rate and flap rate are radians/sec. The aerodynamic lag states are dimensionless.

α_1	=	.0165	
α_2	=	.335	
b	=	3	feet
β_1	=	.041	
β_2	=	.32	
c	=	1.0	
I_α	=	6.04868	$\frac{\text{slug-foot}^2}{\text{feet}}$
I_β	=	.151217	$\frac{\text{slug-foot}^2}{\text{feet}}$
K_α	=	$I_\alpha * 100^2$	
K_β	=	$I_\beta * 500^2$	
K_h	=	$m * 50^2$	
m	=	2.6883	slugs/feet
ρ	=	.002378	* 1
S_α	=	1.61298	* 1.0 slugs
S_β	=	.10081	* 1.0 slugs
V	=	950, 975.6, 1000	feet/sec
Vf	=	975.6	feet/sec

Table 4.1: List of Constants

4.1 Open Loop Simulations

Since A is a 10×10 matrix and x is a 10×1 column vector, the initial condition, x_0 is a 10×1 column vector. The following x_0 is used in these simulations:

$$x_0 = \begin{bmatrix} .05 \\ -.01 \\ .005 \\ -.1 \\ .001 \\ -.0001 \\ 0 \\ 0 \\ 0 \\ 0 \end{bmatrix}. \quad (4.1)$$

We analyze the stability of the system by looking at the eigenvalues of the system matrix A . The eigenvalues of an $n \times n$ matrix A are the roots of the characteristic polynomial

$$p(\lambda) = \det(A - \lambda I) \quad (4.2)$$

where I is the corresponding $n \times n$ identity matrix. If the real parts of all of the eigenvalues of A are negative, i.e., the eigenvalues are in the open left half plane, then the system $\dot{x}(t) = Ax(t)$ is asymptotically stable.

At $V = 950$ feet/sec, the plunge, pitch, flap angle, their respective velocities, and the aerodynamic lag states asymptotically approach zero as shown in Figures (4.1), (4.2), (4.3), and (4.4). At $t = 2$ seconds, almost all oscillations have disappeared. The eigenvalues of this system are given in Table 4.2. Note that for $V = 950$ feet/sec the real parts of the eigenvalues are negative.

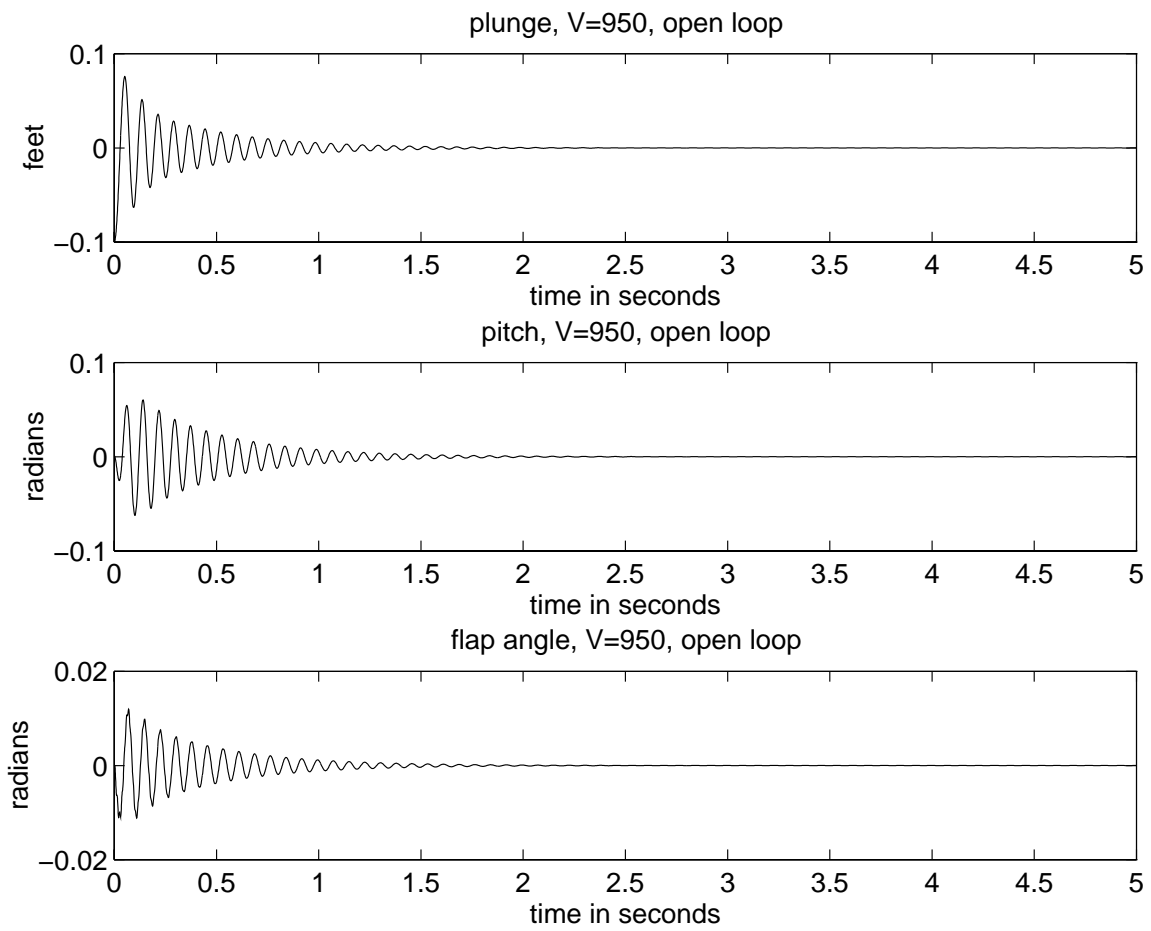


Figure 4.1: The plunge, pitch, and flap angle for the open loop system: Stable, $V=950$.

λ_1	$=$	$-6.20 + 563.58i$
λ_2	$=$	$-6.20 - 563.58i$
λ_3	$=$	$-2.34 + 81.63i$
λ_4	$=$	$-2.34 - 81.63i$
λ_5	$=$	$-17.84 + 66.81i$
λ_6	$=$	$-17.84 - 66.81i$
λ_7	$=$	-93.18
λ_8	$=$	-12.98
λ_9	$=$	-101.33
λ_{10}	$=$	-12.98

Table 4.2: Eigenvalues of open loop system for $V = 950$.

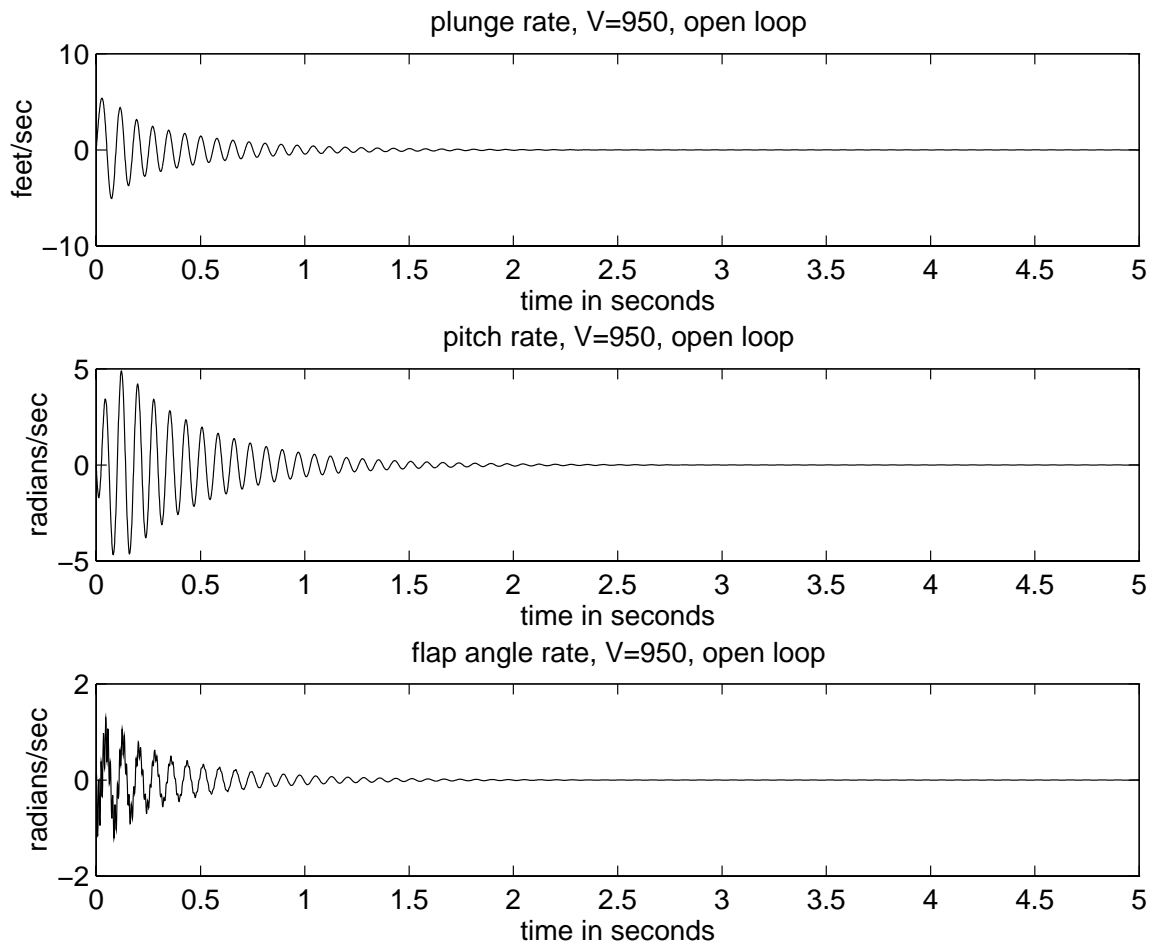


Figure 4.2: The velocities of the plunge, pitch, and flap angle for the open loop system: Stable, $V=950$.

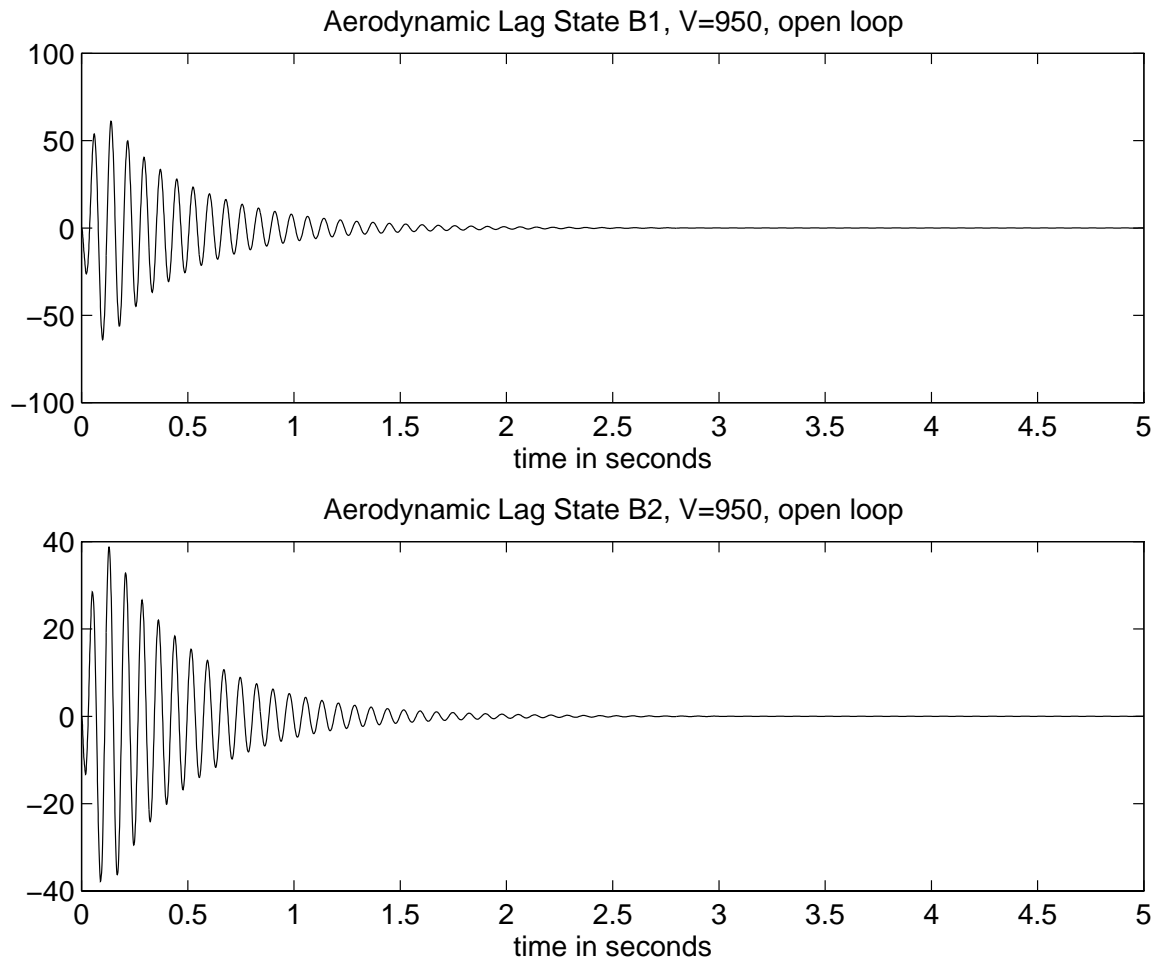


Figure 4.3: The aerodynamic lag states B_1 and B_2 for the open loop system: Stable, $V=950$.

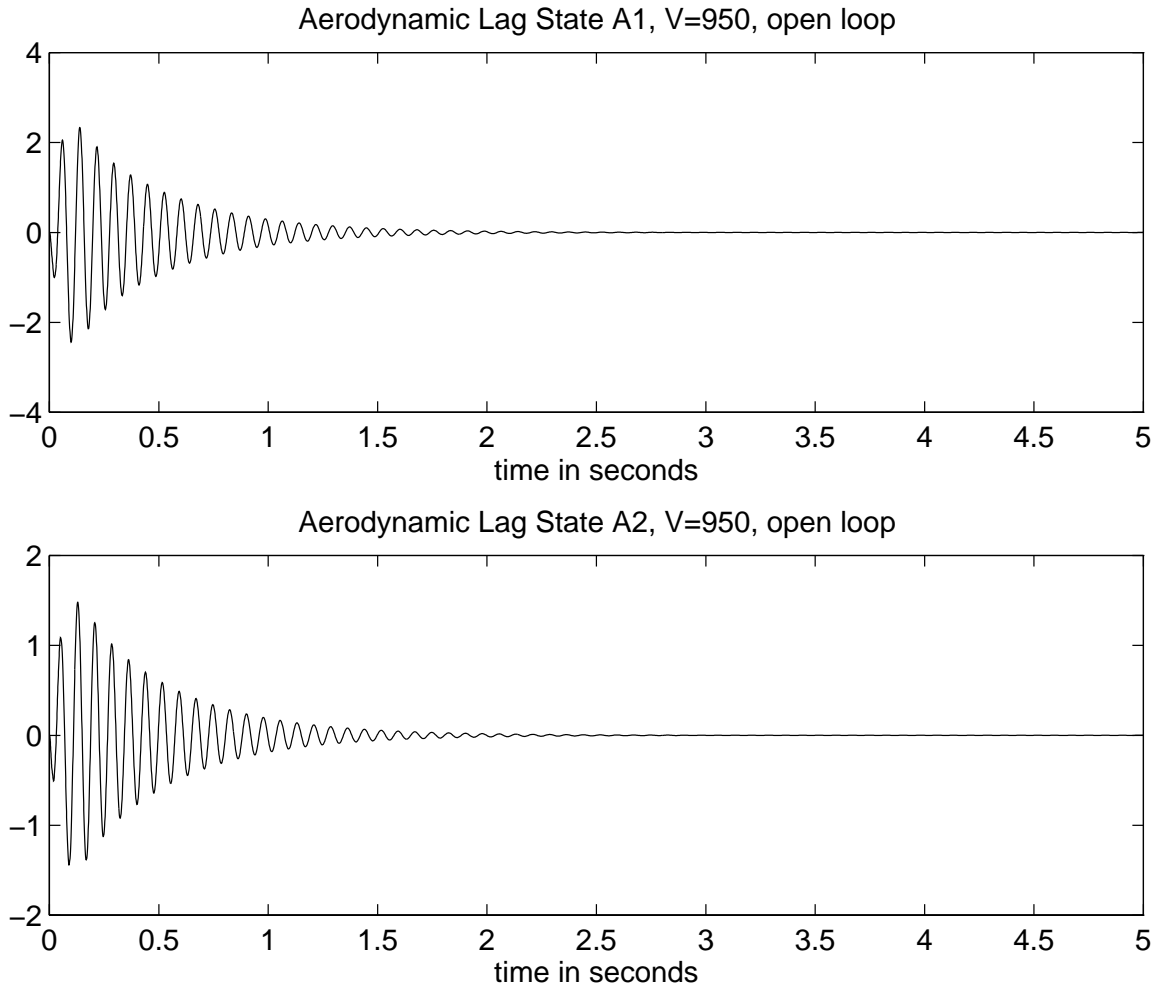


Figure 4.4: The aerodynamic lag states A_1 and A_2 for the open loop system: Stable, $V=950$.

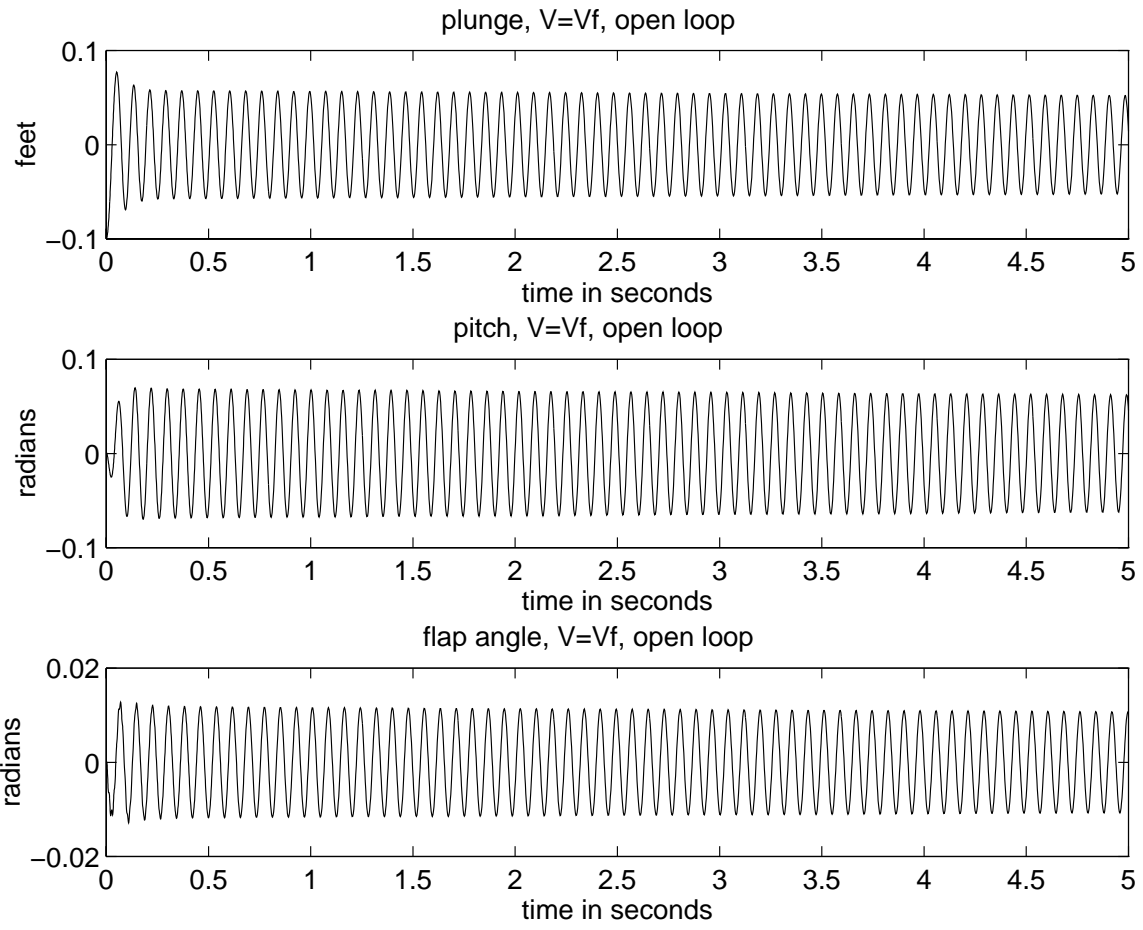


Figure 4.5: The plunge, pitch, and flap angle for the open loop system: Marginally stable, $V=V_f$.

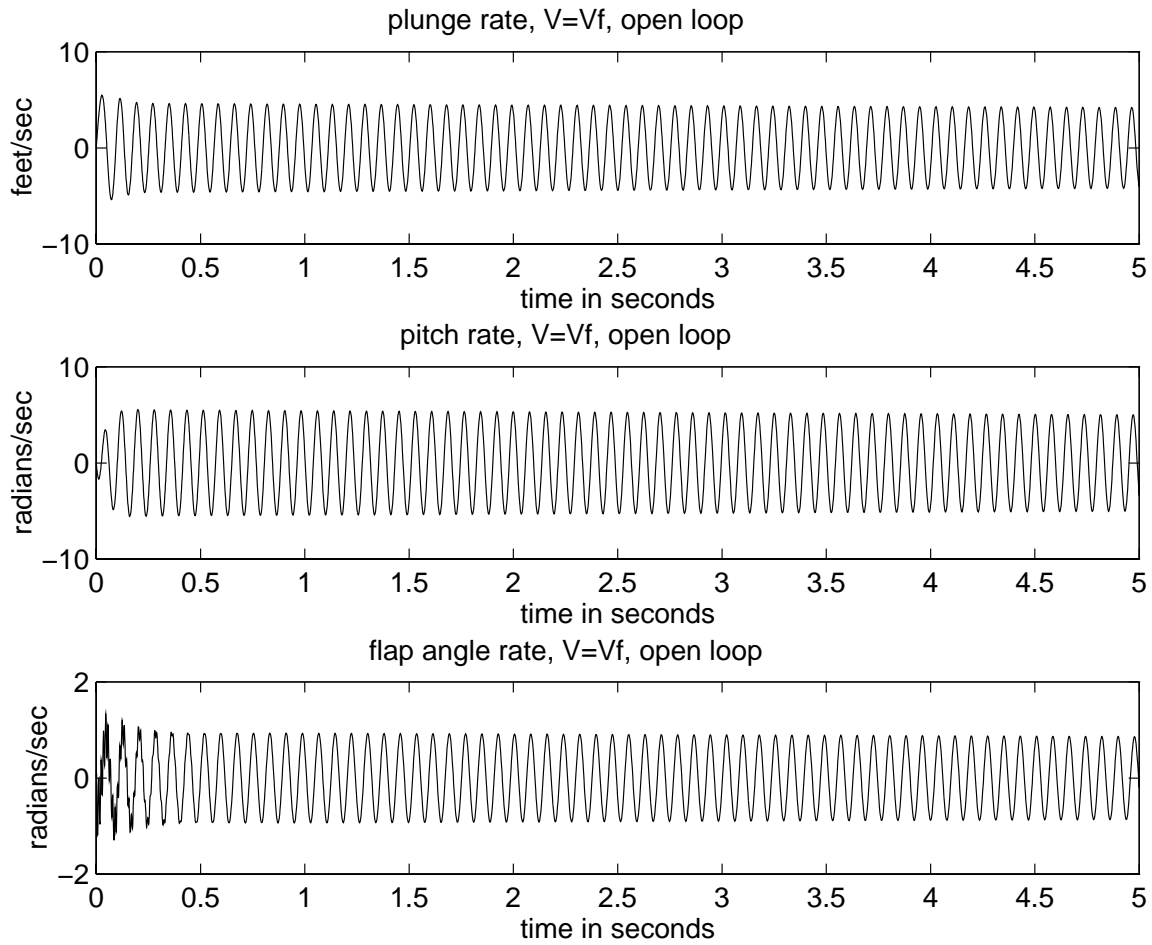


Figure 4.6: The velocities of the plunge, pitch, and flap angle for the open loop system: Marginally Stable, $V=V_f$.

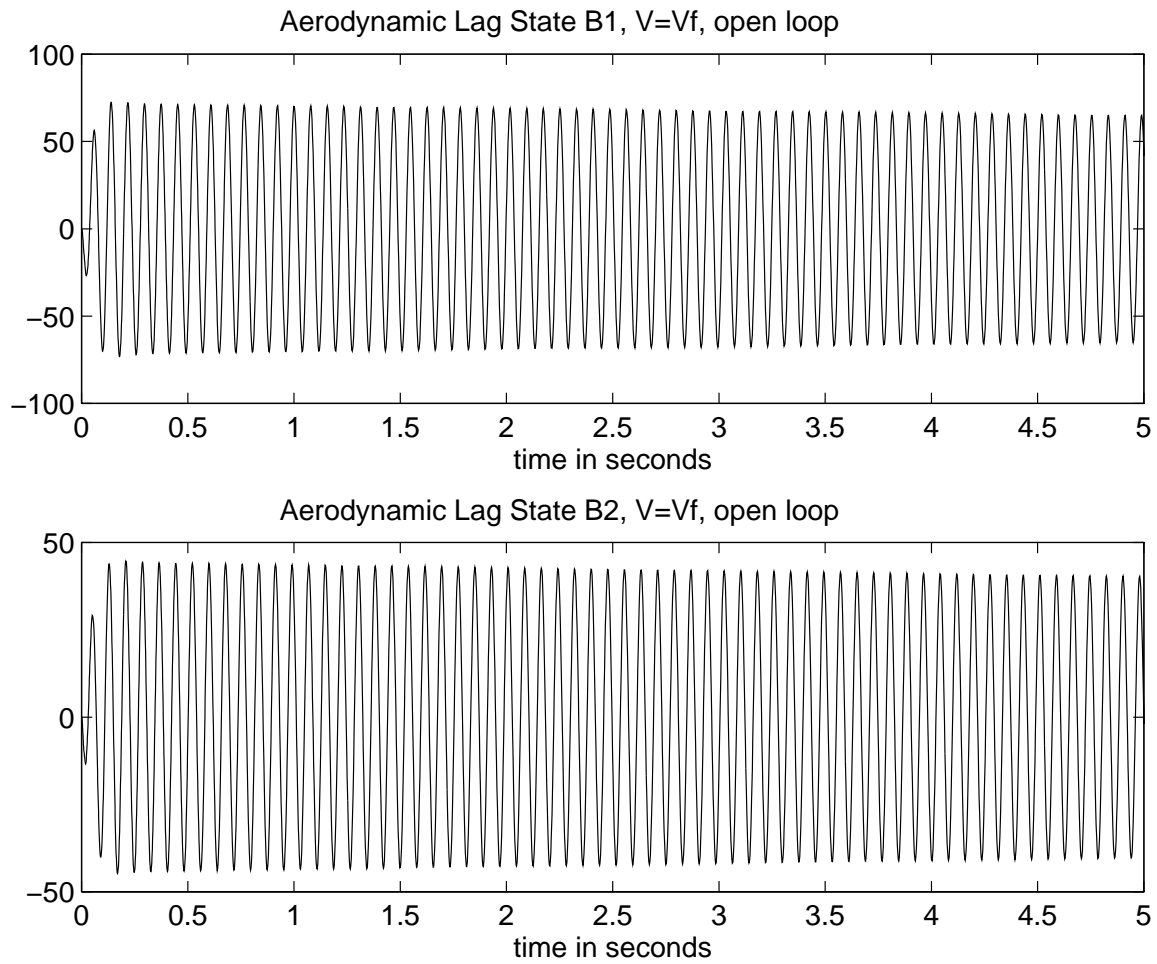


Figure 4.7: The aerodynamic lag states B_1 and B_2 for the open loop system: Marginally Stable, $V=V_f$.

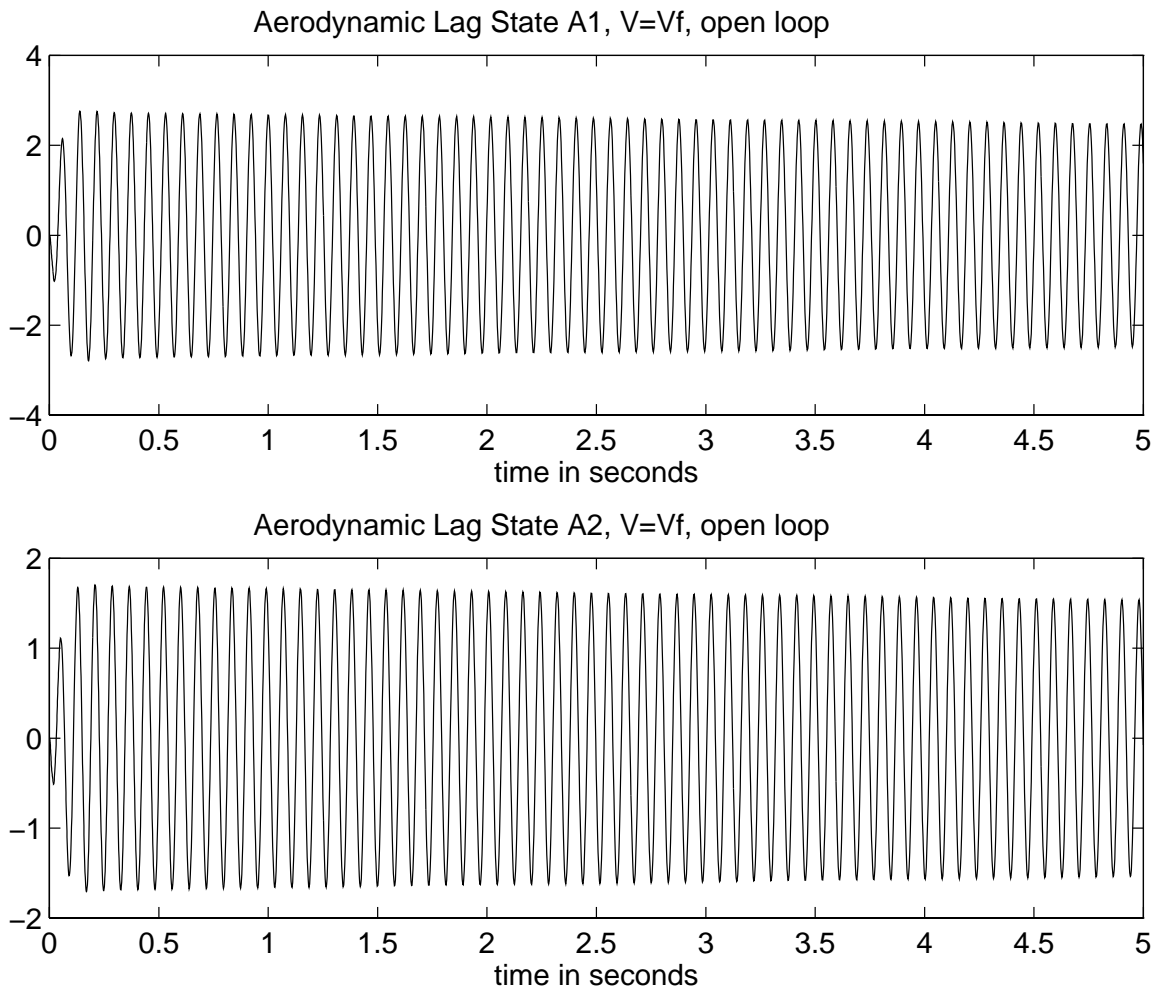


Figure 4.8: The aerodynamic lag states A_1 and A_2 for the open loop system: Marginally Stable, $V=V_f$.

At $V = Vf = 975.6$ feet/sec, the plunge, pitch, flap angle, their respective derivatives, and the aerodynamic lag states all settle into harmonic oscillations as shown in Figures (4.5), (4.6), (4.7), and (4.8). After about .5 seconds, the plunge oscillates between -.075 feet and .075 feet and the pitch oscillates between -.075 and .075 radians. The flap angle settles into oscillations between $\pm .01$ radians. This means that the plunge, pitch, and flap angle oscillate at this constant rate as long as the airplane is flown at this speed. These oscillations never disappear since the system is marginally stable. The eigenvalues of the system, shown in Table 4.3, are all in the open left half plane. However, λ_3 and λ_4 have zero real parts.

λ_1	=	$-6.38 + 563.35i$
λ_2	=	$-6.38 - 563.35i$
λ_3	=	$0.00 + 80.33i$
λ_4	=	$0.00 - 80.33i$
λ_5	=	$-20.92 + 67.37i$
λ_6	=	$-20.92 - 67.37i$
λ_7	=	-95.19
λ_8	=	-13.32
λ_9	=	-104.04
λ_{10}	=	-13.33

Table 4.3: Eigenvalues of open loop system for $V=Vf=975.6$.

At $V = 1000$ feet/sec, a velocity above the flutter speed, the plunge, pitch, flap angle, their respective velocities, and the aerodynamic lag states continue to increase without bound with increasing time as shown in Figures (4.9), (4.10), (4.11), and (4.12). After about 4 seconds, the plunge of the wing is oscillating at an amplitude of about 500 feet. The pitch grows to an amplitude of about 500 radians and the flap angle has an amplitude of about 175 radians. Clearly, the model is no longer valid and in a real system, the airfoil would have become unstable and wing separation would have occurred. In Table 4.4, we see that λ_3 and λ_4 have moved to the right half plane.

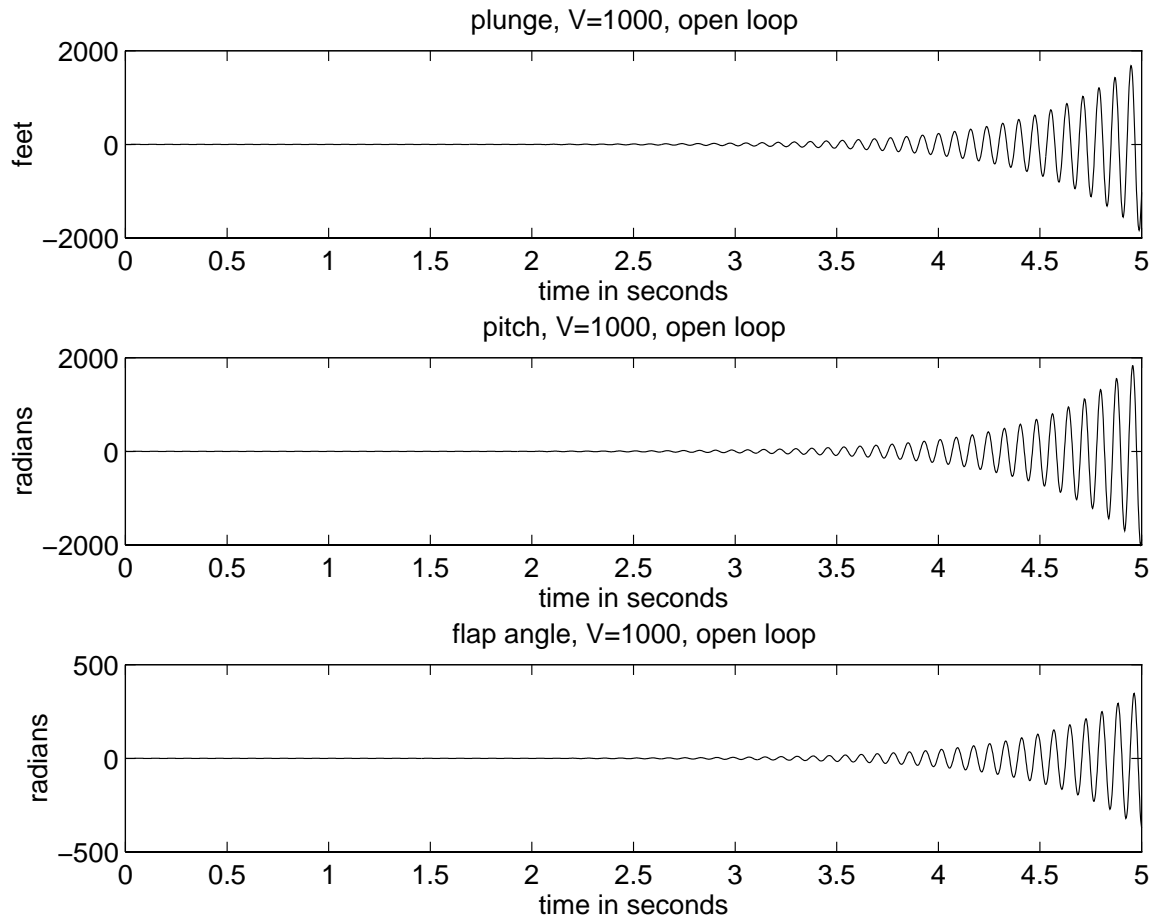


Figure 4.9: The plunge, pitch, and flap angle for the open loop system: Unstable, $V=1000$.

λ_1	$=$	$-6.56 + 563.13i$
λ_2	$=$	$-6.56 - 563.13i$
λ_3	$=$	$2.09 + 79.61i$
λ_4	$=$	$2.09 - 79.61i$
λ_5	$=$	$-23.78 + 67.33i$
λ_6	$=$	$-23.78 - 67.33i$
λ_7	$=$	-97.10
λ_8	$=$	-13.66
λ_9	$=$	-106.67
λ_{10}	$=$	-13.67

Table 4.4: Eigenvalues of open loop system for $V=1000$.

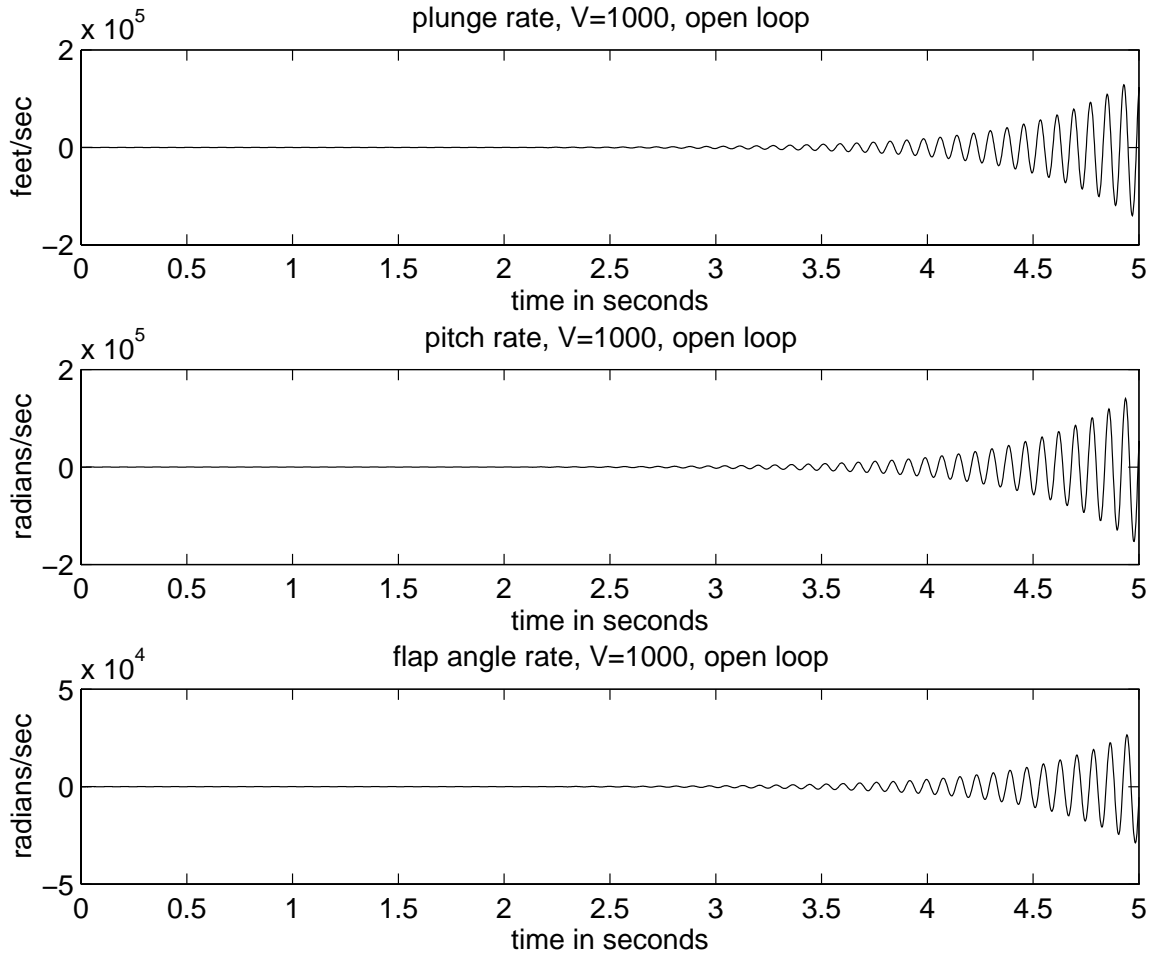


Figure 4.10: The velocities of the plunge, pitch, and flap angle for the open loop system: Unstable, $V=1000$.

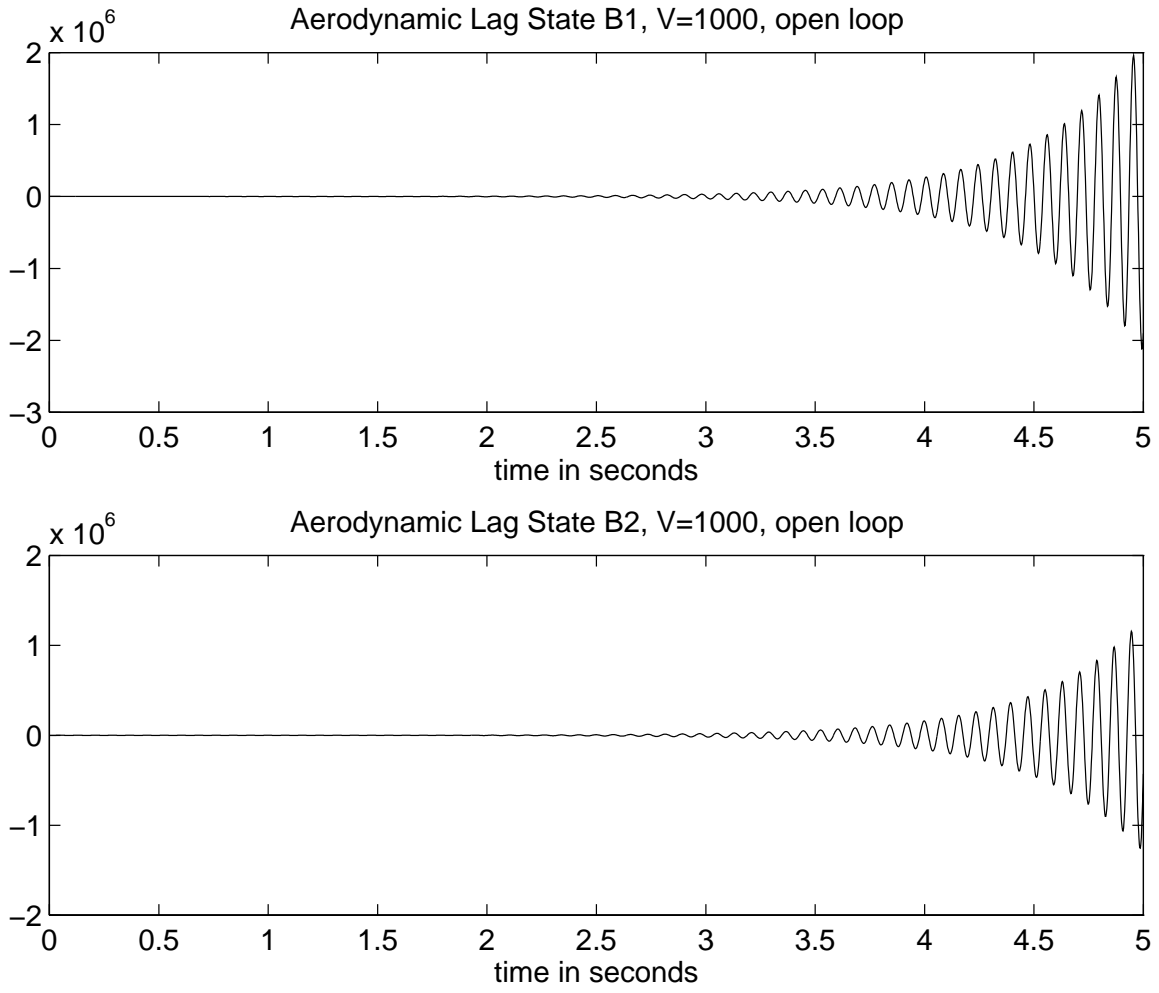


Figure 4.11: The aerodynamic lag states B_1 and B_2 for the open loop system: Unstable, $V=1000$.

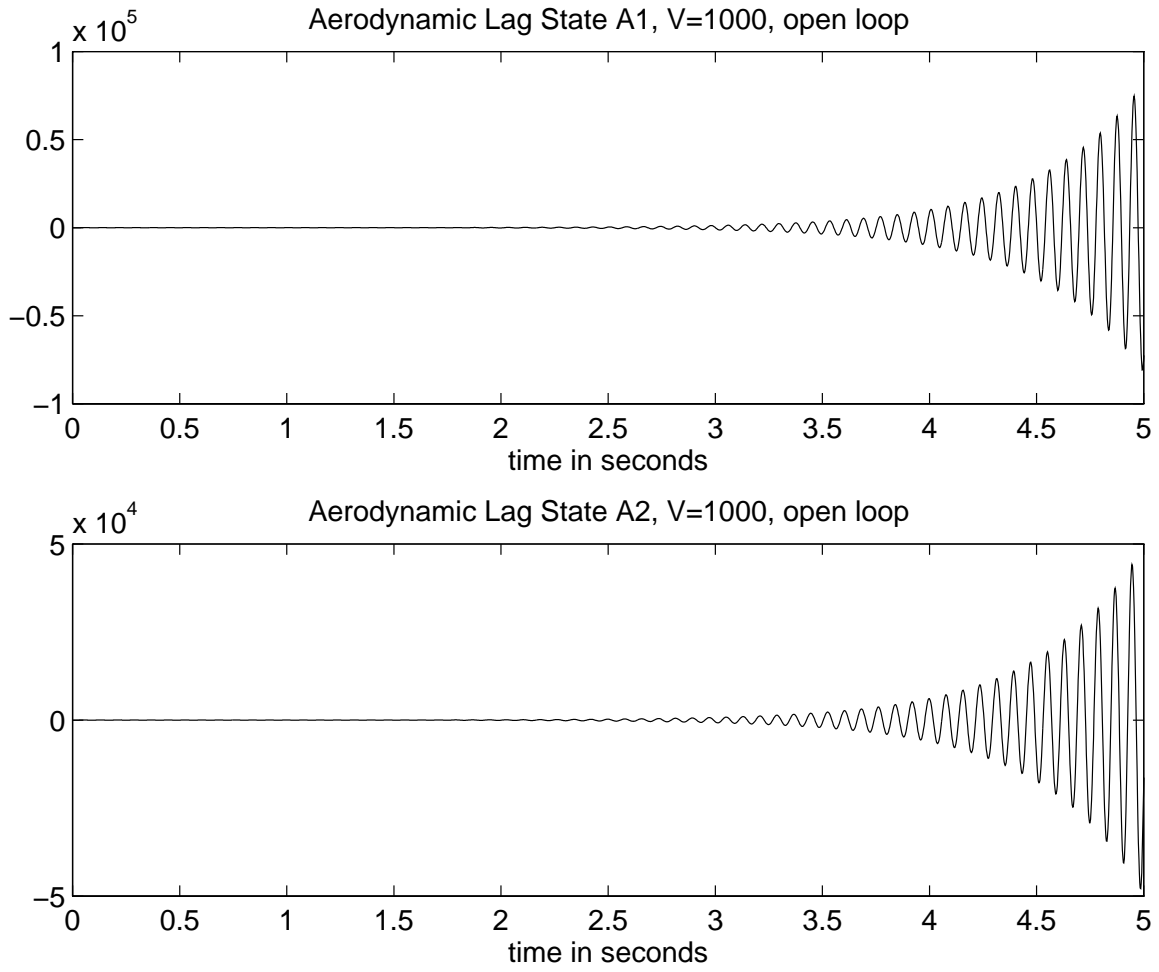


Figure 4.12: The aerodynamic lag states A_1 and A_2 for the open loop system: Unstable, $V=1000$.

Chapter 5

The LQR Problem

In this chapter, the optimal Linear Quadratic Regulator control is discussed and applied to the flutter suppression problem. If $V > V_f = 975.6$ feet/sec, then the airfoil is unstable. In this case, the objective is to find a control function $u(t)$ on $[0, \infty]$ to stabilize the system. From [11], a system is stabilizable if there exists a state feedback control $u = K_c x$ such that the closed loop system is exponentially stable. If the system is stabilizable, then the LQR problem has a solution.

The idea of feedback control is simple. Take the state, multiply it by a gain matrix denoted by K_c , and add it back to the system. In particular, given the system,

$$\dot{x}(t) = Ax(t) + Bu(t) \tag{5.1}$$

we want to find the control input

$$u(t) = -K_c x(t) \tag{5.2}$$

such that the closed loop system

$$\dot{x}(t) = [A - BK_c]x(t) \tag{5.3}$$

is exponentially stable. This means that there exists an $M > 0$ and a $\gamma > 0$ such that if $x(t)$ is the solution to the closed loop system with $x(0) = x_0$, then

$$\|x(t)\| \leq Me^{-\gamma t} \|x_0\|. \tag{5.4}$$

If such a K_c exists, then (5.1) is said to be stabilizable.

5.1 LQR Control

One way of finding K_c is by using Linear-Quadratic Regulator (LQR) design. We will state our problem as follows.

Consider the system

$$\dot{x}(t) = Ax(t) + Bu(t), \quad x(0) = x_0. \quad (5.5)$$

We seek a control $u^*(t)$ that minimizes the performance measure

$$\min_u J = \int_0^\infty \{\langle Qx(t), x(t) \rangle + \langle Ru(t), u(t) \rangle\} dt \quad (5.6)$$

where $x(t)$ is the solution of (5.5). Here $Q = Q^T \geq 0$ and $R = R^T > 0$ are weighting matrices. It is well known that if an optimal control $u^*(t)$ exists, it has the form

$$u^*(t) = -K_c x(t), \quad (5.7)$$

where K_c is a constant gain matrix. Moreover, the closed loop system

$$\dot{x}(t) = Ax(t) - BK_c x(t) = (A - BK_c)x(t) \quad (5.8)$$

is stable. The assumption that $R > 0$ ensures that the energy of the control is finite. The following result may be found in Dorato, Abdallah, and Cerone (see [3], p.21 and 23).

Existence and Stability of the Steady-State LQR Solution: Given the LQR problem with $R > 0$, and $Q = C^T C$, where the pair (A, C) is detectable and the pair (A, B) is stabilizable, it follows that a solution to the steady-state LQR problem exists. In particular, there exists a unique positive semidefinite solution \bar{P} to the algebraic Riccati equation

$$0 = A^T P + PA + Q - PBR^{-1}B^T P, \quad (5.9)$$

and if

$$K_c = R^{-1}B^T \bar{P}, \quad (5.10)$$

then the closed loop system (5.8) is asymptotically stable.

In order to apply this result, we need to show that the system is stabilizable and that (A, C) is detectable. Since $C = Q = I$, it follows that for any velocity V , (A, C) is detectable. If $V < Vf$, then the open loop system is stable, hence (A, B) is stabilizable with $K = [0_{10 \times 1}]$. The only case that needs attention is the problem of stabilizability for velocities $V \geq Vf$.

The pair (A, B) is stabilizable if there exists a state feedback control $u = -K_V x$ at a specific V such that $(A - BK_V)$ is stable. This means that there exists a gain matrix K_V so that the eigenvalues of $(A - BK_V)$ have negative real parts. For $V = 1000$ feet/sec $> Vf$ and the parameters listed in Table 4.1, let

$$K_V = \begin{bmatrix} 9.8 & -39.9 & -1.6 & -1279.7 & -804 & -650.2 & .1 & .9 & 0 & .1 \end{bmatrix}. \quad (5.11)$$

λ_1	=	-44.61 + 563.47i
λ_2	=	-44.61 - 563.47i
λ_3	=	-2.77 + 79.33i
λ_4	=	-2.77 - 79.33i
λ_5	=	-23.93 + 67.29i
λ_6	=	-23.93 - 67.29i
λ_7	=	-96.99
λ_8	=	-13.66
λ_9	=	-106.67
λ_{10}	=	-13.67

Table 5.1: Eigenvalues of $(A - BK_V)$: $V=1000$.

From Table 5.1, we see the eigenvalues of $(A - BK_V)$ have negative real parts. Hence, the pair (A, B) is stabilizable. For $V = Vf = 975.6$ feet/sec let

$$K_V = \begin{bmatrix} .547 & -1.5529 & .6858 & -38.6409 & -39.4681 & -27.4179 & .0017 & .0349 & .0001 & .0173 \end{bmatrix}. \quad (5.12)$$

λ_1	=	-29.05 + 562.64i
λ_2	=	-29.05 - 562.64i
λ_3	=	-.15 + 80.32i
λ_4	=	-.15 - 80.32i
λ_5	=	-20.95 + 67.37i
λ_6	=	-20.95 - 67.37i
λ_7	=	-95.2
λ_8	=	-13.33
λ_9	=	-104.06
λ_{10}	=	-13.33

Table 5.2: Eigenvalues of $(A - BK_V)$: $V=Vf=975.6$.

Again, we see from Table 5.2 that $(A - BK_V)$ is a stable matrix and (A, B) is stabilizable.

For $V = Vf$ and $V = 1000$ feet/sec, we now know that an optimal controller exists. If P is the positive definite solution of the algebraic Riccati equation

$$0 = A^T P + PA + Q - PBR^{-1}B^T P, \quad (5.13)$$

then define

$$K_c = R^{-1}B^T P. \quad (5.14)$$

If $u(t)$ is given as

$$u(t) = -K_c x(t), \quad (5.15)$$

then the closed loop system has the form

$$\dot{x}(t) = (A - BK_c) x(t). \quad (5.16)$$

5.2 Closed Loop Simulations: Control Initiated at $t=0$

We now turn to the closed loop simulations for the velocities $V = 950$ feet/sec, $V = Vf = 975.6$ feet/sec, and $V = 1000$ feet/sec. The constants used will be the same as the ones used for the open loop system in Chapter 4. For $V = 950$ feet/sec, the open loop system is stable. In Figures (5.1)-(5.4) the performance of the closed loop system is comparable to that of the open loop system. The controlled system dampens oscillations slightly faster than does the uncontrolled system. For $V = Vf = 975.6$ feet/sec, the open loop system is marginally stable. The closed loop system shown in Figures (5.5)-(5.8) is asymptotically stable. The performance is better in the controlled system. For $V = 1000$ feet/sec, the open loop system is unstable. The closed loop system shown in Figures (5.9)-(5.12) is again asymptotically stable. Much better performance is obtained using the LQR controller than using the open loop system. As shown in Figure (5.1), Figure (5.5), and Figure (5.9), the pitch, plunge, and flap angle asymptotically approach zero by 1.5 seconds. The velocities of the pitch, plunge, and flap angle and the aerodynamic lag states also asymptotically approach zero. Notice the small spikes near $t = 0$ seconds in the graphs of the flap angle and flap angle rate for all three velocities. This motion indicates that the controller requires fast responses. However, the systems are stabilized in about 1.5 seconds. Clearly, the LQR control performs well and since it uses full state feedback, it is robust. The eigenvalues for the closed loop system at the various velocities are found in Table 5.3, Table 5.4, and Table 5.5. They show that the closed loop system is stable at each of these velocities.

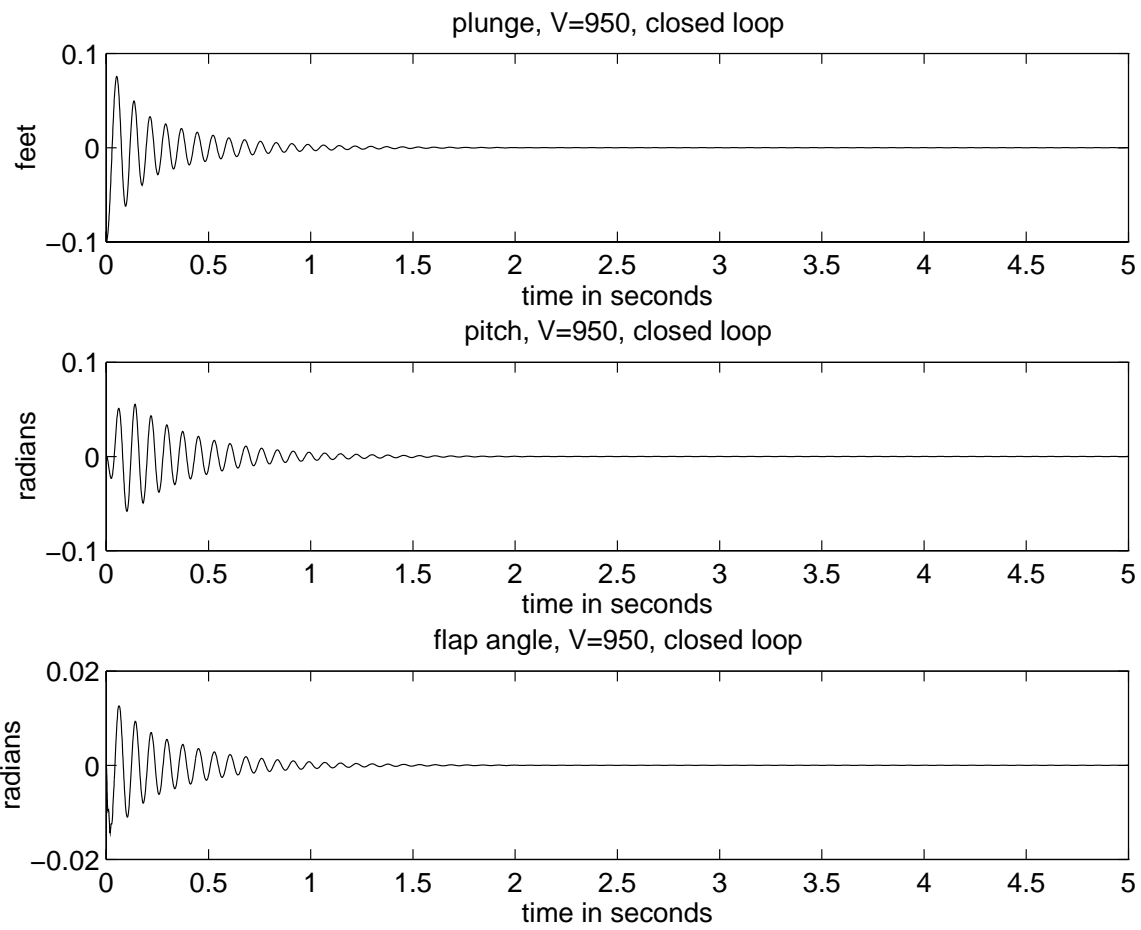


Figure 5.1: The plunge, pitch, and flap angle for the closed loop system: Stable, $V=950$.

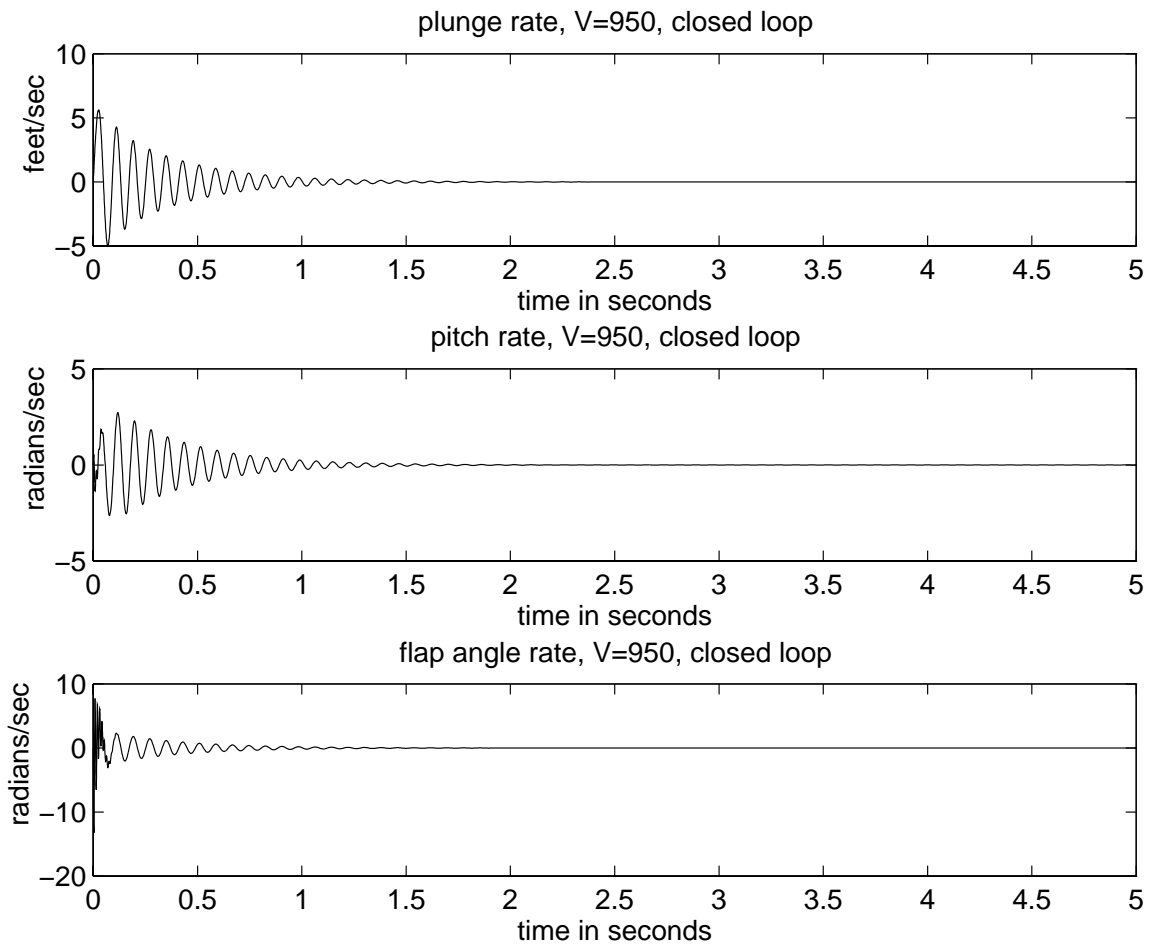


Figure 5.2: The velocities of the plunge, pitch, and flap angle for the closed loop system: Stable, $V=950$.

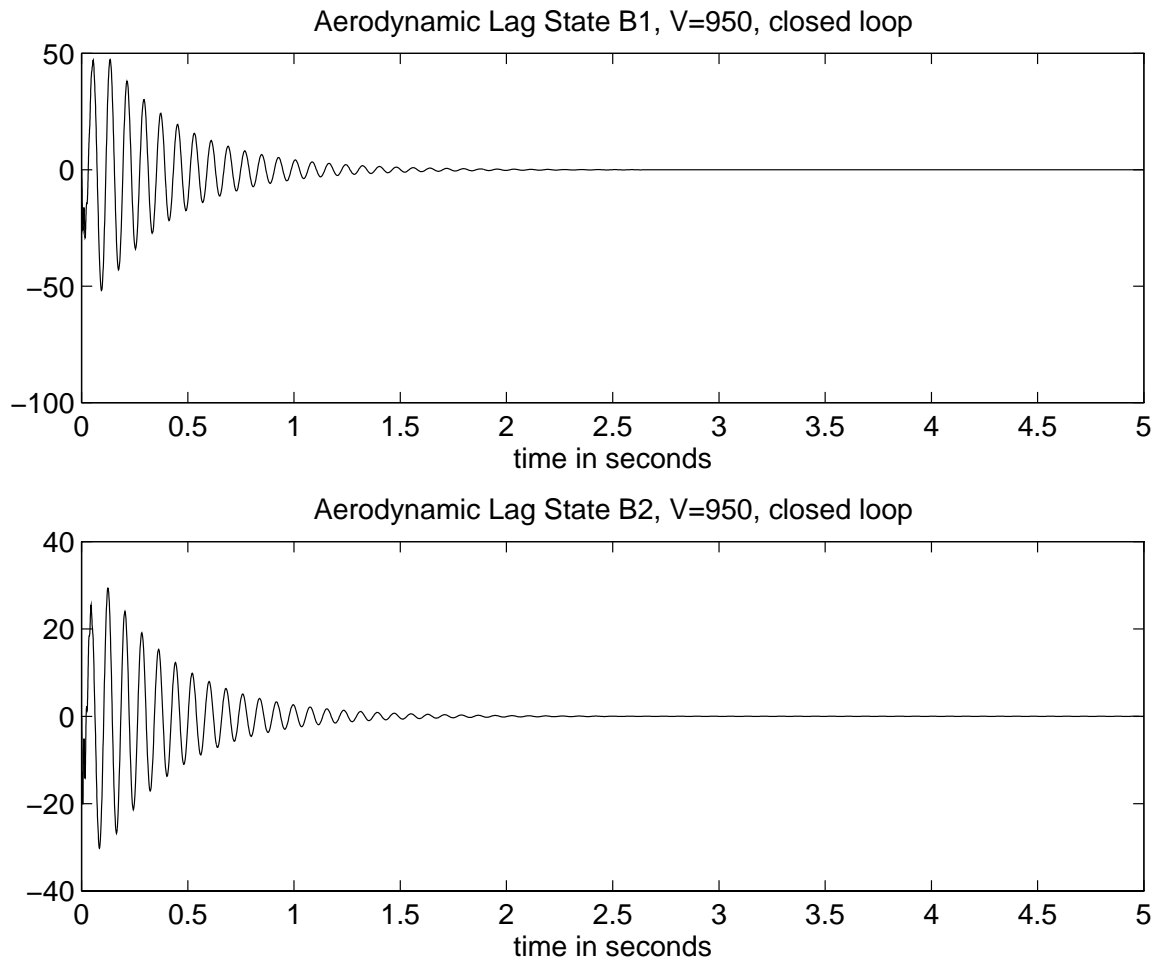


Figure 5.3: The aerodynamic lag states B_1 and B_2 for the closed loop system: Stable, $V=950$.

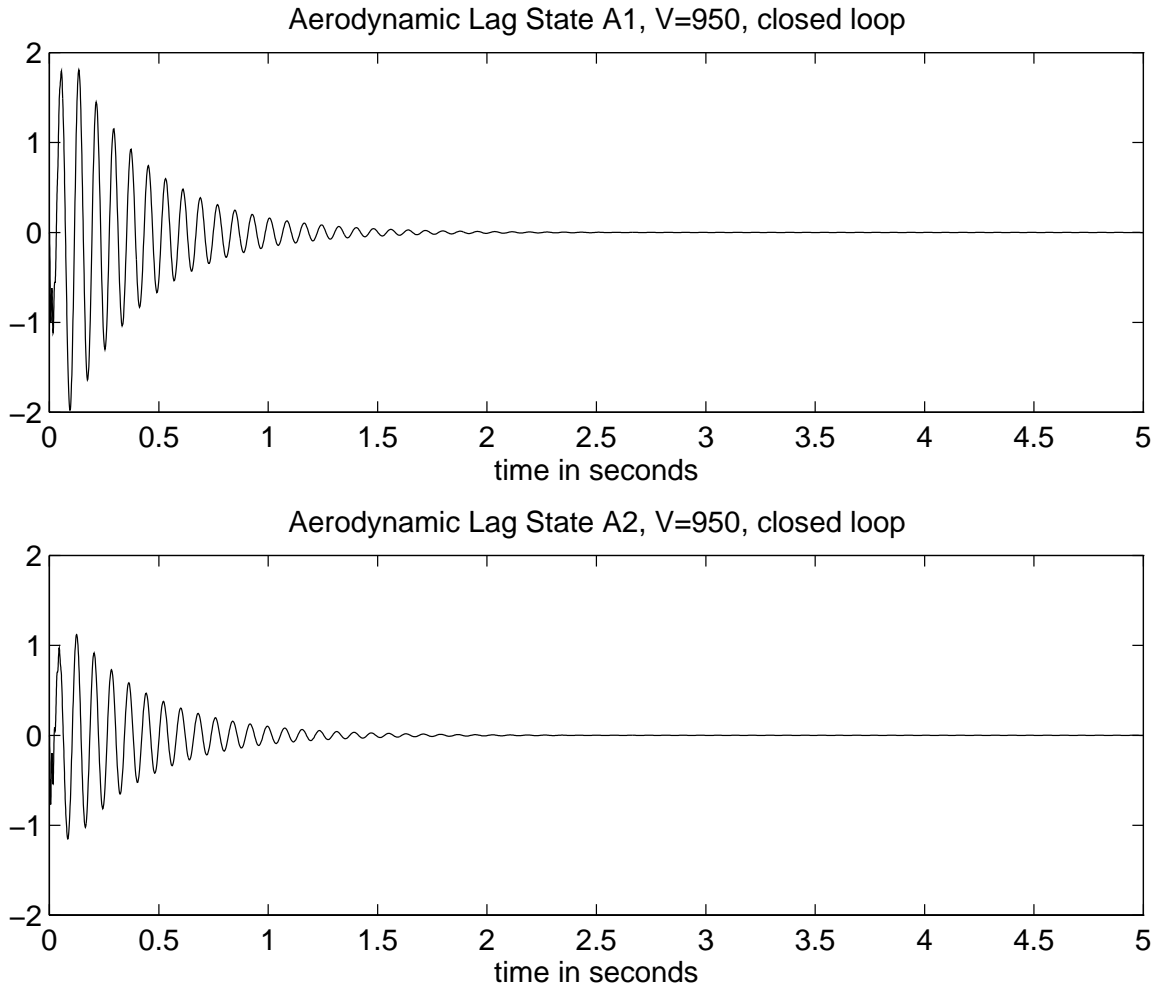


Figure 5.4: The aerodynamic lag states A_1 and A_2 for the closed loop system: Stable, $V=950$.

λ_1	=	$-45.47 + 563.84i$
λ_2	=	$-45.47 - 563.84i$
λ_3	=	$-2.87 + 81.37i$
λ_4	=	$-2.87 - 81.37i$
λ_5	=	$-17.95 + 66.78i$
λ_6	=	$-17.95 - 66.78i$
λ_7	=	-93.06
λ_8	=	-12.98
λ_9	=	-101.33
λ_{10}	=	-12.98

Table 5.3: Eigenvalues of closed loop system for $V=950$.

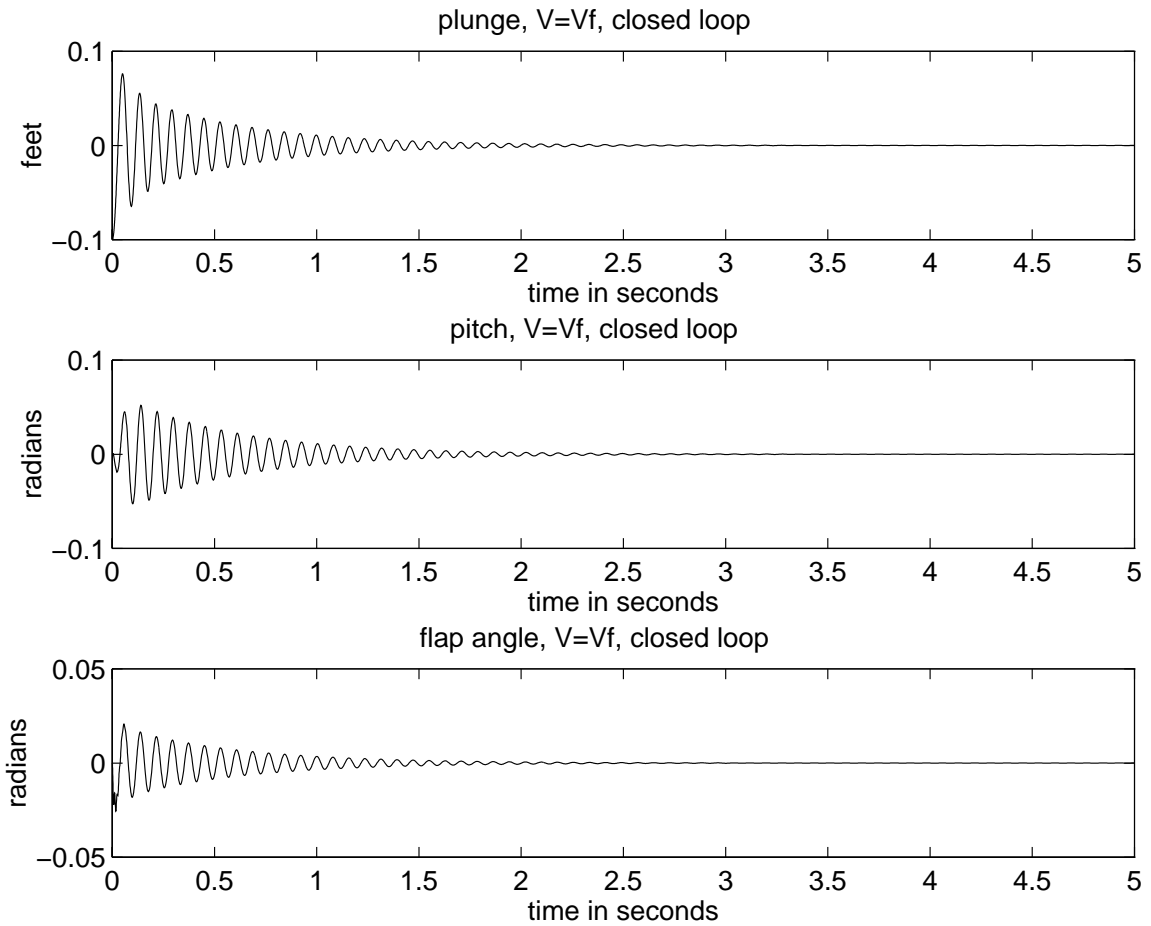


Figure 5.5: The plunge, pitch, and flap angle for the closed loop system: Stable, $V=V_f$.

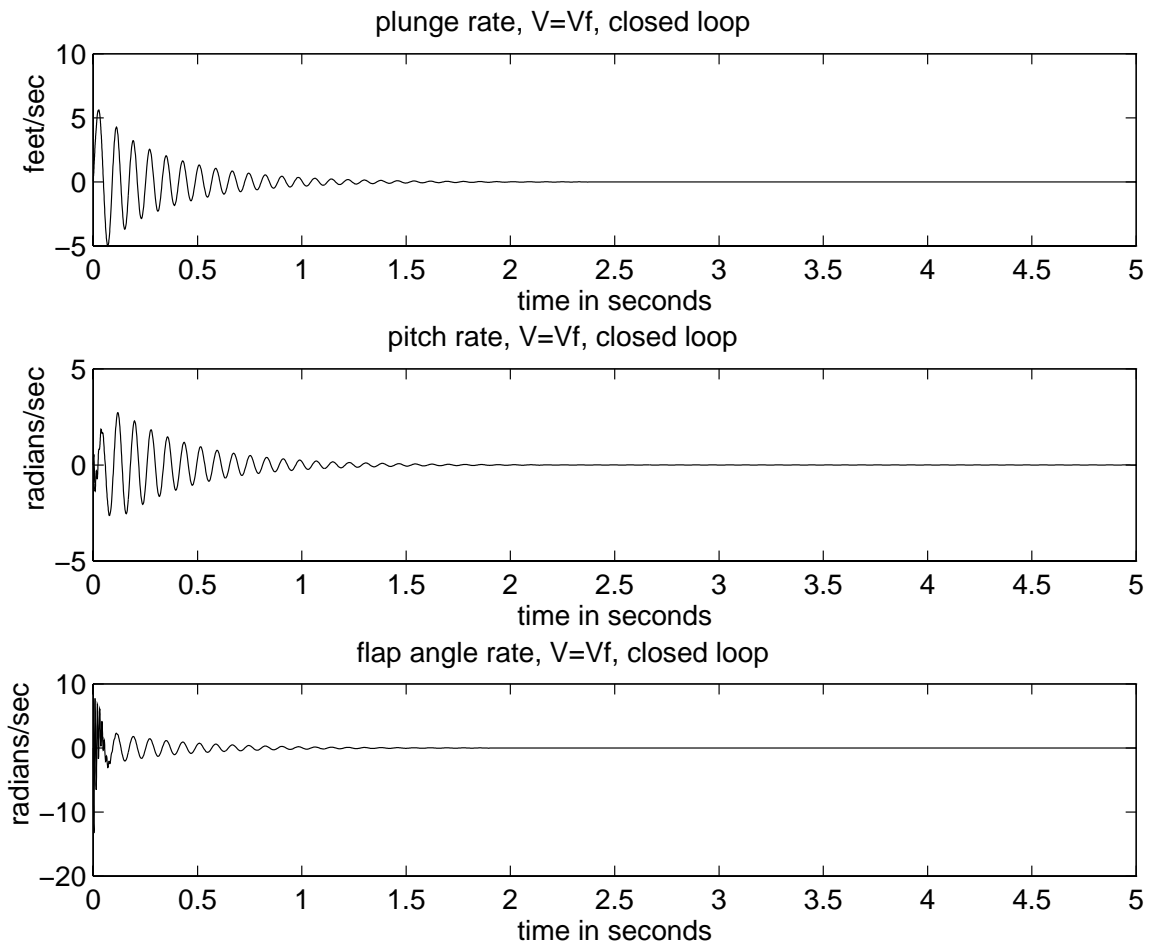


Figure 5.6: The velocities of the plunge, pitch, and flap angle for the closed loop system: Stable, $V=V_f$.

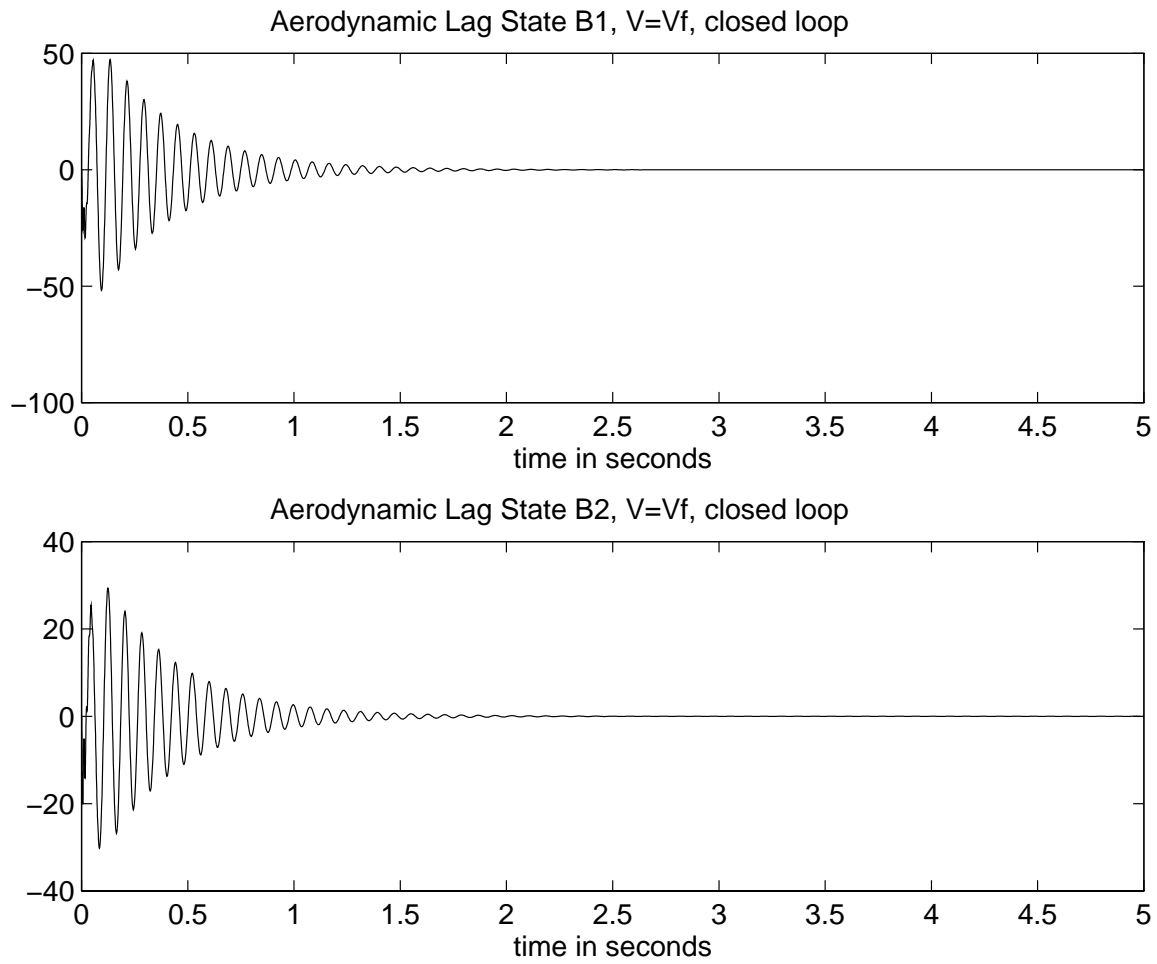


Figure 5.7: The aerodynamic lag states B_1 and B_2 for the closed loop system: Stable, $V=V_f$.

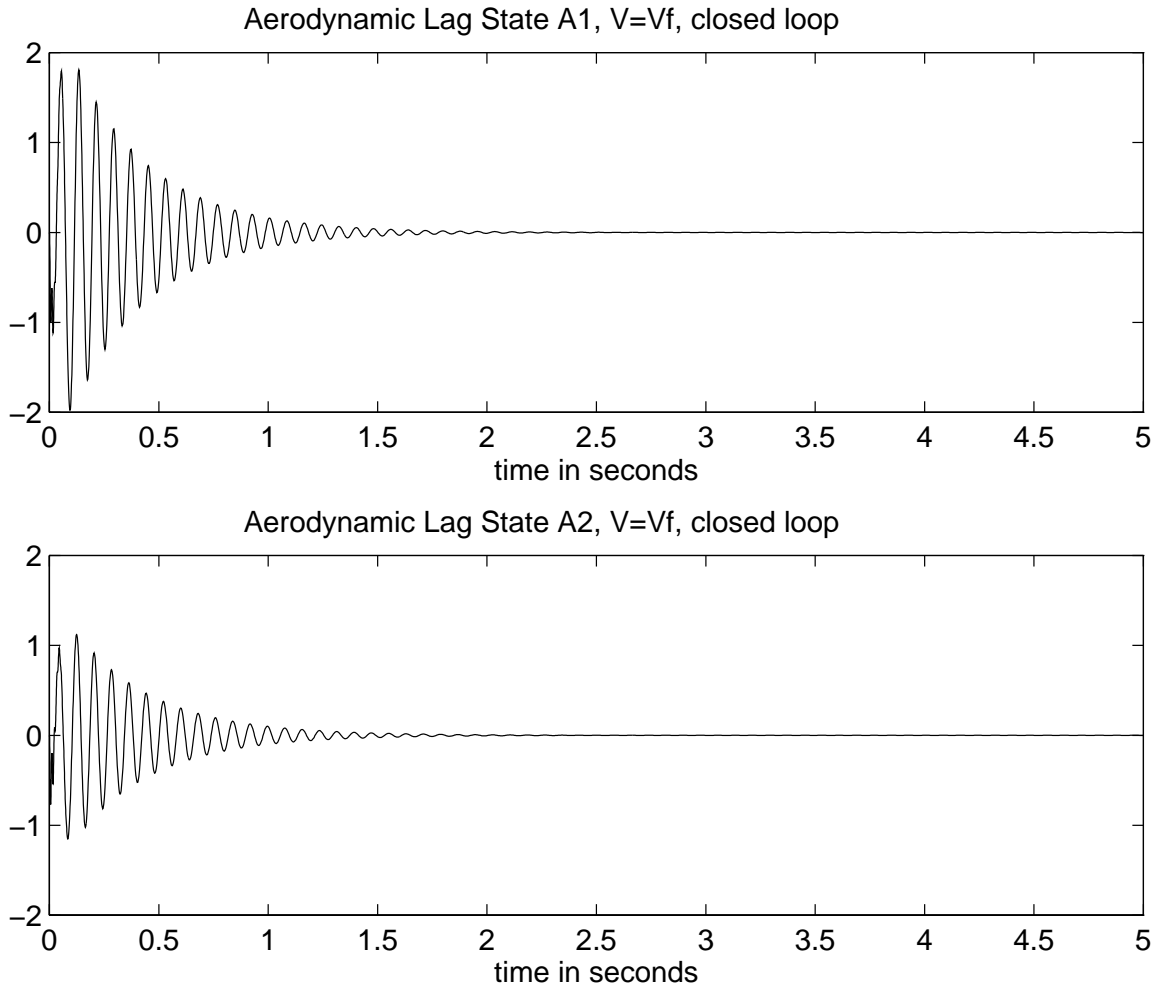


Figure 5.8: The aerodynamic lag states A_1 and A_2 for the closed loop system: Stable, $V=V_f$.

λ_1	=	$-45.02 + 563.66i$
λ_2	=	$-45.02 - 563.66i$
λ_3	=	$-1.75 + 80.07i$
λ_4	=	$-1.75 - 80.07i$
λ_5	=	$-21.06 + 67.33i$
λ_6	=	$-21.06 - 67.33i$
λ_7	=	-95.07
λ_8	=	-13.32
λ_9	=	-104.04
λ_{10}	=	-13.33

Table 5.4: Eigenvalues of closed loop system for $V=V_f=975.6$.

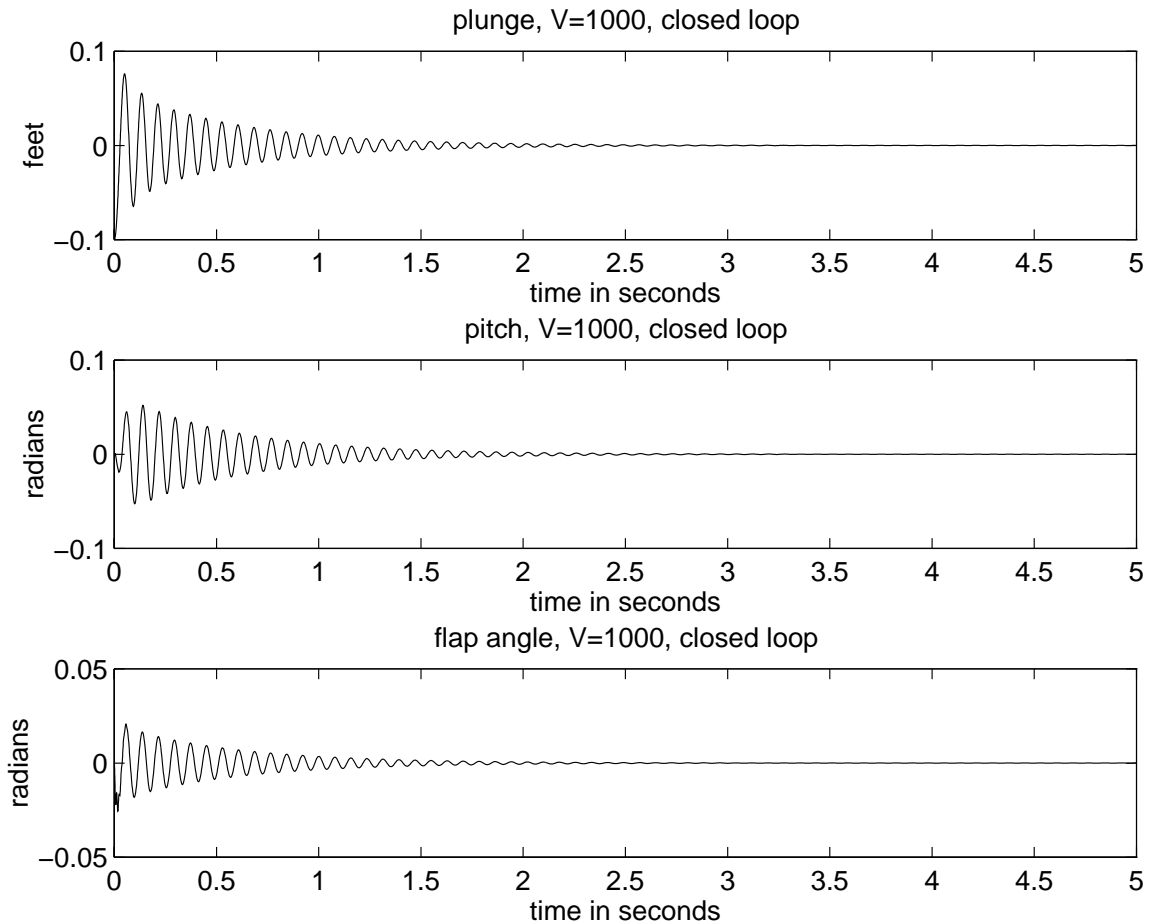


Figure 5.9: The plunge, pitch, and flap angle for the closed loop system: Stable, $V=1000$.

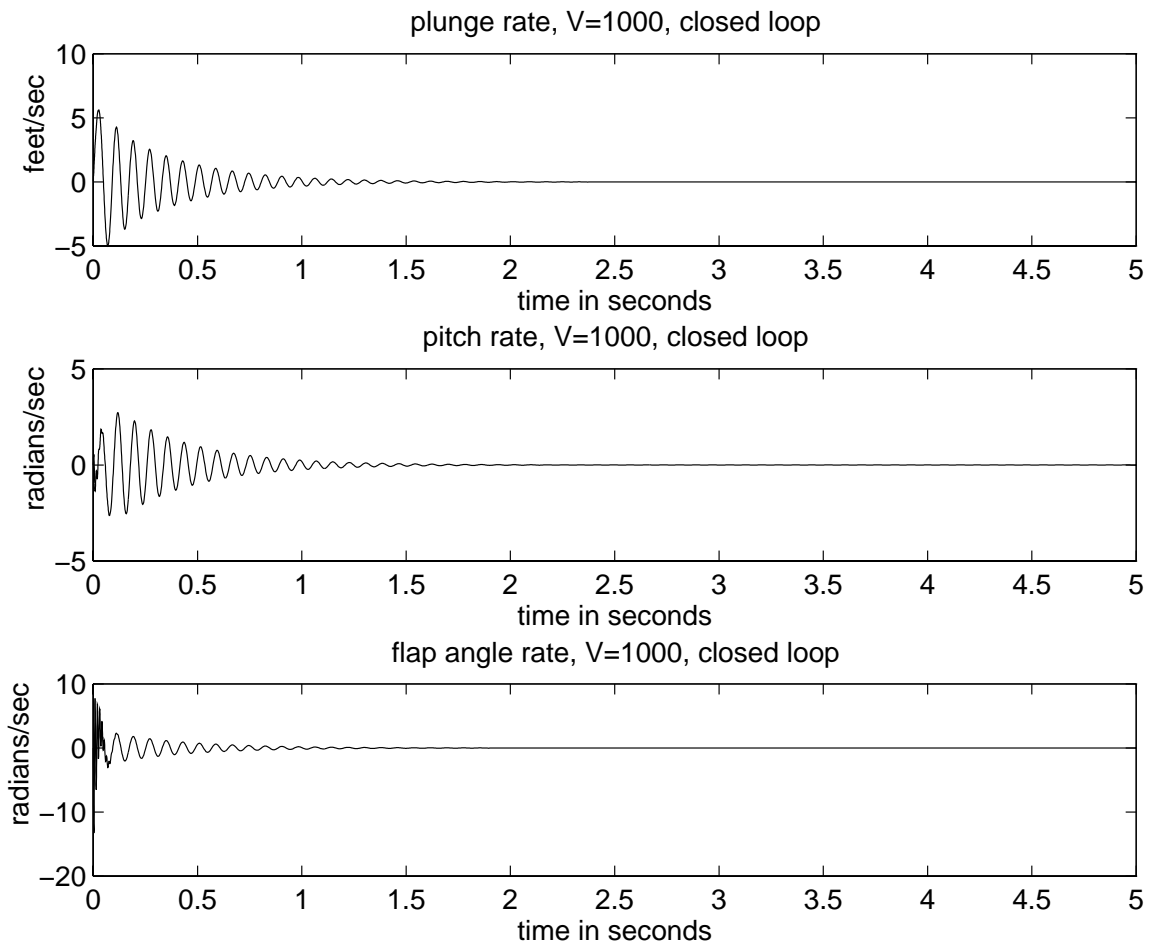


Figure 5.10: The velocities of the plunge, pitch, and flap angle for the closed loop system: Stable, $V=1000$.

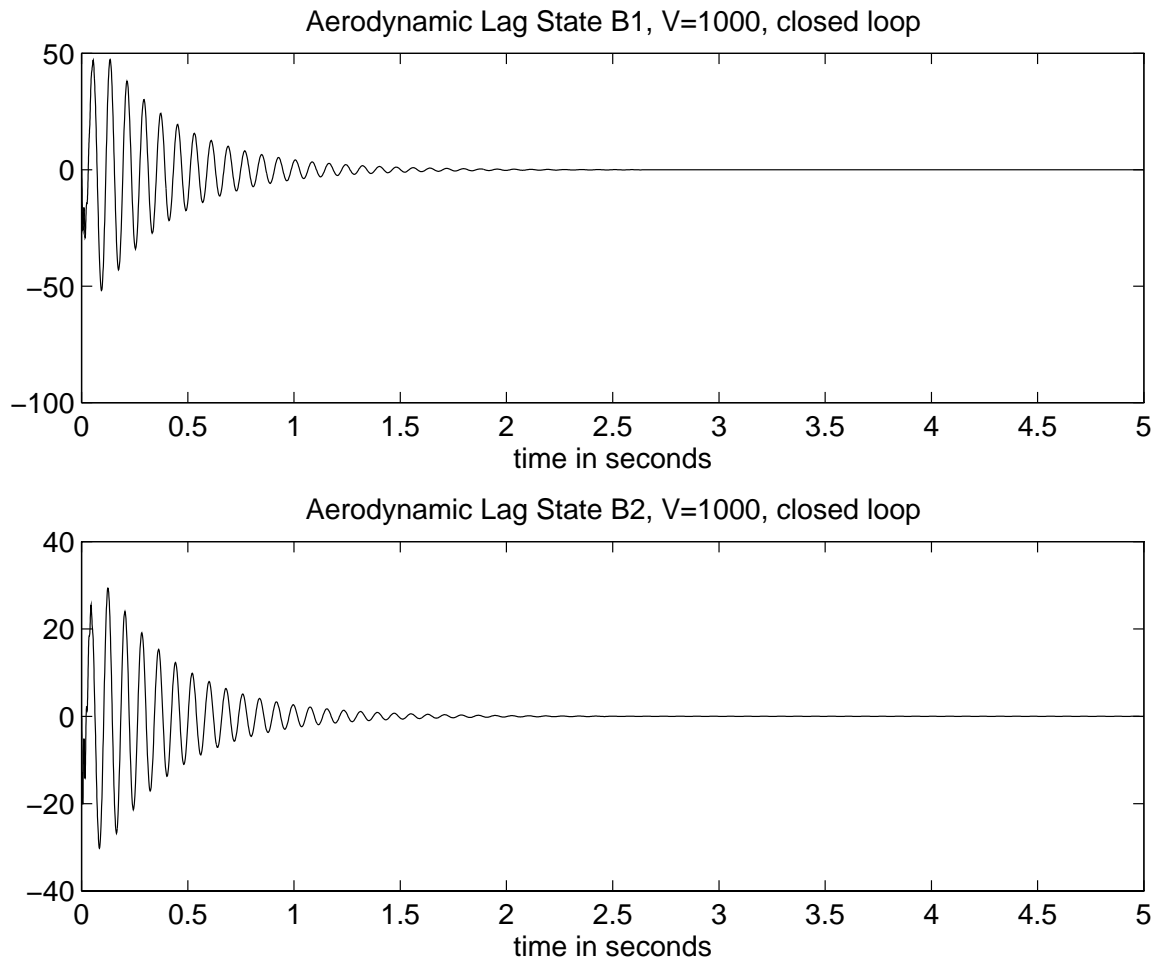


Figure 5.11: The aerodynamic lag states B_1 and B_2 for the closed loop system: Stable, $V=1000$.

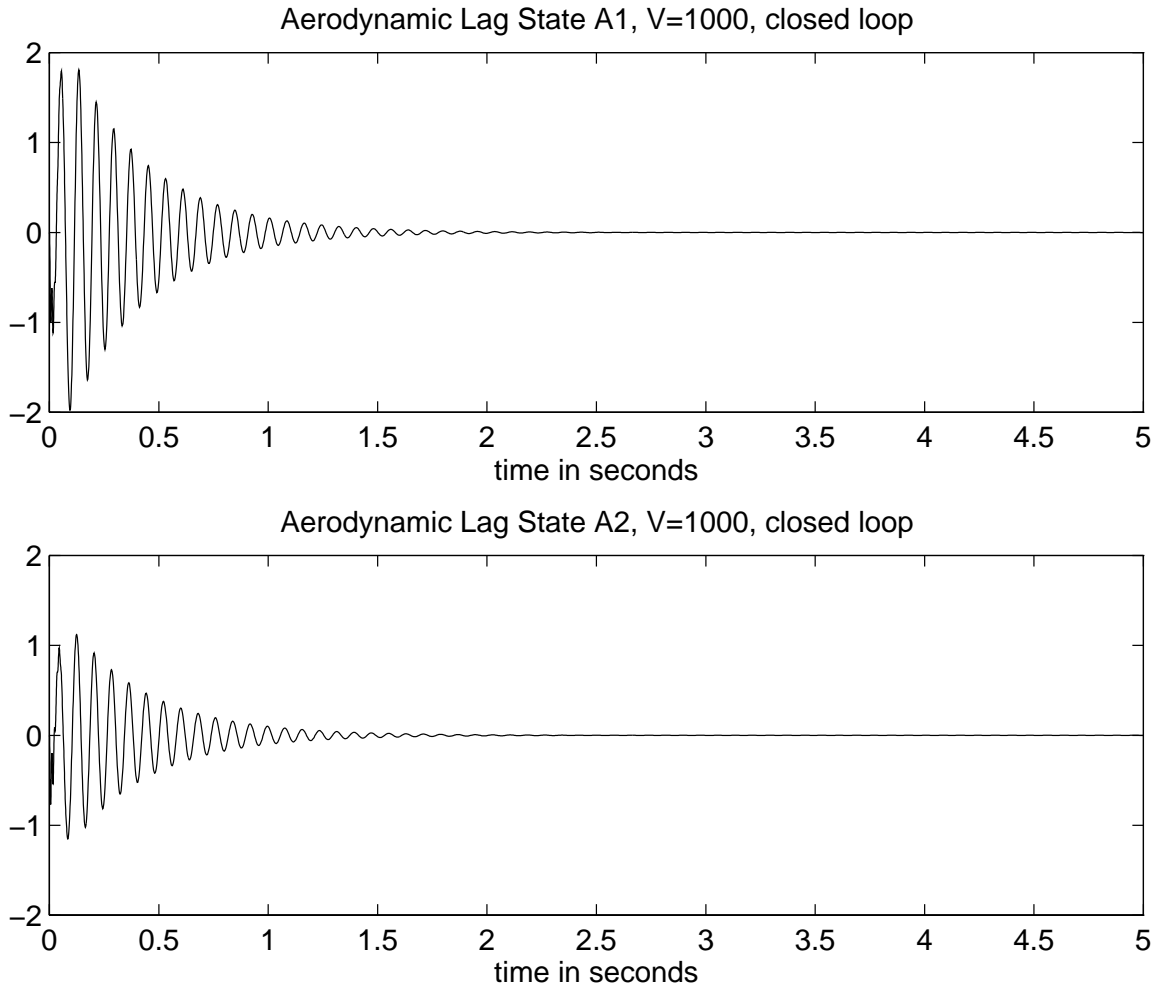


Figure 5.12: The aerodynamic lag states A_1 and A_2 for the closed loop system: Stable, $V=1000$.

λ_1	=	$-44.61 + 563.47i$
λ_2	=	$-44.61 - 563.47i$
λ_3	=	$-2.77 + 79.33i$
λ_4	=	$-2.77 - 79.33i$
λ_5	=	$-23.93 + 67.29i$
λ_6	=	$-23.93 - 67.29i$
λ_7	=	-96.99
λ_8	=	-13.66
λ_9	=	-106.67
λ_{10}	=	-13.67

Table 5.5: Eigenvalues of closed loop system for $V=1000$.

5.3 Closed Loop Simulations: Control Initiated at $t > 0$

Here we investigate the system response when the control is initiated at a time greater than $t = 0$ seconds. In particular, we are interested in performance when the system is flying beyond the flutter speed and the control is delayed by a few seconds. Consequently, we concentrate on the case $V = 1000$ feet/sec, a velocity above the flutter speed. Of course, when the control is turned on at $t = 0$ seconds, the closed loop responses are shown in Figures (5.9)-(5.12). If we initiate the control at .5 seconds as shown in Figures (5.13)-(5.16), the flap has to exert a small amount of force to control the plunge and pitch. The oscillations disappear at $t = 2$ seconds. If we wait 1 second before the control is applied as shown in Figures (5.17)-(5.20), the plunge has oscillates between $\pm .5$ feet and the pitch has oscillates between $\pm .5$ radians. Here the flap has to work harder to control the wing. The sharp spikes in the flap angle rate in Figure (5.18) show that the flap must jump to almost 175 radians/sec very quickly. This may begin to cause some problems for the flap but is still realistic. The oscillations disappear at $t = 2.5$ seconds. If the control is delayed until $t = 2$ seconds as shown in Figures (5.21)-(5.24), then it is likely the system would fail. As shown in Figure (5.21), by the time the control is applied, the plunge is oscillating between -4 feet and 4 feet and the pitch is oscillating between 4 radians and -4 radians. This means that the wing is oscillating up and down 4 feet and twisting back and forth a displacement of 4 radians. Figure (5.22) shows that the velocity of the flap would have to increase to 500 radians/sec at $t = 2$ seconds. For this 6 foot airfoil, wing separation would have occurred by this time. The flap would have to displace about 2.5 radians to control the wing, and that is not realistic. These results show that delaying the control until 2 seconds is too long. Therefore, it follows that if the controller is turned on much later than 1 second, then the wing would separate from the fuselage. Although we have presented the simulation results for one specific velocity $V=1000$ feet/sec, we conducted similar numerical experiments for other velocities and control times. The results presented here are typical of all such runs.

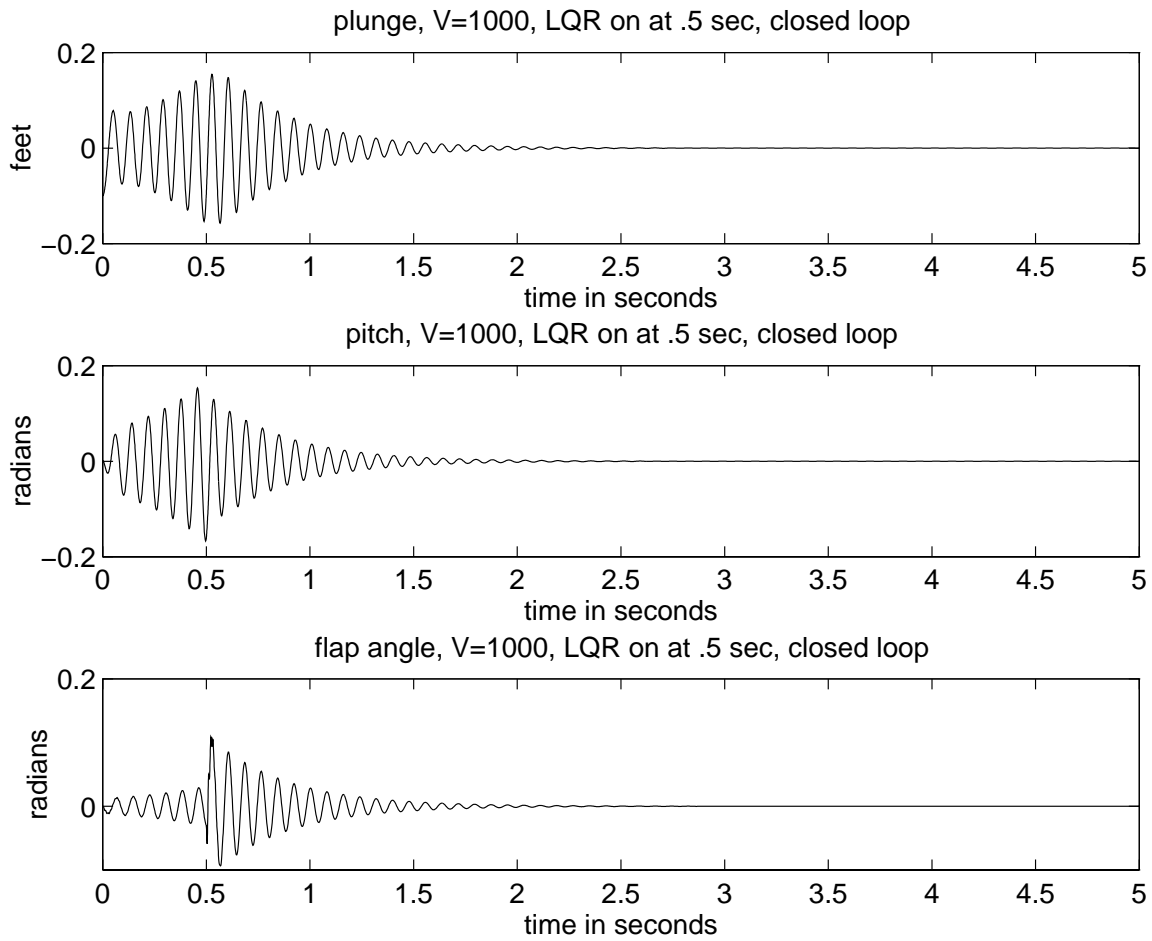


Figure 5.13: The plunge, pitch, and flap angle for the closed loop system with the control initiated at $t = 0.5$ seconds: $V = 1000$.

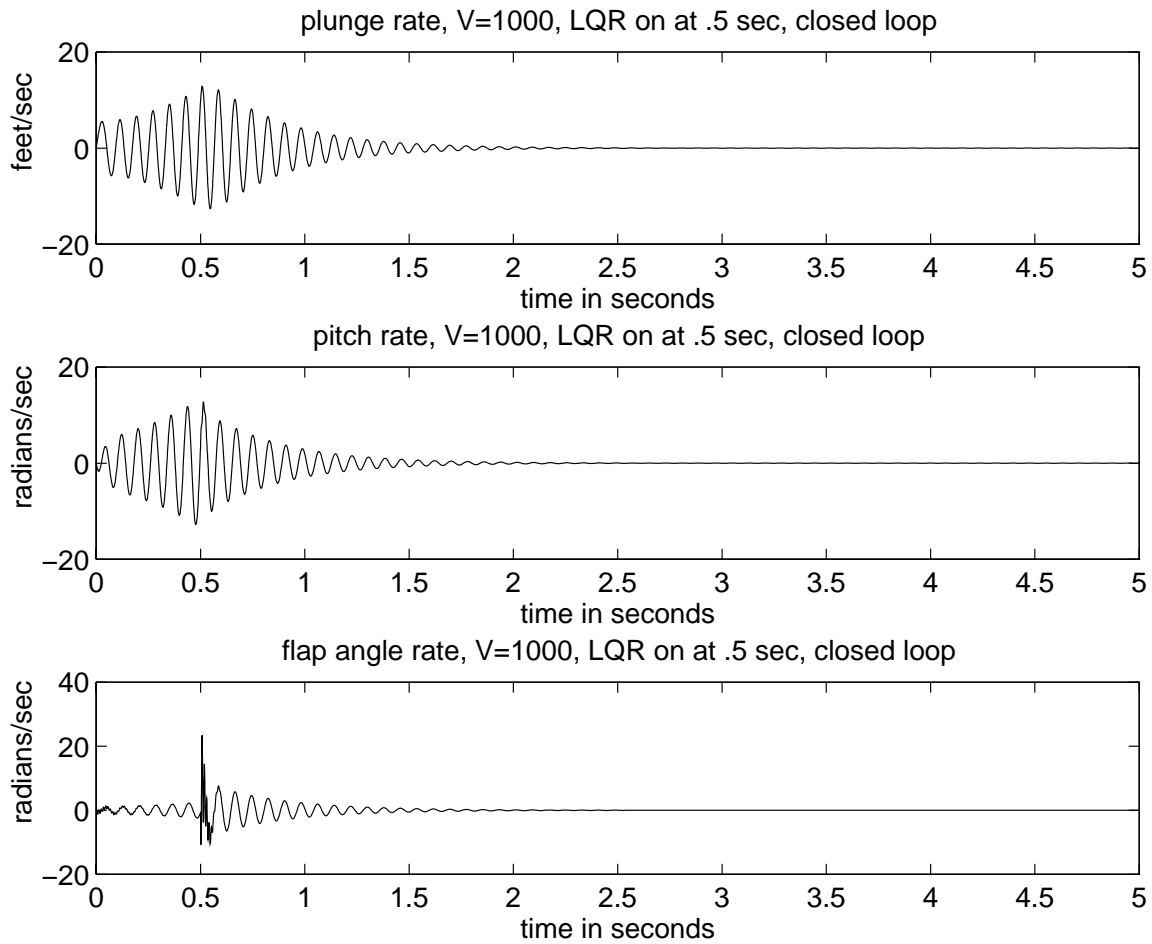


Figure 5.14: The velocities of the plunge, pitch, and flap angle for the closed loop system with the control initiated at $t=0.5$ seconds: $V=1000$.

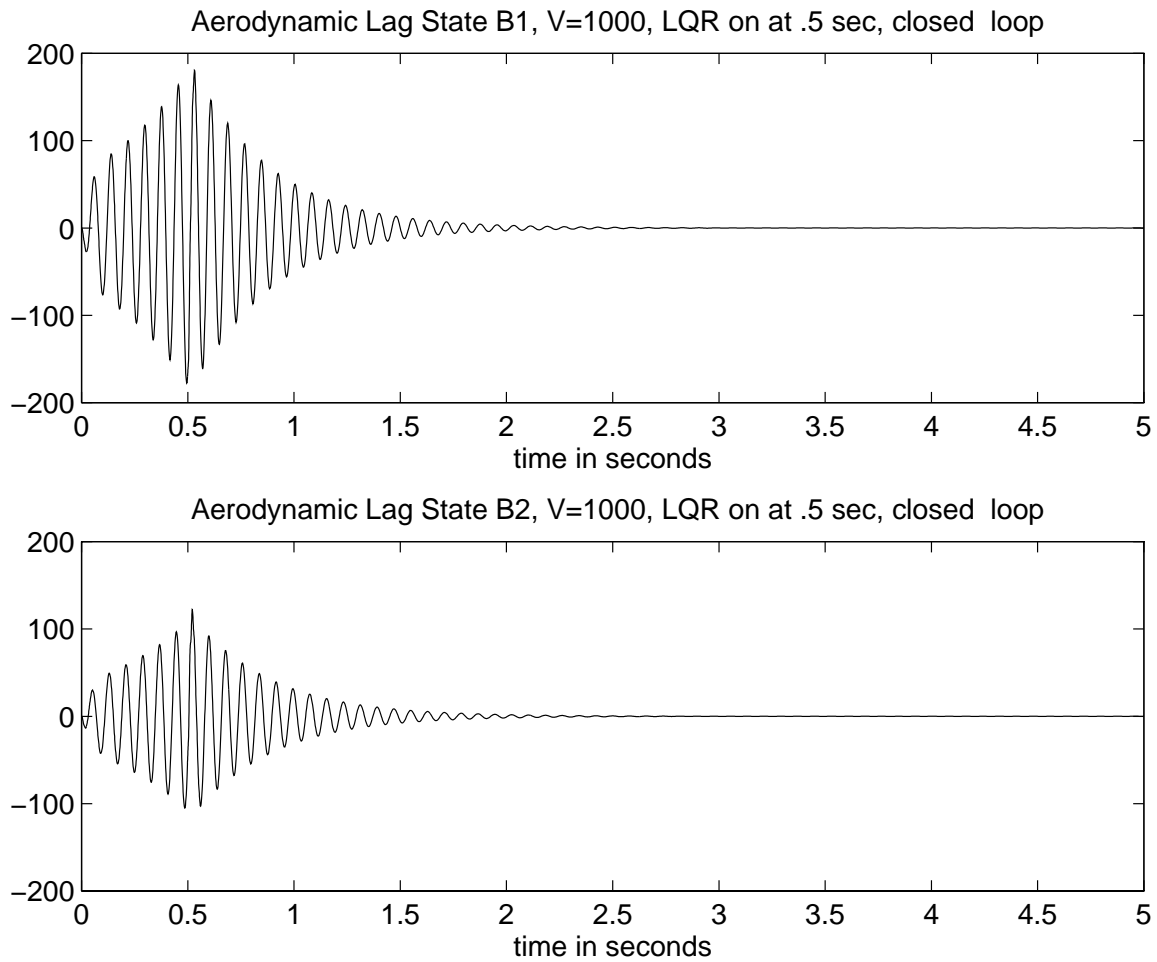


Figure 5.15: The aerodynamic lag states B_1 and B_2 for the closed loop system with the control initiated at $t=.5$ seconds: $V=1000$.

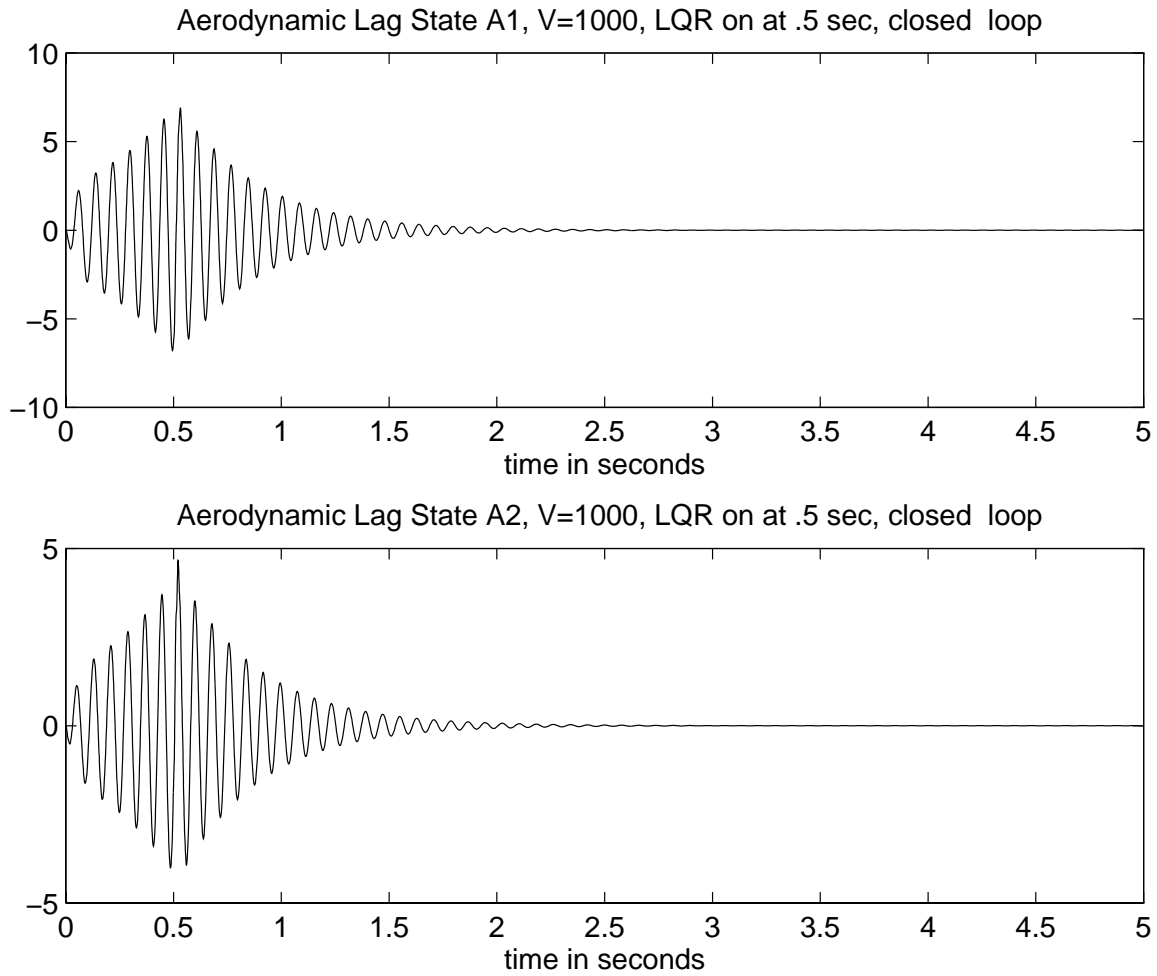


Figure 5.16: The aerodynamic lag states A_1 and A_2 for the closed loop system with the control initiated at $t=.5$ seconds: $V=1000$.

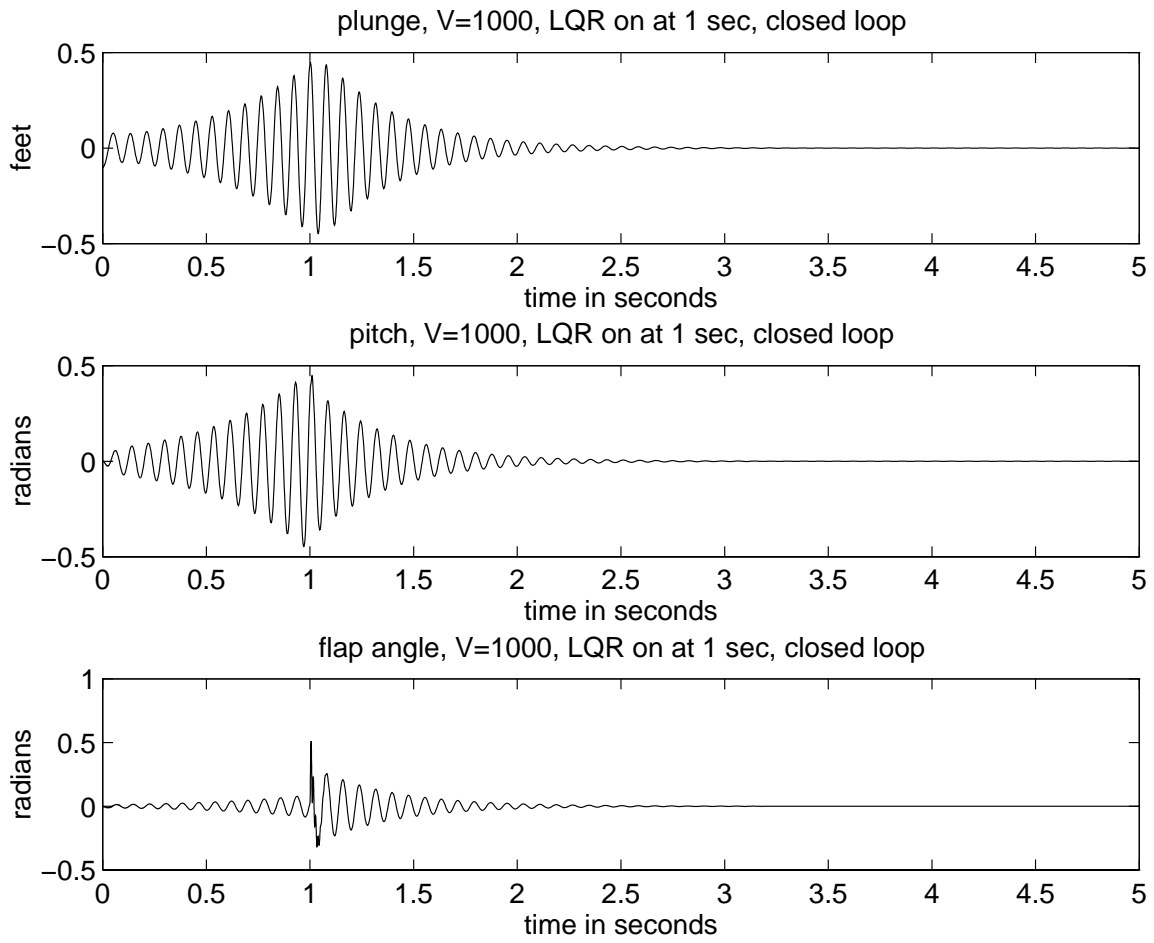


Figure 5.17: The plunge, pitch, and flap angle for the closed loop system with the control initiated at $t=1$ second: $V=1000$.

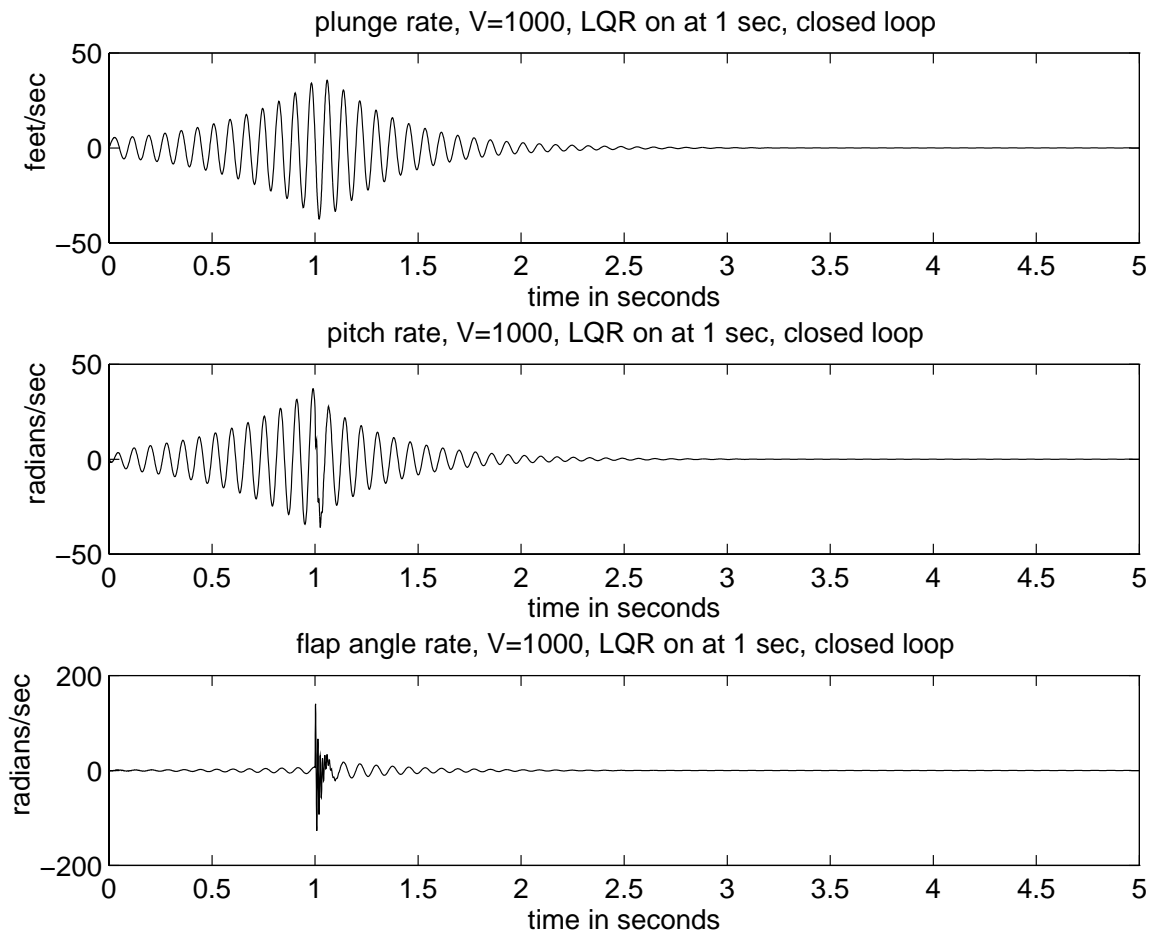


Figure 5.18: The velocities of the plunge, pitch, and flap angle for the closed loop system with the control initiated at $t=1$ second: $V=1000$.

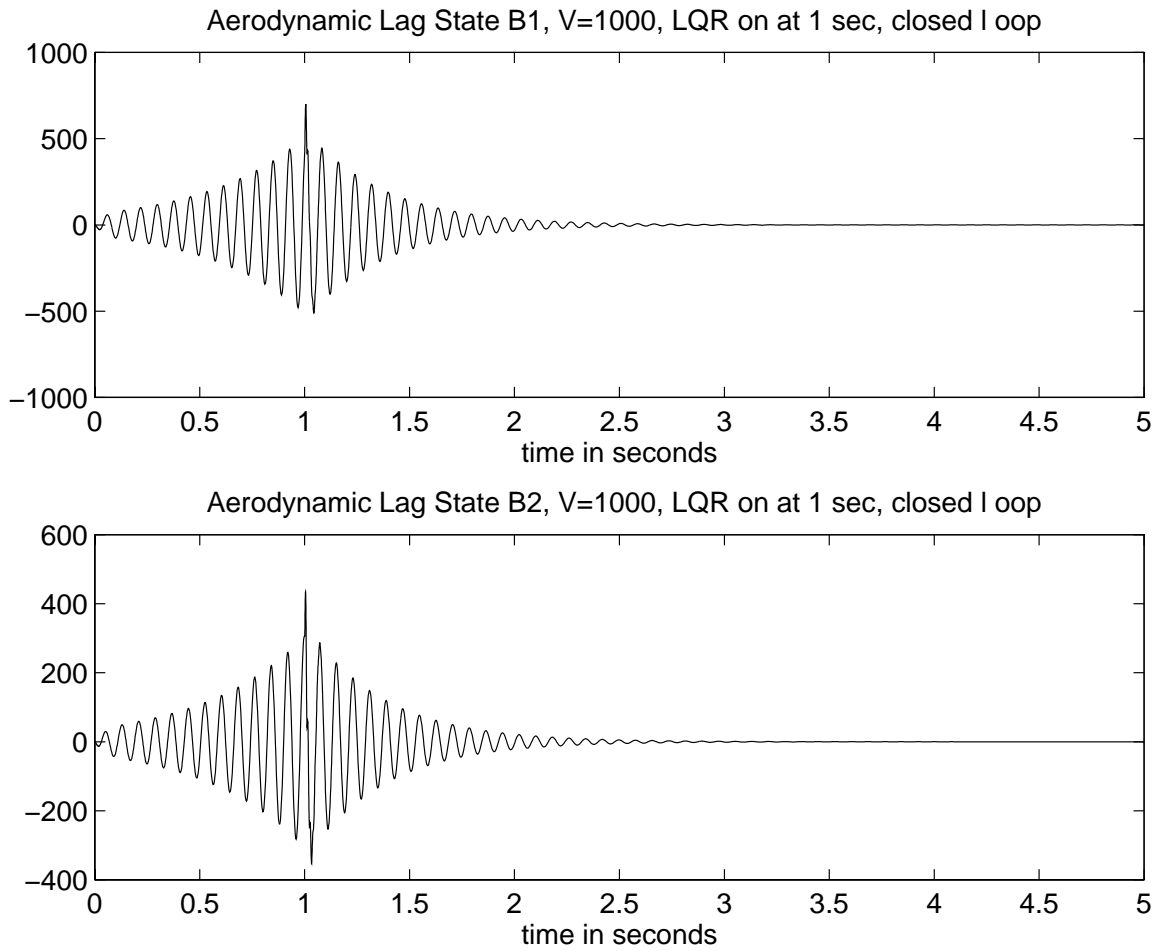


Figure 5.19: The aerodynamic lag states B_1 and B_2 for the closed loop system with the control initiated at $t=1$ second: $V=1000$.

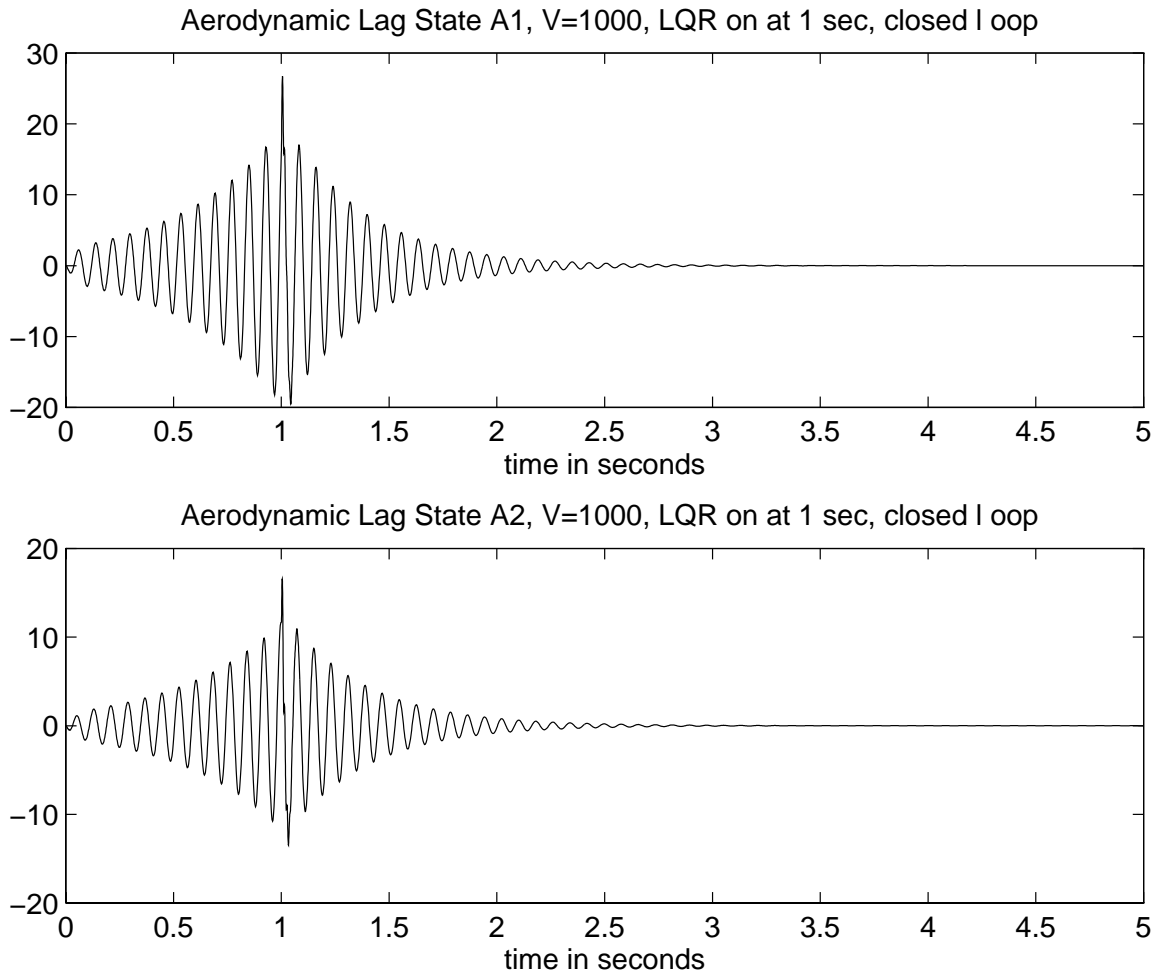


Figure 5.20: The aerodynamic lag states A_1 and A_2 for the closed loop system with the control initiated at $t=1$ second: $V=1000$.

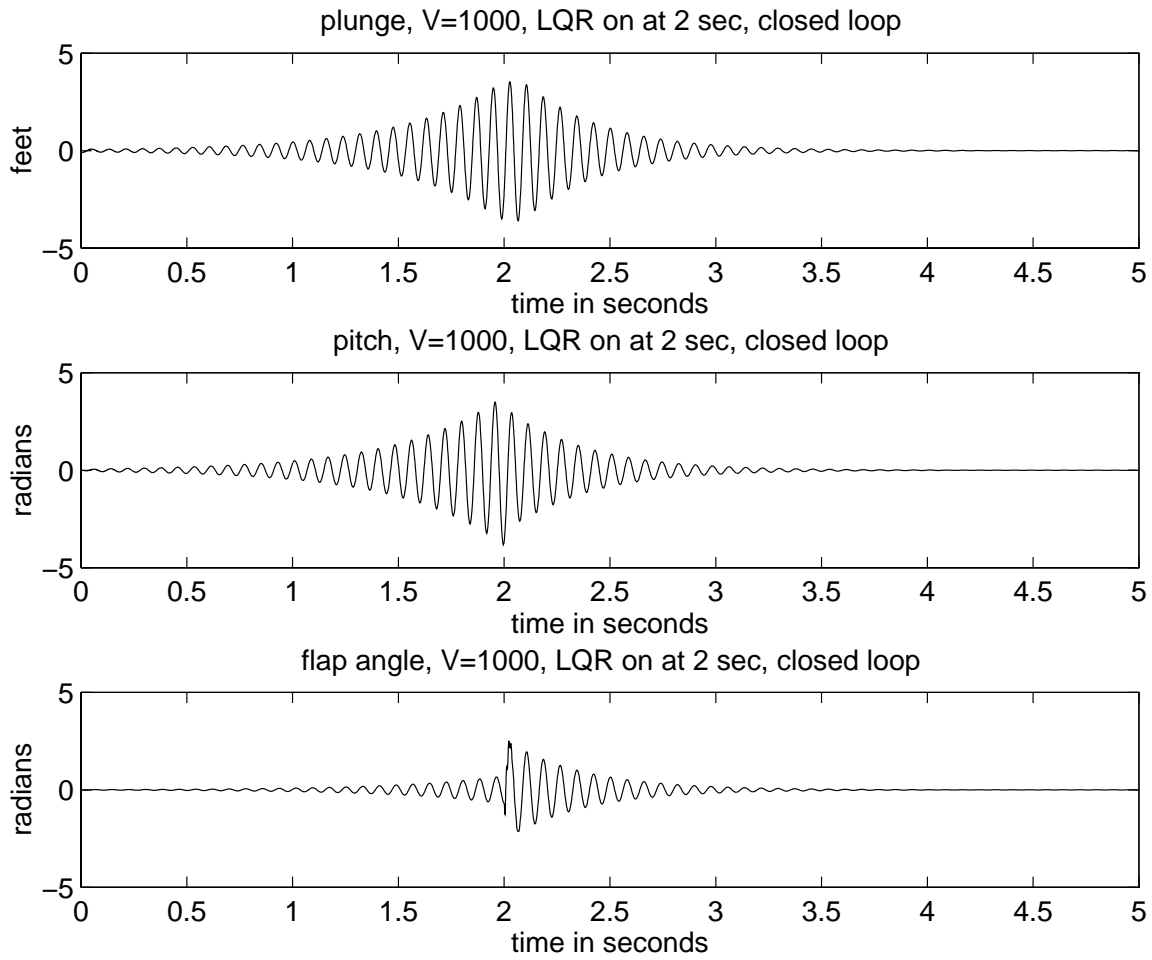


Figure 5.21: The plunge, pitch, and flap angle for the closed loop system with the control initiated at $t=2$ seconds: $V=1000$.

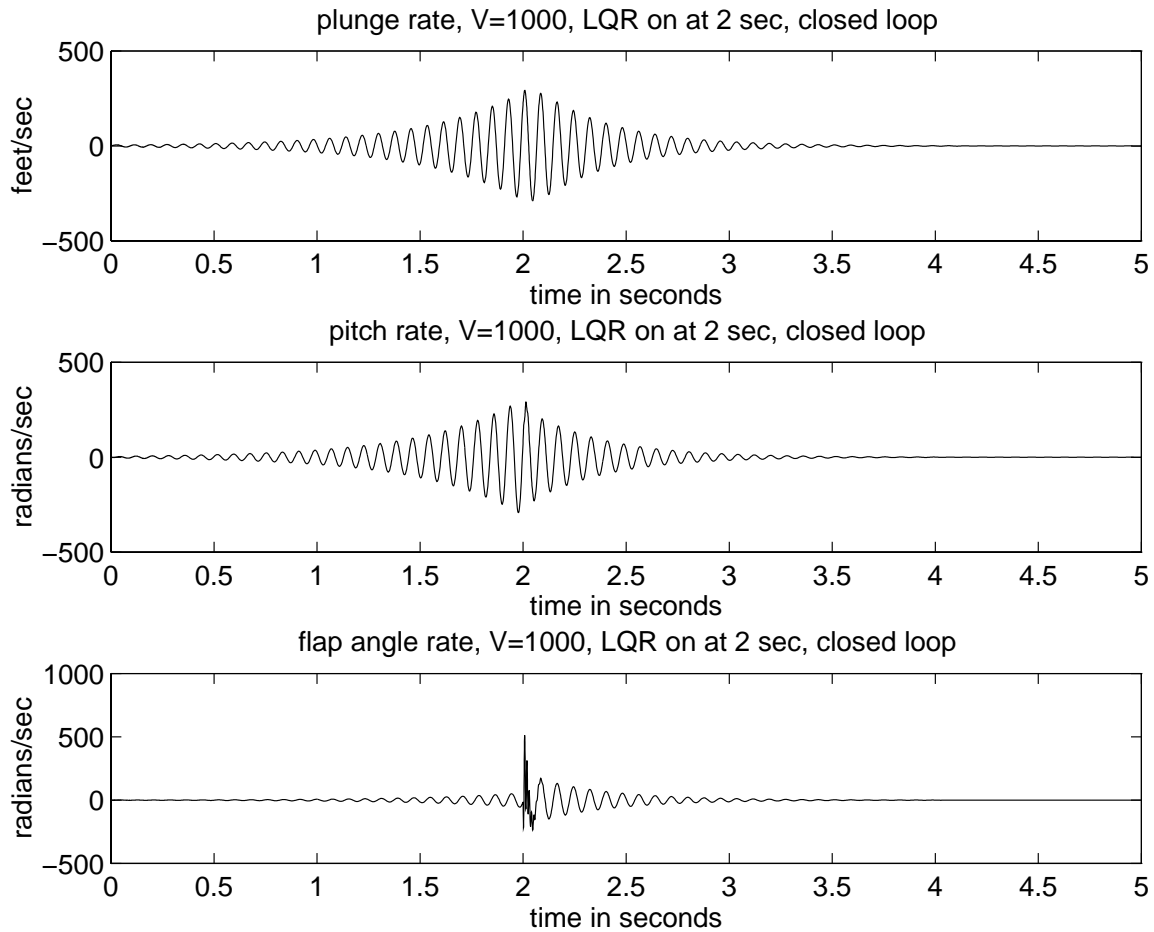


Figure 5.22: The velocities of the plunge, pitch, and flap angle for the closed loop system with the control initiated at $t=2$ seconds: $V=1000$.

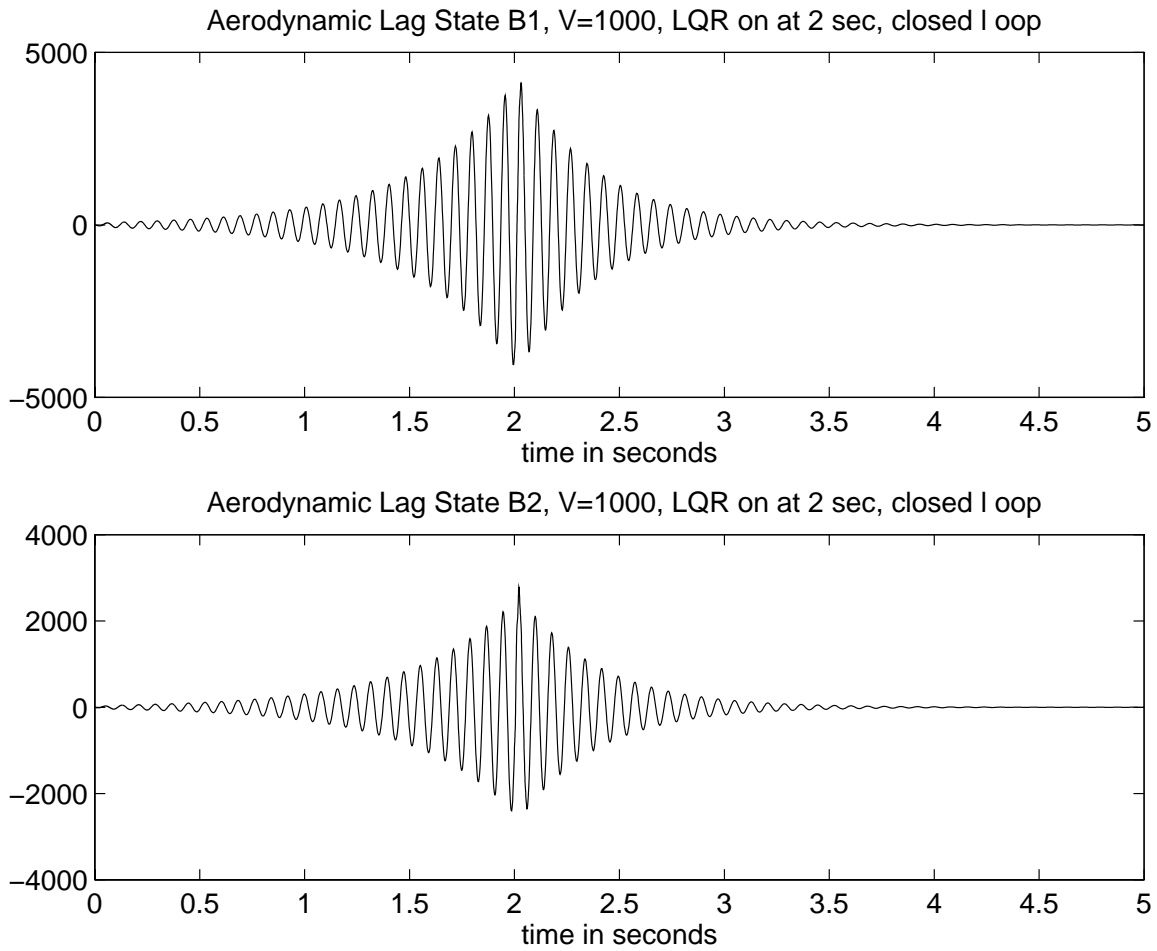


Figure 5.23: The aerodynamic lag states B_1 and B_2 for the closed loop system with the control initiated at $t=2$ seconds: $V=1000$.

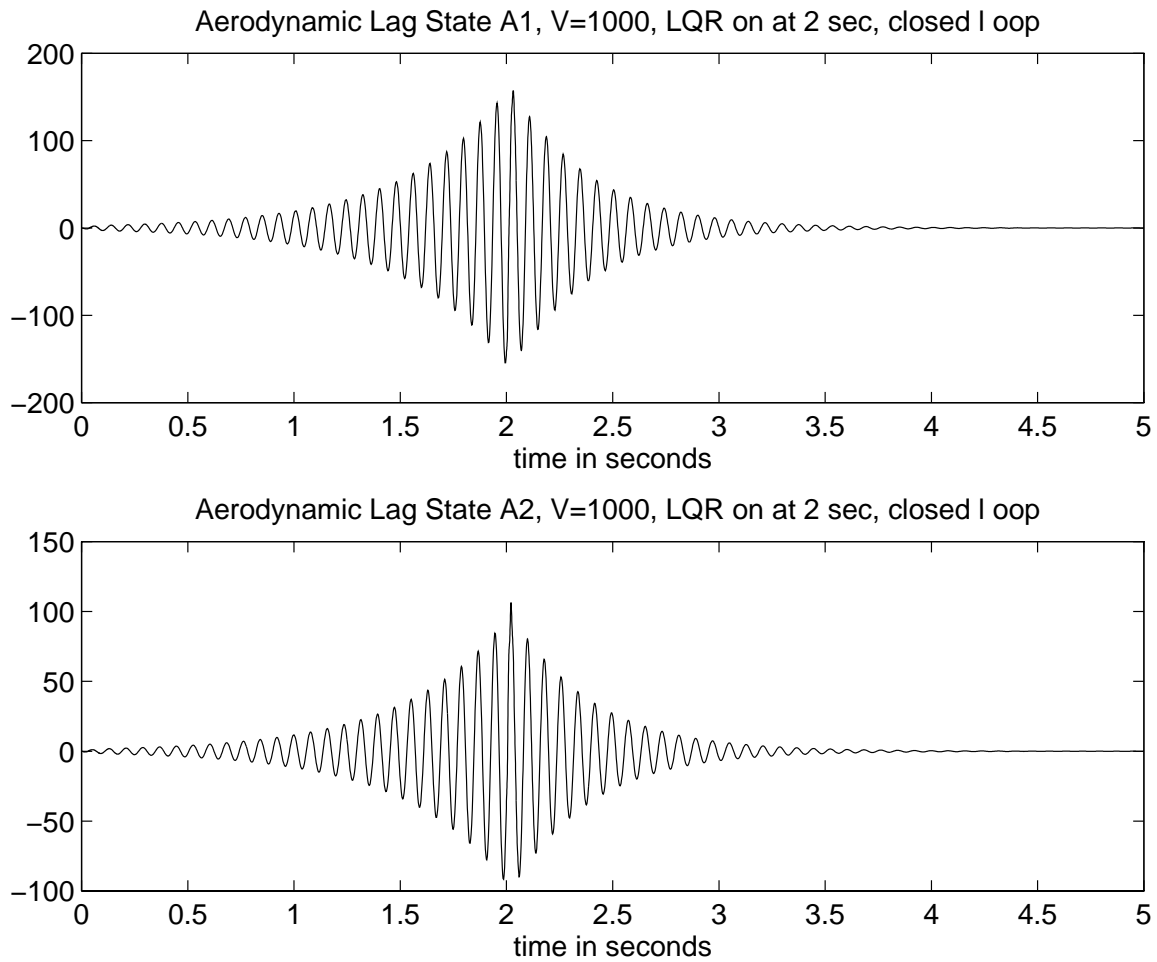


Figure 5.24: The aerodynamic lag states A_1 and A_2 for the closed loop system with the control initiated at $t=2$ seconds: $V=1000$.

Chapter 6

Conclusions

In this paper we developed a state space model for the typical aeroelastic airfoil and investigated the application of LQR control to the flutter suppression problem. We started with Newton's second law of motion and the moment equation for a rigid body in planar motion. By manipulating and linearizing, the equations were transformed into a second order system. These second order equations were then reduced to a first order system of the form $\dot{x} = Ax + Bu$ where A is a 10×10 partitioned matrix and B is a 10×1 column matrix. This open loop system was simulated at speeds below, equal to, and above the flutter speed and the corresponding eigenvalues and dynamic responses were analyzed.

Linear-Quadratic Regulator theory was used to stabilize this system. This closed loop system was also analyzed at speeds below, equal to, and above the flutter speed. It was shown that even above the flutter speed, the LQR controller performs well. We also found that the controller does not have to be applied to the system at $t = 0$ seconds. For the specific speed of $V=1000$ feet/sec the control could be activated anytime up to $t = 1$ second and still stabilize the system. If the control is initiated later, say at $t = 2$ seconds, the system is probably going to become unstable and wing failure will occur.

This work was a preliminary study in modeling and control motivated by York's thesis [10]. The derivation was repeated to correctly identify all of the system's parameters. Further study should be done in describing the motions of the airfoil more explicitly. This would provide a more realistic model. Also, by using more degrees of freedom and better aerodynamics, we could more accurately model the movement of an actual wing. Various approximations of the Wagner Function should be tested to determine which most accurately describes the aerodynamic loads.

LQR control is attractive but unrealistic. Even though, as discussed in [3], LQR is a very robust control law, it is impractical. The LQR controller requires that all states be known at all times in order to use state feedback. In the real world, there is the problem of sensor noise and it is not reasonable to expect that the 10 states used here can be sensed.

In particular, the aerodynamic lag states are not physical states and cannot be sensed. Linear-Quadratic Gaussian (LQG) control and H^∞ control can be used to achieve this goal and is the subject of Bail's thesis [2]. In [2], Bail applies LQG and H^∞ control to the two-dimensional airfoil problem presented in this paper. These methods use state estimators to compensate for the lack of information. The results in [2] are very encouraging and suggest that robust active flutter control is possible.

Appendix A

Nomenclature

A	system matrix for first order differential equation
$\vec{a}_{c.m.}$	acceleration
A_i	aerodynamic lag state variables
A_{ii}	submatrix of A
A^T	transpose of a matrix A
A^*	conjugate transpose of a matrix A
α	pitch angle
B_i	aerodynamic lag state variables
b	normalizing constant
β	flap angle
c	nondimensionalized distance to flap hinge line
C	state matrix
$C(k)$	Theodorsen function
d	nondimensionalized distance to elastic axis from leading edge
D	control input matrix
\vec{F}	force
$\mathcal{F}\{\cdot\}$	Fourier transform of $\{\cdot\}$
$\Phi\left(\frac{Vt}{b}\right)$	Wagner function
g	degree of freedom
G	amplitude of g
h	position with respect to plunge
i	$\sqrt{-1}$
I_α	inertia of pitch angle
I_β	inertia of flap angle
$I_{c.m.}$	inertia
I_G	moment of inertia per unit span of trailing edge flap point G

I_Q	inertia per unit length of total section
K	stiffness matrix
K_c	gain matrix
K_α	stiffness of pitch spring
K_β	stiffness of flap spring
K_h	stiffness of plunge
l	distance to trailing-edge flap center of gravity from c(ft.)
L	lift
L_1	lift per unit span on main section (body 1)of airfoil
L_2	lift per unit span on trailing-edge flap (body 2) of the airfoil
M	pitching moment
M_1	pitching moment per unit span of main section (body 1) about $\frac{1}{4}$ chord
M_2	pitching moment per unit span of trailing-edge flap (body 2) about c
M'	mass matrix
$M_{c.m.}$	momentum
m	mass of airfoil
m_1	mass of main body (body 1) of the airfoil in mass-spring system
m_2	mass of trailing edge control surface (body 2) in mass-spring system
ρ	air density
q_y	vertical flap hinge force
S	static moment
S_α	static moment of pitch angle
S_β	static moment of flap angle
T	torque of flap spring
t	time
u	control vector
V	velocity
V_f	flutter speed
$\dot{\omega}$	angular acceleration
x	state vector
x_A	column vector of aerodynamic lag state variables
x_1	nondimensionalized distance of main section center of gravity
Y	column vector of plunge, pitch, and flap displacement
z	controlled output
$()'$	$\frac{d()}{d\tau}$
$()''$	$\frac{d^2()}{d\tau^2}$
$\dot{()}$	$\frac{d()}{dt}$
$\ddot{()}$	$\frac{d^2()}{dt^2}$

Appendix B

MATLAB Codes

LQROPEN.M

```
%Runs the open loop system,  $\dot{x}=Ax+Bu$ , and prints the  
%graps of the plunge, pitch, and flap angle. Also  
%states the eigenvalues of A.
```

```
runab;  
eig(A);  
global A ;  
[t,w]=ode45('flutrhs',0,5,w0);  
subplot(3,1,1), plot(t,w(:,4))  
title('plunge, V=1000, open loop')  
xlabel('time in seconds')  
ylabel('feet')  
subplot(3,1,2), plot(t,w(:,5))  
title('pitch, V=1000, open loop')  
xlabel('time in seconds')  
ylabel('radians')  
subplot(3,1,3), plot(t,w(:,6))  
title('flap angle, V=1000, open loop')  
xlabel('time in seconds')  
ylabel('radians')
```

RUNAB.M

```
%Calls and runs subprograms to build system.  
%The w0's are the initial conditions.
```

```

cnstnt
phi
tees
arrs
ells
emms
zees
mkprime
biga
bmatrix
gmatrix
save bmatrix B
save amatrix A V
save gmatrix G
clear
load amatrix
load bmatrix
load gmatrix
load gusty
w0=zeros(10,1);
w0(1)=.05;
w0(2)=-.01;
w0(3)=.005;
w0(4)= -.1;
w0(5)=.001;
w0(6)=-.0001;

```

FLUTRHS.M

```
%Solves the right hand side, Ax.
```

```

function y=flutrhs(t,w)
global A
y=A*w;

```

CNSTNT.M

```
%Constants for the flutter problem.
```

```

b = 3;
c = 1;
V = 1000
%V = 975.6
%Vflutter at .6 flap = 975.6
m =2.6883;
Row = .002378*1;
ALPHA1 = .0165;
ALPHA2 = .335;
SALPHA = 1.61298*1.0;
SBETA = .10081*1.0;
IALPHA = 6.04868;
IBETA = .151217;
KH = m*50^2;
BETA1 = .041;
BETA2=.32;
KALPHA = IALPHA*100^2;
KBETA = IBETA*500^2;
Vflutter = 975.6
gvert = 1;
ghoriz = 1;

```

PHI.M

```
%Calculates phi's and sets the location of the flap angle.
```

```

xflap=.6
Phi=acos(-xflap)
%Phi = pi-.75
%xflap=-cos(Phi)
Phi1 = pi - Phi + sin(Phi);
Phi2 = (pi - Phi)*(1 + 2*cos(Phi)) + sin(Phi)*(2 + cos(Phi));
Phi3 = pi - Phi + sin(Phi)*cos(Phi);
Phi4 = (pi - Phi)*2*cos(Phi) + sin(Phi)*2/3*(2 + (cos(Phi))^2);
Phi5 = sin(Phi)*(1 - cos(Phi));
Phi6 = 2*(pi - Phi) + sin(Phi)*2/3*(2-cos(Phi))*(1 + 2*cos(Phi));
Phi7 = (pi - Phi)*(.5 + 2*cos(Phi)) + sin(Phi)*(1/6)*(8 + 5*cos(Phi)
+ 4*cos(Phi)^2 - 2*cos(Phi)^3);
Phi8 = (pi - Phi)*(-1 + 2*cos(Phi)) + sin(Phi)*(2-cos(Phi));
Phi9 = (pi - Phi)*(1 + 2*cos(Phi)) + sin(Phi)*1/3*(2 + 3*cos(Phi)

```

```

+ 4*(cos(Phi))^2);
Phi31= pi - Phi - sin(Phi);
Phi10= Phi31 * Phi5;
Phi11= Phi2 * Phi3;
Phi12= (pi - Phi)^2 * (.5 + 4*cos(Phi)^2)
+(pi - Phi) *sin(Phi)*cos(Phi)*(7 + 2*(cos(Phi))^2)
+ (sin(Phi))^2*(2 + 2.5*(cos(Phi))^2);

```

TEES.M

```

%Generates T's in the Z matrices.
%Phi's defined in PHI.M.
%ALPHA1, ALPHA2, V, b defined in CNSTNT.M.

```

```

TH2 = (b^2/(2*pi))*Phi4;
TALPHA2 = (b^2/(4*pi^2))*Phi7;
TBETA2 = (b^2/(4*pi^2))*Phi12;
TH1 = (V*b/pi)*Phi2;
TALPHA1 = (V*b/pi)*(Phi9/2 + Phi8);
TBETA1 = (V*b/(2*pi^2))*(Phi11 + Phi2*Phi8);
TH0 = 0;
TALPHA0 = (V^2/pi)*Phi8;
TBETA0 = (V^2/pi^2)*(Phi10 + Phi1*Phi8);
TA1 = -V*ALPHA1/b;
TA2 = -V*ALPHA2/b;

```

ARRS.M

```

%Generates R values for the A matrix.
%V, b defined in CNSTN.M.
%Phi's defined in PHI.M.
%R's called from BIGA.M.

```

```

R1 = b^2/V;
R2 = b^2/V;
R3 = (b^2/(2*pi*V))*Phi2;
R4 = V;
R5 = V/pi *Phi1;
R6 = (b^3/(pi*V))*Phi8;
R7 = (b^3/(pi*V))*Phi8;

```

ELLS.M

%Generates the L values for the Z matrices.
%V, b, ALPHA1, ALPHA2 defined in CNSTNT.M.
%Phi's defined in PHI.M.

```
LH2 = b;  
LALPHA2 = b/2;  
LBETA2 = (b/(2*pi))*Phi4;  
LH1 = 2*V;  
LALPHA1 = 3*V;  
LBETA1 = (V/pi)*(Phi3 + Phi2);  
LH0 = 0;  
LALPHA0 = 2*(V^2)/b;  
LBETA0 = (2*(V^2)/(pi*b))*Phi1;  
LB1 = -2*V*ALPHA1/b;  
LB2 = -2*V*ALPHA2/b;
```

EMMS.M

%Generates the M values for the Z matrices.
%V, b defined in CNSTN.M.
%Phi's defined in PHI.M.

```
MH2 = (b^2)/2;  
MALPHA2 = (3*b^2)/8;  
MBETA2 = ((b^2)/(4*pi))*Phi7;  
MH1 = 0;  
MALPHA1 = V*b;  
MBETA1 = (V*b/(2*pi))*Phi6;  
MHO = 0;  
MALPHA0 = 0;  
MBETA0 = ((V^2)/pi)*Phi5;
```

ZEES.M

%Generates the Z matrices used in building the A matrix.

```
Z1 = [LH2 LALPHA2 LBETA2; MH2 MALPHA2 MBETA2; TH2 TALPHA2 TBETA2];
```

```
Z2 = [LH1 LALPHA1 LBETA1; 0 MALPHA1 MBETA1; TH1 TALPHA1 TBETA1];
```

```
Z3 = [0 LALPHA0 LBETA0; 0 0 MBETA0; 0 TALPHA0 TBETA0];
```

```
Z4 = [LB1 LB2 0 0; 0 0 0 0; 0 0 TA1 TA2];
```

MKPRIME.M

```
%Builds the mass and stiffness matrices used in building matrix A.  
%SALPHA, SBETA, IALPHA, IBETA, b, m, c, KH, KALPHA, KBETA  
%defined in CNSTNT.M.
```

```
MPRIME = [ b*m SALPHA SBETA; b*SALPHA IALPHA IBETA+(SBETA*b*c);  
          b*SBETA IBETA+(SBETA*b*c) IBETA];
```

```
KPRIME = [b*KH 0 0; 0 KALPHA 0; 0 0 KBETA];
```

```
global MPRIME KPRIME
```

BIGA.M

```
%Generates the A matrix from the submatrices A11 through A33.  
%This is the A matrix used in y=Ax.  
%R's are defined in ARRS.M.  
%MPRIME, KPRIME defined in MKPRIME.M.  
%Row, pi, b, V, BETA1, BETA2 defined in CNSTNT.M.  
%Z's defined in ZEES.M.
```

```
A11 = -1*inv(MPRIME + (pi*Row*(b^2)*Z1)) * pi*Row*(b^2)*Z2;  
A12 = -1*inv(MPRIME + (pi*Row*(b^2)*Z1)) * (KPRIME + pi*Row*(b^2)*Z3);  
A13 = -1*inv(MPRIME + (pi*Row*(b^2)*Z1)) * pi*Row*(b^2)*Z4;  
A21 = eye(3);  
A22 = zeros(3);  
A23 = zeros(3,4);  
A31 = [[R1 R2 R3]*A11 + [0 R4 R5]; [R1 R2 R3]*A11 + [0 R4 R5];  
       [R6 R7 R8]*A11 + [0 R9 R10]; [R6 R7 R8]*A11 + [0 R9 R10]];  
A32 = [[R1 R2 R3]*A12; [R1 R2 R3]*A12; [R6 R7 R8]*A12; [R6 R7 R8]*A12];  
A330=eye(4);  
A330(1,1)=-BETA1*V/b;
```

```

A330(2,2)=-BETA2*V/b;
A330(3,3)=-BETA1*V/b;
A330(4,4)=-BETA2*V/b;
A33 = [A330 + [[R1 R2 R3]*A13; [R1 R2 R3]*A13; [R6 R7 R8]*A13;
        [R6 R7 R8]*A13]];
A = [A11 A12 A13; A21 A22 A23; A31 A32 A33];
save aparts A11 A12 A13 A21 A22 A23 A31 A32 A33

```

BMATRIX.M

```

%B matrix used in the control system, xdot=Ax + Bu.
%MPRIME defined in MKPRIME.M.
%IBETA defined in CNSTNT.M.

bbb0=[0 0 1];
bbb1=[0 0 0];
bbb2=[0 0 0 0];
bbb0=inv(MPRIME)*bbb0';
B=(1/IBETA)*[bbb0' bbb1 bbb2]';
%save bmatrix

```

LQRRUNS.M

```

%Runs the closed loop system and prints the
%graps of the plunge, pitch, and flap angle. Also
%states the eigenvalues of Acl=A-BK.

runab;
runlqr;
eig(Acl);
global A Acl fk;
[tcl,wcl]=ode45('clrhs',0,5,w0);
subplot(3,1,1), plot(tcl,wcl(:,4))
title('plunge, V=950, closed loop')
xlabel('time in seconds')
ylabel('feet')
subplot(3,1,2), plot(tcl,wcl(:,5))
title('pitch, V=950, closed loop')
xlabel('time in seconds')

```

```

ylabel('radians')
subplot(3,1,3), plot(tcl,wcl(:,6))
title('flap angle, V=950, closed loop')
xlabel('time in seconds')
ylabel('radians')

```

RUNLQR.M

```
%Sets up and runs the LQR problem
```

```

Q=eye(10,10);
Q(1,1)=1000*Q(1,1);
Q(4,4)=1000*Q(4,4);
Q(2,2)=1*Q(2,2);
Q(5,5)=1*Q(5,5);
Q(3,3)=100*Q(3,3);
Q(6,6)=100*Q(6,6);
Q(7,7)=.0001*Q(7,7);
Q(8,8)=.0001*Q(8,8);
Q(9,9)=.0001*Q(9,9);
Q(10,10)=.0001*Q(10,10);
Q=eye(10,10);

```

```

R=V^2/1000000
fk=lqr(A,B,Q,R);
Acl=A-B*fk;

```

CLRHS.M

```
%Solves the closed-looped (controlled) right hand side,
%y=Acl*x where Acl=A-BK.
```

```

function y=clrhs(t,w)
global Acl
y=Acl*w;

```

LQRSTEP.M

```
%Runs the closed loop system with the control turned on at a
%specified time.
```

%Prints the graphs of the plunge, pitch, and flap angle. Also
 %Also states the eigenvalues of $Acl=A-BK$.

```
runab;
runlqr;
eig(Acl);
global A Acl fk B jstep25 tcl;
[ts,ws]=ode45('clrhs25',0,5,w0);
subplot(3,1,1), plot(ts,ws(:,4))
title('plunge, V=1000, LQR on at 2 sec, closed loop')
xlabel('time in seconds')
ylabel('feet')
subplot(3,1,2), plot(ts,ws(:,5))
title('pitch, V=1000, LQR on at 2 sec, closed loop')
xlabel('time in seconds')
ylabel('radians')
subplot(3,1,3), plot(ts,ws(:,6))
title('flap angle, V=1000, LQR on at 2 sec, closed loop')
xlabel('time in seconds')
ylabel('radians')
```

CLRHS25.M

%Solves the right hand side, $Acl*x$. $Acl=A-BK$.
 %Turns the control on at a specified time.

```
function y=clrhs25(t,w)
global Acl A fk B
y=A*w-jstep25(t)*B*fk*w;
```

JSTEP25.M

%Step function that turns on control at specified time, lqron.

```
function z=jstep25(tt)
z=0;
lqron=2;
if tt>lqron
z=1;
end
```

Bibliography

- [1] B.D.O. Anderson and J. B. Moore, *Optimal Control: Linear Quadratic Methods*, Prentice Hall, 1990.
- [2] Thomas R. Bail, *A Disturbance-Rejection Problem for a 2-D Airfoil Exhibiting Flutter*, Thesis, Virginia Polytechnic Institute and State University, 1997.
- [3] Peter Dorato and Chaouki Abdallah and Vito Cerone, *Linear-Quadratic Control: An Introduction*, Prentice Hall, 1995.
- [4] Michael Green and David J. N. Limebeer, *Linear Robust Control*, Prentice Hall, 1995.
- [5] H. G. Kussner and I. Schwarz, *The Oscillating Wing With Aerodynamically Balanced Elevator*, TM 991, Oct. 1941, NACA.
- [6] Douglas K. Linder, *Introduction to Signals and Systems*, 1996.
- [7] Ihnseok Rhee and Jason L. Speyer, "A Game Theoretic Controller and Its Relationship to H^∞ and Linear-Exponential-Gaussian Synthesis," *Proceedings of the Conference on Decision and Control*, Tampa, FL 199: 909-915.
- [8] W. P. Rodden and B. Stahl, "A Strip Method for Prediction of Damping in Subsonic Wind Tunnel and Flight Flutter Tests", *Journal of Aircraft*, Vol. 6, No. 1, pp. 9-17, Jan.-Feb. 1969.
- [9] G. O. Thompson, "Active Flutter Suppression—An Emerging Technology," *Journal of Aircraft*, Vol. 9, pp. 230-235, March 1972.
- [10] York, Darrell L., *Analysis of Flutter and Flutter Suppression Via an Energy Method*, Thesis, Virginia Polytechnic Institute and State University, 1980.
- [11] Kemin Zhou and John C. Doyle and Keith Glover, *Robust and Optimal Control*, Prentice Hall, 1996.

Vita

I was born on November 22, 1973. My parents are Mr. and Mrs. Rudolph M. Olds. I grew up in Chesapeake, VA and graduated from Virginia Tech in May 1995 with a B.S. in Mathematics (Applied Computational Mathematics Option) with a minor in Physics. I decided to stay at Virginia Tech for my M.S. in Mathematics where I have been a graduate teaching assistant. After graduation, I will be working in the Submarine Technology Department of the Johns Hopkins University Applied Physics Lab in Laurel, MD. My hobbies include shopping, cooking, aerobics, reading, and playing with my dog.